

**Distribution Agreement**

In presenting this thesis or dissertation as a partial fulfillment of the requirements for an advanced degree from Emory University, I hereby grant to Emory University and its agents the non-exclusive license to archive, make accessible, and display my thesis or dissertation in whole or in part in all forms of media, now or hereafter known, including display on the world wide web. I understand that I may select some access restrictions as part of the online submission of this thesis or dissertation. I retain all ownership rights to the copyright of the thesis or dissertation. I also retain the right to use in future works (such as articles or books) all or part of this thesis or dissertation.

Signature:

---

Brenda Milagros Calderon

---

Date

Non-coding RNA 886 is a novel regulator of viral dsRNA sensors

By

Brenda Milagros Calderon

Doctor of Philosophy

Graduate Division of Biological and Biomedical Science

Biochemistry, Cell and Developmental Biology

\_\_\_\_\_  
[Advisor's signature]  
Graeme L. Conn, Ph.D.  
Advisor

\_\_\_\_\_  
[Member's signature]  
Anita H. Corbett, Ph.D.  
Committee Member

\_\_\_\_\_  
[Member's signature]  
Eric A. Ortlund, Ph.D.  
Committee Member

\_\_\_\_\_  
[Member's signature]  
Daniel Reines, Ph.D.  
Committee Member

\_\_\_\_\_  
[Member's signature]  
Nicholas T. Seyfried, Ph.D.  
Committee Member

Accepted:

\_\_\_\_\_  
Lisa A. Tedesco, Ph.D.  
Dean of the James T. Laney School of Graduate Studies

\_\_\_\_\_  
Date

Non-coding RNA 886 is a novel regulator of viral dsRNA sensors

By

Brenda Milagros Calderon

B.S., University of Florida, 2011

Advisor: Graeme L. Conn, Ph.D.

An abstract of

A dissertation submitted to the Faculty of the

James T. Laney School of Graduate Studies of Emory University

in partial fulfillment of the requirements for the degree of

Doctor of Philosophy

in Biochemistry, Cell and Developmental Biology

2017

## Abstract

Non-coding RNA 886 is a novel regulator of viral dsRNA sensors

By Brenda Milagros Calderon

The innate immune response acts as a critical first line of defense against viral pathogens. Pattern recognition receptors on the cell surface and in the cytosol detect pathogen-associated molecular patterns and initiate signaling cascades to halt viral replication and establish an antiviral state. The double-stranded RNA-activated protein kinase (PKR) and the 2'-5'-oligoadenylate synthetases (OASes) sense dsRNA in the cytosol, a potent signal of viral infection, and limit viral replication through translational control. The central importance of PKR and OAS1 is highlighted by the abundance of viral strategies to inhibit their actions. The accurate discrimination of self from non-self is essential for normal cell function. Aberrant detection of self nucleic acids can lead to autoimmune disorders and improper activation of these sensors can contribute to human diseases including cancer. Thus, precise regulation of these sensors is required for proper cell function.

In this dissertation, the molecular mechanisms of PKR and OAS1 regulation by a cellular non-coding RNA, nc886, are investigated. Structural and biochemical studies reveal that nc886 adopts two stable conformations with stark differences in their functions towards PKR and OAS1. nc886 conformers differ structurally in their apical region with Conformer 1 adopting a unique tertiary structure. The presence of this structural motif confers high affinity PKR-binding and potent inhibition of PKR and its downstream activity on translation initiation factor 2. In contrast, Conformer 2 is a weak activator of PKR. Both conformers activate OAS1, but only Conformer 1 is capable of potent activation *in vitro* and in A549 cells. Functional analysis of various nc886 deletion variants reveals that PKR and OAS1 share overlapping, but distinct, requirements for nc886-mediated regulation and suggests they compete for binding. We present a model for nc886-mediated regulation of basal PKR activity in uninfected cells and propose that during infection nc886 activates OAS1 to stimulate the immune response. Finally, using growth arrest-specific 5 (Gas5), a long intergenic ncRNA, we demonstrate potential ncRNA-mediated regulation of immune sensors in response to diverse cell needs. Detailed knowledge of the cellular regulation of these sensors is essential for the development of therapeutic approaches to enhance or suppress the immune system.

Non-coding RNA 886 is a novel regulator of viral dsRNA sensors

By

Brenda Milagros Calderon

B.S., University of Florida, 2011

Advisor: Graeme L. Conn, Ph.D.

A dissertation submitted to the Faculty of the  
James T. Laney School of Graduate Studies of Emory University  
in partial fulfillment of the requirements for the degree of  
Doctor of Philosophy  
in Biochemistry, Cell and Developmental Biology

2017

## Acknowledgements

I would like to thank my mentor, Dr. Graeme L. Conn, for the support and guidance throughout my graduate career. I have grown both as a scientist and as a person in this lab. Thank you for always believing in me and for allowing me to pursue all my interests, even when they have been in completely different directions than you had in mind. Thank you for challenging me in every aspect from my experiment design to my choice in colors for manuscript figures and everything in between. I am so glad that you convinced me to join the dark side of RNA structure. It has been a joy to work with you and I am grateful for your thoughtfulness and caring.

Thank you to my committee members Drs. Anita H. Corbett, Eric A. Ortlund, Daniel Reines, and Nicholas T. Seyfried for constantly challenging me and developing me into a well-rounded scientist. I have greatly appreciated the guidance, input, and constant support during my training. You have been wonderful role models and I feel equipped to take on whatever comes next.

To all the members of the Conn lab, past and present, thank you for creating such a collaborative, supportive, and friendly environment. I have loved working in “the fun lab” and I will miss you all dearly. A special thank you to Drs. Emily Kuiper, Sunita Subramanian, and Virginia Vachon for teaching me everything I know about RNA, PKR and OAS. To Dr. Natalia Zelinskaya, thank you for being so sweet and for making sure I am as organized and thorough as any great scientist should be. To Dr. Marta Witek and Samantha Schwartz, thank you for the laughs and the friendship. To Zane Laughlin, Dr. Meisam Nosrati, and Dr. Debayan Dey thank you for continuing the spirit of the fun lab. Thank you to Dr. Christine Dunham for recruiting me to Emory and to the members of her lab for all the great discussions at our joint lab meetings.

Thank you to the members of the Corbett lab for the laughs and the cell biology guidance. Thank you to Dr. Anice Lowen, Dr. John Steel, and Shamika Danzy for the support and guidance in my ventures into cell culture.

To my friends and loved ones, thank you for being my cheerleaders on this journey. I am especially grateful for Dr. Skye Comstra, Kevin Morris, and Julia Omotade for being an endless source of love and support. I am in constant awe of what amazing humans you are. Thank you to my San Diego crew (Eduardo, Jamie, Makendra, Mfon, and Osric) for keeping me humble. It is truly a blessing to know so many talented scientists who are equally dedicated to making this world better. I am grateful for your friendship and excited to be there to celebrate all of your future successes. I also want to thank my friends back home: Vanessa, Lidice, Fiona, Linet, Jani, and Katie. Thank you for all the support even before I was a scientist and for all the phone calls and visits throughout the years. You each inspire me in different ways and keep me grounded. A heartfelt thanks to Russell Jeter, and to our two puppies Raven and Rosie, for joining me on this journey. Everything is easier with your love.

Most importantly, thank you to my mother Marisol and my late father Jose. I would not be where I am if it were not for all the sacrifices you have made. From moving, to helping me with my homework, fostering my curiosity, and ecstatically supporting every choice I have made. Words could never capture the immense love and gratitude I feel. You have both always been my role models and whom I have always looked to for support. This dissertation is dedicated to you both.

## Table of Contents

<b>Chapter 1: Introduction .....</b>	<b>1</b>
<b>1.1 The innate immune response to viral infections.....</b>	<b>1</b>
<b>1.2 Nucleic acid sensing in innate immunity.....</b>	<b>2</b>
<b>1.3 Discriminating self from non-self in innate immunity.....</b>	<b>5</b>
<b>1.4 Translational control by PKR .....</b>	<b>7</b>
1.4.1 PKR cellular function .....	7
1.4.2 Strategies viruses employ to evade activation of PKR .....	9
<b>1.5 Viral RNA degradation by the OAS/RNase L pathway .....</b>	<b>10</b>
1.5.1 OAS/RNase L cellular functions .....	10
1.5.2 Strategies viruses employ to evade the OAS/RNase L pathway .....	13
<b>1.6 Non-coding RNA 886 .....</b>	<b>14</b>
<b>1.7 Research questions addressed by this work .....</b>	<b>15</b>
<b>1.8 References.....</b>	<b>22</b>
<b>Chapter 2: Human noncoding RNA 886 (nc886) adopts two structurally distinct conformers that are functionally opposing regulators of PKR .....</b>	<b>32</b>
<b>2.1 Abstract.....</b>	<b>32</b>
<b>2.2 Introduction.....</b>	<b>33</b>
<b>2.3 Results .....</b>	<b>35</b>
2.3.1 nc886 RNA adopts two noninterconverting conformers with distinct stabilities .....	35
2.3.2 nc886 RNA conformers have opposing activities against PKR .....	37

2.3.3 Differences in apical stem-loop structure distinguish the two nc886 RNA conformers .....	38
2.3.4 The unique Conformer 1 apical stem-loop structure is critical for PKR repression .....	40
<b>2.4 Discussion .....</b>	<b>43</b>
<b>2.5 Materials and Methods.....</b>	<b>46</b>
2.5.1 RNA <i>in vitro</i> transcription and purification.....	46
2.5.2 PKR and eIF2 $\alpha$ protein expression and purification.....	47
2.5.3 RNA UV thermal melting analysis .....	48
2.5.4 Electrophoretic mobility shift assays (EMSA) .....	48
2.5.5 PKR inhibition assays .....	49
2.5.6 PKR activation assays.....	49
2.5.7 Selective 2'-hydroxyl acylation analyzed by primer extension (SHAPE).....	50
<b>2.6 Acknowledgements .....</b>	<b>51</b>
<b>2.7 References .....</b>	<b>61</b>
<b>Chapter 3: Activation of the OAS/RNase L pathway by a human cellular non-coding RNA .....</b>	<b>64</b>
<b>3.1 Abstract.....</b>	<b>64</b>
<b>3.2 Introduction.....</b>	<b>65</b>
<b>3.3 Results and Discussion.....</b>	<b>67</b>
3.3.1 OAS1 is potently activated by a single nc886 RNA conformer .....	67
3.3.2 nc886 Conformer 1 activates the OAS/RNase L pathway in human A549 cells .....	68

3.3.3 The nc886 terminal stem is dispensable for activation of OAS1.....	68
3.3.4 OAS1 activation requires an intact apical stem-loop.....	70
<b>3.4 Conclusions.....</b>	<b>71</b>
<b>3.5 Materials and Methods.....</b>	<b>72</b>
3.5.1 RNA <i>in vitro</i> transcription and purification.....	72
3.5.2 OAS1 expression and purification.....	73
3.5.3 <i>In vitro</i> chromogenic assay of OAS1 activity.....	73
3.5.4 OAS/RNase L activation in A549 cells.....	74
3.5.5 RNA UV thermal melting analysis.....	75
3.5.6 Selective 2'-hydroxyl acylation analyzed by primer extension (SHAPE).....	75
<b>3.6 Acknowledgements.....</b>	<b>76</b>
<b>3.6 References.....</b>	<b>85</b>
<b>Chapter 4: Conclusion.....</b>	<b>88</b>
<b>4.1 Structural differences in nc886 conformers have functional consequences.....</b>	<b>89</b>
<b>4.2 PKR and OAS1 interact overlapping segments of nc886 RNA.....</b>	<b>92</b>
<b>4.3 Gas5 lincRNA activates PKR.....</b>	<b>94</b>
<b>4.4 Roles for nucleic acid sensors outside of immunity.....</b>	<b>95</b>
<b>4.5 References.....</b>	<b>100</b>
<b>Appendix: Gas5 lincRNA is a novel, cellular non-coding RNA activator of PKR ..</b>	<b>102</b>
<b>A.1 Abstract.....</b>	<b>102</b>
<b>A.2 Introduction.....</b>	<b>102</b>
<b>A.3 Results.....</b>	<b>104</b>
A.3.1 Gas5 activates PKR <i>in vitro</i> .....	104

A.3.2 Gas5 induces PKR T446 phosphorylation in HEK293T cells.....	105
A.3.3 PKR recognition of Gas5 is length but not sequence dependent.....	106
<b>A.4 Discussion.....</b>	<b>106</b>
<b>A.5 Materials and Methods.....</b>	<b>108</b>
A.5.1 RNA <i>in vitro</i> transcription and purification.....	109
A.5.2 PKR protein expression and purification.....	109
A.5.3 eIF2 $\alpha$ protein expression and purification.....	109
A.5.4 PKR activation assays.....	110
A.5.5 Cell lines, transfections and immunoblotting.....	110
<b>A.6 Acknowledgements.....</b>	<b>111</b>
<b>A.7 References.....</b>	<b>116</b>

## Table of Figures

### Chapter 1

Figure 1.1 Type I Interferon (IFN) signaling cascade .....	18
Figure 1.2 RNA sensing in innate immunity .....	19
Figure 1.3 Structure and function of the double-stranded RNA-activated protein kinase (PKR).....	20
Figure 1.4 Structure and function of the 2'-5'-oligoadenylate synthetase (OAS) family.....	21

### Chapter 2

Figure 2.1 nc886 forms two distinct, noninterconverting conformers that can be isolated and characterized separately .....	52
Figure 2.2 nc886 conformer stability and refolding .....	53
Figure 2.3 The individual nc886 conformers have distinct activities against PKR .....	54
Figure 2.4 The apical stem-loop of nc886 distinguishes the two RNA conformers .....	55
Figure 2.5 Binding and inhibition of PKR by terminal stem and apical stem-loop deletion variants .....	56
Figure 2.6 Inhibition of PKR phosphorylation of eIF2 $\alpha$ substrate by wild-type and nc886 RNA variants .....	58
Figure 2.7 Alteration of loop 5 (nucleotides 44-48; nc886 $\Delta$ L5) disrupts the structure specific to nc886 Conformer 1 and abrogates PKR inhibition .....	59

### Chapter 3

Figure 3.1 Differential activation of OAS1 by the two nc886 conformers.....	77
Figure 3.2 nc886 Conformer 1 activates the OAS/RNase L pathway in human A549 cells .....	79
Figure 3.3 The apical stem-loop of nc886, but not the terminal stem, is critical for OAS1 activation .....	80
Figure 3.4 Activation of OAS1 is dependent on an intact apical stem of nc886 RNA.....	81
Figure 3.5 Model for coordinated nc886-mediated regulation of the viral dsRNA sensors PKR and OAS.....	82
Figure 3.6 SHAPE probing of nc886 variants .....	83

### Chapter 4

Figure 4.1 Model for coordinated nc886-mediated regulation of the viral dsRNA sensors PKR and OAS.....	97
Figure 4.2 PKR is activated by a variety of Gas5 secondary structures.....	98
Figure 4.3 PKR regulation by cellular RNAs with varied structures .....	99

### Appendix

Figure A.1 Gas5 activates PKR <i>in vitro</i> .....	112
Figure A.2 Gas5 activates PKR in HEK293T cells .....	113
Figure A.3 Gas5 deletion variants retain PKR activity <i>in vitro</i> in a length- dependent manner .....	114

## **Table of Tables**

### **Chapter 2**

<b>Table 2.1 Apparent melting temperatures (<math>T_m</math>) for wild-type and variant nc886 unfolding .....</b>	<b>60</b>
---	-----------

### **Chapter 3**

<b>Table 3.1 Apparent melting temperatures (<math>T_m</math>) for wild-type and variant nc886 unfolding .....</b>	<b>84</b>
---	-----------

## **Abbreviations**

2-5A, 2'-5'-oligoadenylate

3'-ssPy, 3'-single-stranded pyrimidine motif

ADAR1, Adenosine deaminase acting on RNA 1

AGS, Aicardi-Goutieres syndrome

AIM2, Absent in melanoma 2

ANK, Ankyrin

AS, Apical stem

AMP, Adenosine monophosphate

ATP, Adenosine triphosphate

cGAMP, 2'-5'-cyclic guanosine monophosphate-adenosine monophosphate

cGAS, cyclic GMP-AMP synthase

DNA, Deoxyribonucleic acid

DNase, Deoxyribonuclease

dsDNA, Double-stranded DNA

dsRBD, Double-stranded RNA-binding domain

dsRBM, Double-stranded RNA-binding motif

dsRNA, Double-stranded RNA

eIF2 $\alpha$ , eukaryotic translation initiation factor 2 alpha subunit

EMSA, Electrophoretic mobility shift assay

Gas5, Growth arrest-specific 5

GCN2, General control non-derepressible protein 2

GDP, Guanosine monophosphate

GTP, Guanosine triphosphate

HDV, Hepatitis delta virus

HRI, Heme-regulated inhibitor

IFN, Interferon

IFNAR, Interferon-alpha/beta receptor

IL-1 $\beta$ , Interleukin-1 beta

IPTG, Isopropyl  $\beta$ -D-1-thiogalactopyranoside

IRF, Interferon regulatory factor

ISG, Interferon-stimulated gene

ISRE, Interferon-stimulated response element

JAK, Janus kinase

LGP2, Laboratory of genetics and physiology 2

lincRNA, long intergenic non-coding RNA

MAVS, Mitochondrial antiviral signaling protein

MDA5, Melanoma differentiation-associated gene 5

Met-tRNA<sup>i</sup>, Methionyl initiator tRNA

mRNA, messenger RNA

MYD88, Myeloid differentiation primary response protein 88

nc886, non-coding RNA 886

ncRNA, non-coding RNA

NF- $\kappa$ B, Nuclear factor kappa-light-chain enhancer of activated B cells

NMIA, N-methylisatoic anhydride

OAS, 2'-5'-oligoadenylate synthetase

OASL, OAS-like protein

PACT, Protein interferon-inducible double-stranded RNA-dependent protein kinase  
activator A

PAGE, Polyacrylamide gel electrophoresis

PAMP, Pathogen-associated molecular pattern

PERK, PKR-like endoplasmic reticulum kinase

PKR, Double-stranded RNA-activated protein kinase

PPi, Pyrophosphate

PRR, Pattern recognition receptor

RIG-I, Retinoic acid-inducible gene I

RNA, Ribonucleic acid

RNase L, Ribonuclease L

rRNA, ribosomal RNA

RT, Reverse transcription

SHAPE, 2'-hydroxyl acylation analyzed by primer extension

siRNA, small interfering RNA

ssRNA, single-stranded RNA

STAT, Signal transducer and activator of transcription

STING, Stimulator of interferon genes

TBE, Tris-Borate-EDTA

TE, Tris-EDTA

TLR, Toll-like receptor

TNF, Tumor necrosis factor

TRAF, Tumor necrosis factor receptor-associated factors

tRNA, transfer RNA

TS, Terminal stem

TYK2, Tyrosine kinase 2

## Chapter 1

### Introduction

#### 1.1 The innate immune response to viral infections

The innate immune system acts as the first line of defense against invading pathogens and is crucial for host survival. Unlike adaptive immunity, this system confers resistance to a broad set of pathogens and acts during initial exposure. Pattern recognition receptors (PRRs) on the cell surface and in the cytosol of immune and non-immune cells recognize pathogen-associated molecular patterns (PAMPs), such as viral coat proteins and nucleic acids. Upon activation, these receptors initiate signaling cascades that ultimately limit viral replication and prime neighboring cells to respond similarly by inducing a heightened antiviral state.

A key function of cellular PRRs is to induce the production of Type I Interferon (IFN), a family of cytokines that are secreted and can act in an autocrine or paracrine manner (1-3). IFNs are classified by the receptor complex to which they bind but all signal through the Janus kinase-signal transducer and activator of transcription (JAK-STAT) signaling pathway (4). Type I IFN is the largest class of IFNs and nearly every cell type can produce two members, IFN- $\alpha$  and IFN- $\beta$ . Type I IFNs bind to the IFN-alpha/beta receptor 1 and 2 (IFNAR1/2) at the cell surface (Figure 1.1). The intracellular domains of these receptors are normally bound by the tyrosine kinases Janus kinase 1 (JAK1) and tyrosine kinase 2 (TYK2) in an inactive conformation (5). IFN binding-induced conformational changes bring the cytoplasmic chains into close proximity

facilitating the transphosphorylation and activation of JAK1 and TYK2 (6). The activated kinases phosphorylate IFNAR1/2 on cytoplasmic tyrosine residues, promoting recruitment of the STAT proteins STAT1 and STAT2 via Src homology 2 domain interactions (7-9). STATs are subsequently phosphorylated and released from the receptor (9, 10). Phosphorylation stimulates STAT1/2 heterodimerization and recruitment of IFN regulatory factor 9 (IRF-9) (11). This trimeric complex is then translocated to the nucleus where it binds to DNA at IFN-stimulated response elements (ISRE) upstream of IFN-stimulated genes (ISGs), leading to the expression of thousands of genes with diverse antiviral effector functions (12-14). Proteins encoded by ISGs protect cells against viral infection by limiting virus entry, replication, and assembly through direct activity on viral components or through inhibition of core cellular processes (15). Type I IFNs can also initiate the process of adaptive immunity through recruitment of immune cells to the site of infection (16).

## **1.2 Nucleic acid sensing in innate immunity**

Viruses propagate inside host cells, thus making nucleic acids an important PAMP and nucleic acid sensing the dominant antiviral defense pathway in vertebrates (17, 18). Many PRRs in innate immunity detect foreign nucleic acids in endosomes and in the cytosol with some redundancy in their nucleic acid recognition and downstream signaling pathways. These nucleic acid sensing receptors fall into two categories: receptors that directly or indirectly induce immune responses through transcription factors and cytokines, and receptors that have direct antiviral activities.

The receptors stimulated by nucleic acids to induce downstream innate immune

responses consist of the family of Toll-like receptors (TLR) including TLR3, TLR7, TLR8, and TLR9; absent in melanoma 2 (AIM2); the cyclic GMP-AMP synthase (cGAS); and the RIG-I like receptors including retinoic acid-inducible gene I (RIG-I), melanoma differentiation-associated gene 5 (MDA5), and laboratory of genetics and physiology 2 (LGP2). DNA in the endosomes of immune cells is detected by TLR9, which recognizes unmethylated CpG motifs, resulting in TLR9 dimerization and activation (19-21). Active TLR9 induces Type I IFN through recruitment of the adaptor protein myeloid differentiation primary response protein 88 (MYD88) and the transcription factor IFN regulatory factor 7 (IRF-7) (22). DNA, which is not normally found in the cytosol and is thus a potent indicator of infection, is detected by AIM2 and cGAS. AIM2 senses cytoplasmic dsDNA through its hematopoietic interferon-inducible nuclear antigens with a 200-amino-acid repeat (HIN) domain and interacts with the adaptor molecule apoptosis-associated speck-like protein containing a Caspase activation and recruitment domain (CARD) (ASC) through its pyrin domain (23-25). The AIM2-ASC complex drives formation of inflammasomes and recruits caspase-1, resulting in the release of the pro-inflammatory cytokine interleukin-1 beta (IL-1 $\beta$ ) (26, 27). cGAS on the other hand, synthesizes 2'-5'-cyclic guanosine monophosphate-adenosine monophosphate (cGAMP) in response to dsDNA (28-30). This second messenger then activates the mitochondrial adaptor protein stimulator of interferon genes (STING) leading to production of Type I IFN through the transcription factor IRF-3 (31-33).

While DNA sensing is an important component of innate immunity, detection of RNA, and specifically double-stranded RNA (dsRNA), is crucial (Figure 1.2). dsRNA is produced as a consequence of RNA virus genome replication, transcription from RNA

viruses, overlapping convergent transcription from DNA viruses, or secondary structures formed by viral RNA or RNA virus genomes. dsRNA thus serves as a PAMP for detecting both DNA and RNA viruses. In the endosomes of immune cells, dsRNA and ssRNA is detected by TLR3 and TLR7/TLR8, respectively, and these receptors induce production of Type I IFN and IL-1 $\beta$  through pathways shared with TLR9 (34-37). In the cytosol, dsRNA is detected by the RNA helicases RIG-I, MDA5, and LGP2. In response to dsRNA, RIG-I and MDA5 activate their shared signaling adaptor molecule, the mitochondrial antiviral signaling protein (MAVS), through interaction of CARD domains on each protein (38, 39). LGP2 also activates MAVS in response to dsRNA, despite lacking a CARD domain, through interactions with MDA5 (40, 41). Activation of MAVS recruits tumor necrosis factor (TNF) receptor-associated factors (TRAF) 2, 5 and 6, and leads to production of Type I IFN through activation of IRF-3/IRF-7, and can also induce apoptosis through activation of caspase-8 (40-44).

The second class of nucleic acid sensing receptors possesses direct antiviral activities, although they may also induce immune responses indirectly. These include the adenosine deaminase acting on RNA 1 (ADAR1), the double-stranded RNA-activated protein kinase (PKR), and the 2'-5'-oligoadenylate synthetase family of enzymes (OAS) of the OAS/ ribonuclease L (RNase L) pathway. These receptors detect cytosolic dsRNA, a potent signal of viral infection, and act directly on the RNA to prevent viral replication. ADAR1 binds to dsRNA and catalyzes the conversion of adenosine to inosine through a deamination reaction, thus disrupting normal A:U pairing and causing destabilization of the RNA (45-49). The RNA editing function of ADAR1 can be both antiviral by inhibiting viral replication and pro-viral by reducing recognition of long dsRNA by other

dsRNA sensors (50). PKR and OAS are also activated by dsRNA-binding and halt viral replication through distinct translational control mechanisms (51). As described further in Section 1.4, PKR is a kinase that targets the translation initiation factor 2 alpha subunit (eIF2 $\alpha$ ), halting protein synthesis through a block in translation initiation (52-56). OAS, on the other hand, inhibits viral protein synthesis by activating RNase L to degrade viral RNA (57-61), as described in more detail in Section 1.5.

### **1.3 Discriminating self from non-self in innate immunity**

Nucleic acid sensors play a critical role in the detection of viral infection and must be broad in order to detect nucleic acids from a diverse range of viral pathogens. However, they must also be sufficiently specialized to avoid the incorrect detection of host cellular nucleic acids as foreign. This is achieved by exploiting both the aberrant location of nucleic acids and the absence of features present in nucleic acids of cellular origins (62, 63). The aberrant presence of DNA in endosomes or in the cytoplasm is a potent signal of infection and is detected by TLR9, and AIM2/cGAS, respectively. Furthermore, DNA modifications such as CpG methylation can be used to distinguish host DNA from bacterial and viral DNA (27). Long stretches of dsRNA are not typically found in cellular RNAs and can thus signal infection when detected in endosomes or in the cytoplasm by TLR3, MDA5, and PKR. As cellular RNAs are transcribed and processed in the nucleus, unprocessed RNA features can distinguish viral RNAs from host cell nucleic acids. These features can include a 5'-triphosphate that in cellular mRNAs is replaced with a 7-methylguanosine cap, modifications such as methylation of the 2'-hydroxyl groups of the ribose sugar, and incorporation of modified nucleosides such as

pseudouridine (64). RIG-I, for example, detects dsRNA with 5' di- and triphosphates and capped dsRNA lacking 2'-O-methylation (44, 65). Modifications such as ribose 2'-O-methylation and incorporation of modified nucleosides abrogate the ability of dsRNA to activate sensors such as TLRs, RIG-I, and PKR (66-70). However, some viruses express cap analogues, such as the VPg protein that is covalently linked to the 5'-end of viral RNA in a number of RNA viruses, while others acquire their 5' caps through "cap snatching" from host nuclear mRNAs. Alternatively, some viruses encode their own phosphatases to remove the 5'-triphosphate or methyltransferases to directly alter their RNAs to appear more host-like (71, 72).

Recently, the RNA editing function of ADAR1 was shown to be crucial in preventing self-dsRNA recognition (73). ADAR1 deletion in uninfected cells was shown to be lethal but could be rescued by the additional deletion of RNase L, the ribonuclease that degrades cellular and viral RNA in response to activation by the dsRNA sensor OAS (73, 74). ADAR1 is thus required to edit and destabilize otherwise activating cellular dsRNA. Loss of this protein results in accumulation of self-dsRNA that is recognized by OAS leading to the production of 2'-5'-oligoadenylate (2-5A) second messengers, RNase L activation, rRNA cleavage, and cell death, all in the absence of exogenous dsRNA (73). Mutations in the *ADAR1* gene have also been previously shown to cause the autoimmune disorder Aicardi-Goutieres syndrome (AGS) and to mirror *Adar1* mouse gene knockout (75). Taken together, these data suggest that ADAR1 limits the cytoplasmic accumulation of dsRNA and thus prevents recognition of endogenous RNA by nucleic acid sensors of the innate immune response. Accumulation of self-DNA and self-DNA/RNA hybrids have already been implicated in autoimmune disorders such as AGS, due to loss of

proteins, such as the DNase TREX1 and the RNase H2, that clear these species and prevent them from activating the innate immune response (76, 77). These findings highlight the critical role nucleic acid sensors play in the accurate detection of viruses and also demonstrate how aberrant function of these sensors can cause or contribute to autoimmune disorders. Finally, these findings emphasize that endogenous nucleic acids are not so different from those of viral origins, instead, host cells have a multitude of factors working together to mask activating features and the precise regulation of these factors is crucial for proper cell function.

## **1.4 Translational control by PKR**

### **1.4.1 PKR cellular function**

PKR is a member of the eIF2 $\alpha$  kinase family that also consists of PKR-like endoplasmic reticulum kinase (PERK), general control non-derepressible protein 2 (GCN2), and heme-regulated inhibitor (HRI). Members of this family respond to different stimuli and halt general translation through phosphorylation of eIF2 $\alpha$  as part of the integrated stress response (78). PKR is ubiquitously expressed in human cells, although its expression is also stimulated by IFN. PKR is a 551 amino acid protein that contains an N-terminal dsRNA-binding domain (dsRBD) composed of tandem dsRNA-binding motifs (dsRBMs) and a C-terminal kinase domain (Figure 1.3A). PKR activation occurs through RNA-mediated dimerization and autophosphorylation (79-82) (Figure 1.3B). RNA recognition is primarily conferred by the dsRBMs, which interact with the 2'-hydroxyl group in the minor groove of A-form helix dsRNA, thus making RNA recognition by PKR sequence-independent (81, 83). PKR dimerization is low-affinity thus binding to dsRNA via the

dsRBDs on separate PKR monomers promotes PKR dimerization and autophosphorylation (80, 84). This places a minimum length requirement of 30 bp of dsRNA for activation (85). RNA-mediated dimerization leads to the critical autophosphorylation of Threonine 446 in the activation loop of the kinase, although other Serine/Threonine residues in the protein can also be phosphorylated (86). Activated PKR can then phosphorylate its cellular target eIF2 $\alpha$  on Serine 51 (87, 88). eIF2 is composed of the three subunits  $\alpha$ ,  $\beta$  and  $\gamma$  and functions in translation initiation by binding to methionyl initiator tRNA (Met-tRNA<sub>i</sub>) in a GTP-dependent manner to form a ternary preinitiation complex that delivers the Met-tRNA<sub>i</sub> to the small 40S ribosomal subunit (89). Phosphorylated eIF2 $\alpha$  has greater affinity for its guanine nucleotide exchange factor eIF2B than unphosphorylated eIF2 $\alpha$ . Due to the relatively low abundance of eIF2B, this non-productive sequestering of eIF2B effectively halts GDP/GTP recycling on eIF2 $\alpha$  and results in inhibition of general translation (90) (Figure 1.3C). However, this process allows for the specific translation of stress response genes, which are normally not translated due to the presence of upstream open reading frames (uORF): at high levels of phosphorylated eIF2 $\alpha$  many ribosomal subunits fail to initiate at the uORFS and thus can scan to reach the real start codons (91, 92). PKR activation thus allows for inhibition of viral protein synthesis while allowing the cell to recover through initiation of the integrated stress response. Continued stimulation of PKR eventually leads to cell death due to the enhanced expression of the pro-apoptotic C/EBP homologous protein (CHOP) (93).

In addition to viral dsRNA activation of PKR during infection, specific cellular RNAs and proteins can also activate the kinase, including interferon-gamma (IFN- $\gamma$ )

mRNA, cytoskeletal mRNAs, Inverted Alu repeat-containing RNAs, and the protein interferon-inducible double-stranded RNA-dependent protein kinase activator A (PACT) (94-97). This endogenous PKR activation is a result of the many roles PKR plays outside of innate immunity including regulation of gene expression, cell differentiation, cell proliferation, and other stress responses (98). Thus, tight regulation of PKR activity is required to regulate these cellular activities and achieve accurate detection of foreign nucleic acids while preventing spurious activation that would be deleterious to the cell.

#### **1.4.2 Strategies viruses employ to evade activation of PKR**

PKR's critical role in innate immunity is highlighted by the abundance of viral encoded genes targeting every step of PKR function. These include proteins that bind to dsRNA and prevent detection by PKR including the NS1 protein produced by Influenza A virus, US11 produced by Herpes Simplex virus, E3L produced by Vaccinia virus, VP35 produced by Ebola virus, TRS1 produced by human cytomegalovirus, and the sigma 3 outer capsid protein of reoviruses (99-104). Another distinct mechanism involves the production of competitive inhibitors of PKR such as the viral non-coding RNAs VA RNA<sub>I</sub>/VA RNA<sub>II</sub> and EBER-1 produced by Adenovirus and Epstein-Barr virus, respectively. These small viral non-coding RNAs bind to PKR with high-affinity (mid-nanomolar range for VA RNA<sub>I</sub> and EBER-1) and prevent PKR dimerization thus sequestering the protein and preventing it from binding other viral dsRNA (105-108). While activating dsRNA also binds PKR with nanomolar affinity, autophosphorylation of PKR reduces its affinity for RNA, thus allowing for the release of RNA after kinase phosphorylation (109). There are also several viral proteins that bind to PKR and prevent

it from binding to and phosphorylating its cellular target eIF2 $\alpha$ . Vaccinia virus produces the K3L protein, which shares homology with eIF2 $\alpha$  and thus acts as a pseudosubstrate for PKR (110, 111). Similarly, Hepatitis C virus encodes a nonstructural protein, NS5A, that binds to PKR and prevents dimerization, and an envelope protein, E2, that contains a sequence identical to the phosphorylation site on eIF2 $\alpha$  thus allowing it to bind to and inhibit PKR activity (112, 113). Furthermore, some viral factors can induce the dephosphorylation of eIF2 $\alpha$  through recruitment of the cellular protein phosphatase 1 $\alpha$  (PP1 $\alpha$ ). These include the E6 protein produced by Human Papilloma virus which associates with the GADD34/PP1 $\alpha$  holophosphatase complex, and IC-34.5 produced by Herpes Simplex virus which is homologous to GADD34 and directly binds PP1 $\alpha$  (114, 115). Some viruses can even induce PKR degradation, including Rift Valley virus which uses its non-structural proteins to bind the host F-box protein FBXW11, leading to assembly of Cullin-RING E3 ligases that target PKR for ubiquitination and subsequent proteosomal degradation (116). Moreover, some viruses can bypass the PKR/eIF2 $\alpha$  pathway activation altogether. For example, Sindbis virus uses a hairpin loop structure in its viral 26S mRNA to initiate translation on the 40S ribosome in the absence of eIF2 (117). Poliovirus is also able to switch to an eIF2-independent mechanism of translation which uses a cleavage fragment of eIF5B produced by the viral 3C proteinase (118). Through this variety of mechanisms, viruses can neutralize PKR antiviral activity and thus continue to replicate.

## **1.5 Viral RNA degradation by the OAS/RNase L pathway**

### **1.5.1 OAS/RNase L cellular functions**

The OAS family of enzymes are nucleotidyl transferases that catalyze the synthesis of 2'-5'-linked oligoadenylate (2-5A) from adenosine triphosphate (ATP) (119). This family consists of four Type I IFN-inducible genes: the catalytically active OAS1, OAS2, OAS3, and the catalytically inactive OAS-like protein (OASL) (120) (Figure 1.4A). These genes in humans are expressed as the isoforms p42/p46 for OAS1, p69/p70 for OAS2, and p100 for OAS3 (121). OAS1, OAS2, and OAS3 differ by the number of OAS units, polymerase beta-like nucleotidyl transferase domains, present in each protein. However, in each protein only the C-terminal OAS unit is catalytically active (122, 123). OASL exists as a single isoform p59 and contains two ubiquitin-like (UBL) domains, in addition to a catalytically inactive OAS domain (124) (Figure 1.4A).

Unlike other dsRNA-binding proteins, the OAS proteins do not possess dsRNA-binding domains or other recognizable RNA recognition motifs. Instead, OAS proteins interact with dsRNA through patches of positive residues on the protein surface, and the presence of additional domains in OAS2 and OAS3 confer specificity for longer dsRNA (58, 125). The crystal structure of human OAS1 bound to dsRNA revealed that OAS1 contains two dsRNA-binding sites that recognize two adjacent minor grooves, making the minimum dsRNA length requirement 17 bp. (58). Small-angle X-ray scattering analysis of human OAS3 suggested that OAS3 adopts a non-spherical, elongated shape (126). The crystal structure and biochemical analyses of the human OAS3 catalytically-inactive domain I, demonstrated that this domain serves as an essential dsRNA-binding module, and thus places a minimum length requirement of 50 bp of dsRNA for OAS3 due to the placement of its RNA-binding and catalytic domains at opposite ends of the protein (58, 127). While nucleic acid sensors recognize dsRNA in a sequence-independent manner,

OAS1 has been shown to recognize a consensus sequence motif (WWN<sub>9</sub>WG; where W is A or U) (128). This sequence strongly promotes OAS1 activation by short RNAs and is present in viral RNA activators of OAS1, including the Adenovirus non-coding RNAs VA RNA<sub>I</sub> and VA RNA<sub>II</sub> (129). The structure of OAS1 in complex with an 18 bp dsRNA containing a consensus sequence motif revealed a single direct contact between OAS1 and dsRNA, made to the G residue of the WWN<sub>9</sub>WG motif (58). Another recently identified RNA feature important for OAS1 activation is the 3'-single-stranded pyrimidine motif (3'-ssPy), which dramatically affects the level of OAS1 activation in simple duplex dsRNA and in the viral non-coding RNAs VA RNA<sub>I</sub> and EBER-1 (130).

Activation of OAS1, OAS2, and OAS3 is mediated by dsRNA-binding, although the mechanistic details are only known for OAS1 and OAS3. In OAS1, binding of dsRNA induces a conformational rearrangement in the N-terminal lobe that brings residues D75, D77, and D148 into proximity to coordinate binding of two Mg<sup>2+</sup> ions and ATP (58) (Figure 1.4B, inset). This results in a more than 20,000-fold increase in 2-5A synthesis activity in response to dsRNA-binding (58). The 2-5A in turn serves as a second messenger for the ubiquitously expressed, and Type 1 IFN-stimulated, latent ribonuclease RNase L, inducing dimerization and subsequent activation (131, 132). Specifically, 2-5A interacts with the ankyrin (ANK) domain repeats 1-4 on one RNase L monomer and ANK domain repeat 9 of another RNase L monomer, thus facilitating dimerization (57, 132) (Figure 1.4B). Active RNase L cleaves single-stranded loops within double-stranded RNA and, in addition to cleaving viral RNA, can also cleave cellular RNAs including ribosomal RNA (rRNA) and specific messenger RNA (mRNA) transcripts involved in cell proliferation and adhesion (133-135). Activation of the

OAS/RNase L pathway establishes an antiviral state in several ways including inhibition of protein synthesis by degradation of viral RNA, cleavage of specific mRNAs resulting in an anti-proliferative state, and the degradation of rRNA leading to ribosome stalling, and eventually apoptosis (74, 133) (Figure 1.4B). Furthermore, RNase L cleavage products can further elicit induction of Type 1 IFN by serving as activating RNAs for the sensors RIG-I and MDA5 (136, 137). OASL, while catalytically inactive, still binds dsRNA and exerts antiviral activity through an interaction with RIG-I that results in IFN production (138, 139).

### **1.5.2 Strategies viruses employ to evade the OAS/RNase L pathway**

For efficient replication, viruses must employ mechanisms to halt OAS/RNase L function in the host cell. The same viral dsRNA-binding proteins used to sequester activating nucleic acids away from PKR are used against OAS. Such strategies include the NS1 protein produced by Influenza A virus, US11 produced by Herpes Simplex virus, E3L produced by Vaccinia virus, VP35 produced by Ebola virus, TRS1 produced by human cytomegalovirus, and the sigma 3 outer capsid protein of reoviruses (99-104). Viruses also produce proteins that bind to OAS1 thus competing with dsRNA for binding, such as the Hepatitis C virus non-structural protein NS5A that binds to OAS at a site distinct from its PKR-binding domain (140). As noted above, activation of RNase L is mediated by 2-5A-induced dimerization. Thus, RNase L activity can be inhibited by the degradation of 2-5A by viral phosphodiesterases that degrade this second messenger into ATP and AMP (141). Such phosphodiesterases include mouse Hepatitis virus protein NS2 and rotavirus encoded core protein VP3 (142, 143). Furthermore, some viruses

encode 2-5A analogs that compete for RNase L binding. For example, HSV-1 and HSV-2 produce viral 2-5A analogs that bind and very weakly activate RNase L, thus leading to a significant decrease in RNase L-mediated RNA cleavage (144). Simian virus 40 and Vaccinia virus also produce analogs of 2-5A, but the structural details and mechanism of action of these molecules are unknown (145, 146). Some viruses also encode proteins that bind directly to RNase L and inhibit activity, such as the L\* accessory protein encoded by Theiler's murine encephalomyelitis (TMEV) (147). Additionally, some viruses can bypass the OAS/RNase L pathway activation altogether such as poliovirus which contains a highly structured hairpin in its 3C protein coding region that is RNase L cleavage resistant thus allowing it to persist despite activation of this pathway in cells (148).

### **1.6 Non-coding RNA 886**

The cellular non-coding RNA 886 (nc886) is a 101 nucleotide RNA Polymerase III transcript that is ubiquitously expressed in human cells (149-152). While nc886 is expressed to high levels in the cytoplasm of normal cells and tissues, its expression was found to be downregulated in small-cell lung carcinoma and this loss correlated with increased PKR activity as measured by PKR and eIF2 $\alpha$  phosphorylation (149). While PKR functions in an anti-proliferative manner during infection through translation inhibition, activation of PKR in other cell contexts can lead to the activation of NF- $\kappa$ B, thus functioning in a proliferative manner (153, 154). nc886 expression was further shown to be downregulated or absent in many other types of cancers (155). Specifically, epigenetic silencing of nc886 expression by CpG DNA methylation at the gene promoter

was observed in esophageal squamous-cell carcinoma, small-cell lung cancer, gastric cancer, and acute myeloid leukemia (156-158). Furthermore, knockdown of nc886 RNA in non-cancer derived cells using small interfering RNAs (siRNA) led to the phosphorylation of PKR in the absence of exogenous RNA, suggesting a potential role for nc886 as a negative regulator of basal PKR activity (159). Downstream activation of NF- $\kappa$ B was also observed in response to deletion of nc886 (156). Importantly, these data support the existence of unknown cellular activators of PKR, further highlighting the need for tight regulation of PKR activity for proper cell function. PKR and nc886 were shown to interact through complementary *in vitro* immunoprecipitation assays using cell extracts and pull down with PKR or pull down with biotinylated nc886 RNA (149). The interaction between nc886 and PKR was further probed using purified components and electrophoretic mobility shift assays (EMSA). While direct binding was clearly established, analysis of these data were complicated by the observation that nc886 adopted two different conformers which could be seen as separate bands by native polyacrylamide gel electrophoresis (PAGE) (160). Despite this limitation, however, all subsequent investigations were carried out using a mixture of the conformers and thus failed to clearly define the contributions of each. The lack of structural details of these two forms of nc886 and any potential functional differences between them therefore represent a big gap in our understanding of nc886-mediated PKR regulation.

### **1.7 Research questions addressed by this work**

While the role of nc886 in the cellular regulation of PKR activity was investigated in cells, this work centered on the role PKR plays in cell proliferation and focused

specifically on cancer cells (156-159, 161, 162). None of the studies addressed how nc886-mediated PKR regulation affects its main role as a nucleic acid sensor in innate immunity. Furthermore, published studies on the interaction between nc886 and PKR used a mixture of nc886 conformers without addressing if they were functionally equivalent. We set out to isolate and separately dissect the nc886 conformers for their function towards PKR. We approach this work first through the isolation of nc886 conformers by native PAGE purification and the determination of their secondary structures using chemical probing methods. In Chapter 2, we define the structural identities of the two forms of nc886 and the functional consequences of these differences towards PKR. We find that not only are these forms not functionally equivalent, they actually have opposing functions towards PKR. In Chapter 3, we address the question of whether nc886 can also regulate OAS1 activity as many of the RNAs that interact with PKR and OAS1 are shared. To our surprise, one nc886 conformer potently activates OAS1 both *in vitro* and in human A549 cells. This raises the question of why nc886 would regulate PKR and OAS1 in opposing manners. We propose a model where nc886 can mediate cross talk between these two arms of the innate immune response, discussed in Chapter 4. In uninfected cells nc886 binds to and inhibits basal PKR activity, which is supported by the current literature. During infection, displacement of nc886 by viral dsRNA would allow it to be free to bind to and activate OAS1, resulting in an amplified immune response. We expand our studies of cellular non-coding RNA-mediated regulation of innate immune sensors in Appendix 1 to include a long intergenic non-coding RNA (lincRNA), growth arrest-specific 5 (Gas5), and demonstrate its ability to activate PKR *in vitro* and in HEK293T cells. Gas5-mediated PKR activation supports the

idea that other non-coding RNAs may regulate these dsRNA sensors for specific cellular needs. This work highlights the expanding roles for non-coding RNAs in various cell functions and illustrates the importance of RNA structures to these functions.

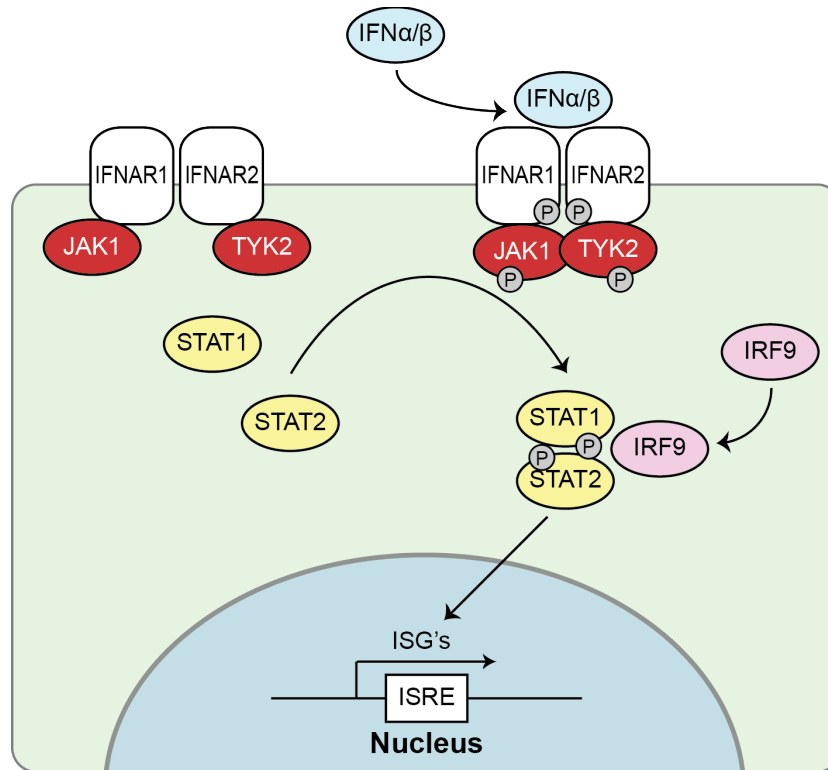


**Figure 1.1 Type I Interferon (IFN) signaling cascade.** Type I IFNs signal through IFN-alpha/beta receptors 1 and 2 (IFNAR1/2). Binding of IFN to these receptors induces conformational changes that trigger the transphosphorylation of pre-associated Janus Kinase 1 (JAK1) and Tyrosine Kinase 2 (TYK2). These activated kinases then phosphorylate tyrosine residues on the receptors leading to the recruitment of the signal transducers and activators of transcription 1 and 2 (STAT1/2), which are also phosphorylated by the tyrosine kinases. Phosphorylated STATs are released and form heterodimers that recruit IFN regulatory factor 9 (IRF-9). This trimeric complex can translocate to the nucleus and induce genes that are under the control of IFN-stimulated response elements (ISRE).

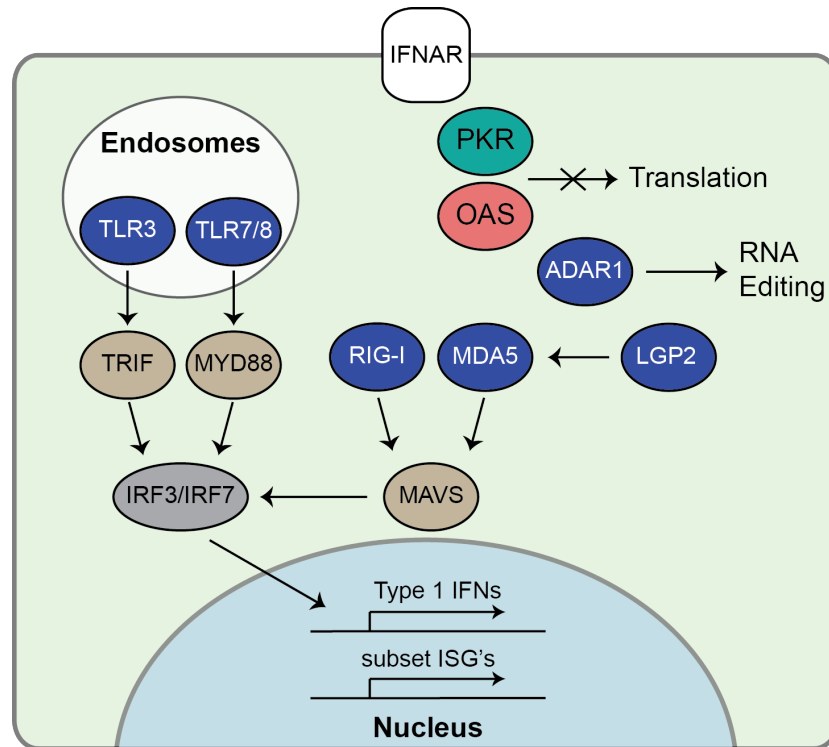


**Figure 1.2 RNA sensing in innate immunity.** RNA in the endosomes is detected by the Toll-like receptors (TLR) 2, 7 and 8. RNA in the cytoplasm is detected by retinoic acid-inducible gene 1 (RIG-I), melanoma differentiation-associated gene 5 (MDA5), laboratory of genetics and physiology 2 (LGP2), adenosine deaminase acting on RNA 1 (ADAR1), dsRNA-activated protein kinase (PKR), and 2'-5'-oligoadenylate synthetase (OAS). These sensors can induce Type I IFN and a subset of ISGs directly or indirectly through shared adaptor proteins such as TIR-domain-containing adapter-inducing interferon beta (TRIF), myeloid differentiation primary response protein 88 (MYD88), and mitochondrial antiviral signaling protein (MAVS), which in turn activate the transcription factors IFN-regulatory factors 3 and 7 (IFR3/7). PKR, OAS and ADAR1, however, directly act on viral RNAs to inhibit viral replication through translational control or RNA editing.

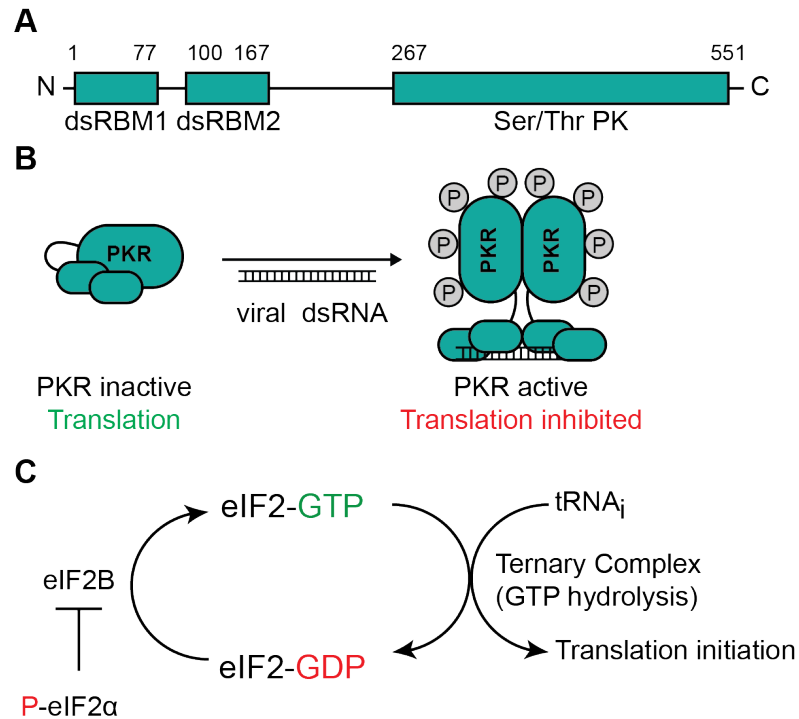


**Figure 1.3 Structure and function of the double-stranded RNA-activated protein**

**kinase (PKR).** A. Human PKR is a 551 amino acid protein kinase composed of tandem

N-terminal dsRNA-binding motifs (dsRBM) and a C-terminal Serine/Threonine Protein

Kinase (Ser/Thr PK) domain. B. PKR has low self-affinity in the absence of dsRNA and

remains inactive in uninfected cells allowing for general translation. During viral

infection, binding of viral dsRNA induces PKR dimerization and autophosphorylation

yielding the active enzyme that can inhibit general translation through the

phosphorylation of the eukaryotic translation initiation factor 2 (eIF2)  $\alpha$  subunit. C. eIF2

functions in translation initiation by binding to Met-tRNA<sub>i</sub> in a GTP-dependent manner.

After GTP hydrolysis, eIF2-GDP can be recycled through the action of its guanine

nucleotide exchange factor eIF2B. Phosphorylation of eIF2  $\alpha$  increases the affinity for

eIF2B, which sequesters eIF2B and prevents recycling, thus blocking general translation.

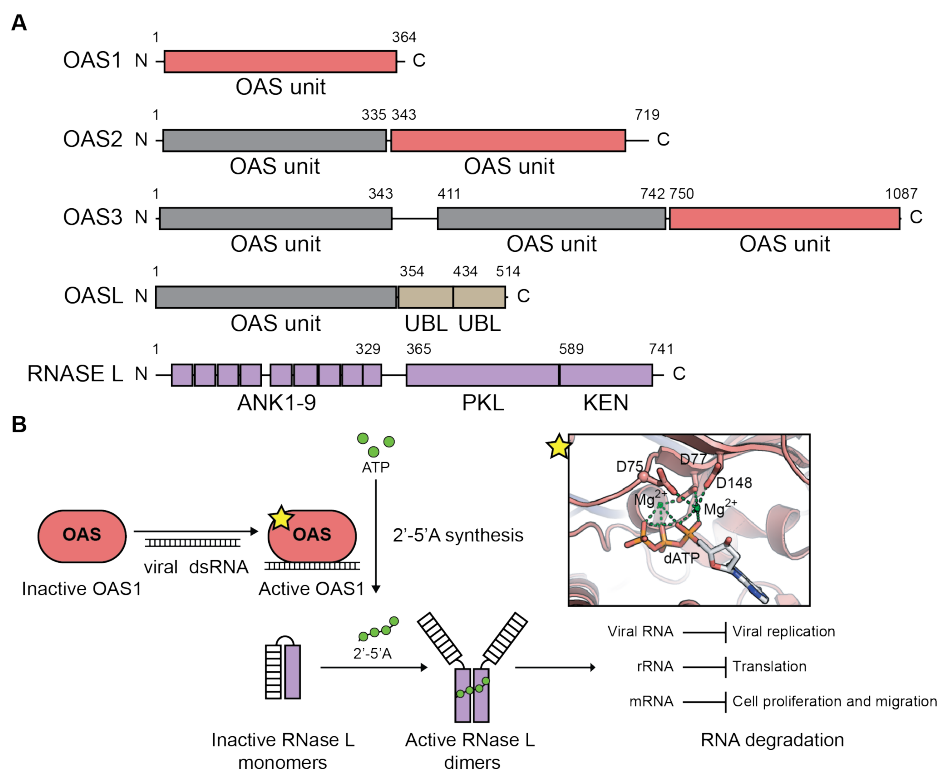


### Figure 1.4 Structure and function of the 2'-5'-oligoadenylate synthetase (OAS)

**family.** A. The human OAS family consists of three catalytically active enzymes (OAS1-3) that differ in the number of OAS units, and a catalytically inactive OAS-like (OASL) protein. Only the C-terminal OAS unit is active in each enzyme (shown in salmon); inactive OAS domains are shown in gray. The latent ribonuclease (RNase L) acts downstream of OAS1-3. The N-terminus of RNase L consists of 9 ankaryin (ANK) repeats which bind the 2'-5'-oligoadenylate (2-5A) synthesized by OAS and its C-terminus contains a catalytically inactive Protein Kinase (PKL) domain and a ribonuclease KEN domain. B. OAS is activated by dsRNA-binding, which induces a conformational rearrangement and brings residues D75, D77 and D148 into proximity to form the catalytic triad to coordinate two Mg ions and ATP (PDB= 4IG8). Active OAS synthesizes 2-5A second messengers from ATP, which induce RNase L dimerization and activation. RNase L degrades viral and cellular RNA to block viral replication.

## 1.8 References

1. Isaacs A & Lindenmann J (1957) Virus Interference. I. The Interferon. *Proceedings of the Royal Society of London. Series B - Biological Sciences* 147(927):258.
2. Isaacs A, Lindenmann J, & Valentine RC (1957) Virus interference. II. Some properties of interferon. *Proceedings of the Royal Society of London. Series B, Biological sciences* 147(927):268-273.
3. Lindenmann J, Burke DC, & Isaacs A (1957) Studies on the Production, Mode of Action and Properties of Interferon. *British Journal of Experimental Pathology* 38(5):551-562.
4. Pestka S (2007) The interferons: 50 years after their discovery, there is much more to learn. *J Biol Chem* 282(28):20047-20051.
5. Colamonici OR, Uyttendaele H, Domanski P, Yan H, & Krolewski JJ (1994) p135tyk2, an interferon-alpha-activated tyrosine kinase, is physically associated with an interferon-alpha receptor. *J Biol Chem* 269(5):3518-3522.
6. Gauzzi MC, *et al.* (1996) Interferon-alpha-dependent activation of Tyk2 requires phosphorylation of positive regulatory tyrosines by another kinase. *J Biol Chem* 271(34):20494-20500.
7. Heim MH, Kerr IM, Stark GR, & Darnell JE, Jr. (1995) Contribution of STAT SH2 groups to specific interferon signaling by the Jak-STAT pathway. *Science* 267(5202):1347-1349.
8. Colamonici O, *et al.* (1994) Direct binding to and tyrosine phosphorylation of the alpha subunit of the type I interferon receptor by p135tyk2 tyrosine kinase. *Mol Cell Biol* 14(12):8133-8142.
9. Greenlund AC, *et al.* (1995) Stat recruitment by tyrosine-phosphorylated cytokine receptors: an ordered reversible affinity-driven process. *Immunity* 2(6):677-687.
10. Schindler C, Shuai K, Prezioso VR, & Darnell JE, Jr. (1992) Interferon-dependent tyrosine phosphorylation of a latent cytoplasmic transcription factor. *Science* 257(5071):809-813.
11. Darnell JE, Jr. (1997) STATs and gene regulation. *Science* 277(5332):1630-1635.
12. Darnell JE, Kerr IM, & Stark GR (1994) Jak-STAT pathways and transcriptional activation in response to IFNs and other extracellular signaling proteins. *Science* 264(5164):1415.
13. Chen K, Liu J, & Cao X (2017) Regulation of type I interferon signaling in immunity and inflammation: A comprehensive review. *J Autoimmun.*
14. Levy DE, Kessler DS, Pine R, Reich N, & Darnell JE, Jr. (1988) Interferon-induced nuclear factors that bind a shared promoter element correlate with positive and negative transcriptional control. *Genes Dev* 2(4):383-393.
15. Schneider WM, Chevillotte MD, & Rice CM (2014) Interferon-stimulated genes: a complex web of host defenses. *Annu Rev Immunol* 32:513-545.
16. González-Navajas JM, Lee J, David M, & Raz E (2012) Immunomodulatory functions of type I interferons. *Nature Reviews Immunology* 12(2):125-135.
17. Schlee M & Hartmann G (2016) Discriminating self from non-self in nucleic acid sensing. *Nat Rev Immunol* 16(9):566-580.
18. Yoneyama M & Fujita T (2010) Recognition of viral nucleic acids in innate

- immunity. *Rev. Med. Virol.* 20(1):4-22.
19. Takeshita F, *et al.* (2001) Cutting edge: Role of Toll-like receptor 9 in CpG DNA-induced activation of human cells. *J Immunol* 167(7):3555-3558.
  20. Haas T, *et al.* (2008) The DNA sugar backbone 2' deoxyribose determines toll-like receptor 9 activation. *Immunity* 28(3):315-323.
  21. Hemmi H, *et al.* (2000) A Toll-like receptor recognizes bacterial DNA. *Nature* 408(6813):740-745.
  22. Kumagai Y, Takeuchi O, & Akira S (2008) TLR9 as a key receptor for the recognition of DNA. *Advanced Drug Delivery Reviews* 60(7):795-804.
  23. Luecke S & Paludan SR (2016) Molecular requirements for sensing of intracellular microbial nucleic acids by the innate immune system. *Cytokine*.
  24. Hornung V, *et al.* (2009) AIM2 recognizes cytosolic dsDNA and forms a caspase-1-activating inflammasome with ASC. *Nature* 458(7237):514-518.
  25. Burckstummer T, *et al.* (2009) An orthogonal proteomic-genomic screen identifies AIM2 as a cytoplasmic DNA sensor for the inflammasome. *Nat Immunol* 10(3):266-272.
  26. Fernandes-Alnemri T, Yu J-W, Datta P, Wu J, & Alnemri ES (2009) AIM2 activates the inflammasome and cell death in response to cytoplasmic DNA. *Nature* 458(7237):509-513.
  27. Rathinam VAK, *et al.* (2010) The AIM2 inflammasome is essential for host defense against cytosolic bacteria and DNA viruses. *Nat Immunol* 11(5):395-402.
  28. Ablasser A, *et al.* (2013) cGAS produces a 2'-5'-linked cyclic dinucleotide second messenger that activates STING. *Nature* 498(7454):380-384.
  29. Civril F, *et al.* (2013) Structural mechanism of cytosolic DNA sensing by cGAS. *Nature* 498(7454):332-337.
  30. Sun L, Wu J, Du F, Chen X, & Chen ZJ (2013) Cyclic GMP-AMP synthase is a cytosolic DNA sensor that activates the type I interferon pathway. *Science* 339(6121):786-791.
  31. Gao P, *et al.* (2013) Cyclic [G(2',5')pA(3',5')p] is the metazoan second messenger produced by DNA-activated cyclic GMP-AMP synthase. *Cell* 153(5):1094-1107.
  32. Ishikawa H, Ma Z, & Barber GN (2009) STING regulates intracellular DNA-mediated, type I interferon-dependent innate immunity. *Nature* 461(7265):788-792.
  33. Wu J, *et al.* (2013) Cyclic GMP-AMP Is an Endogenous Second Messenger in Innate Immune Signaling by Cytosolic DNA. *Science* 339(6121):826.
  34. Liu L, *et al.* (2008) Structural Basis of Toll-Like Receptor 3 Signaling with Double-Stranded RNA. *Science* 320(5874):379.
  35. Heil F, *et al.* (2004) Species-Specific Recognition of Single-Stranded RNA via Toll-like Receptor 7 and 8. *Science* 303(5663):1526.
  36. Alexopoulou L, Holt AC, Medzhitov R, & Flavell RA (2001) Recognition of double-stranded RNA and activation of NF- $\kappa$ B by Toll-like receptor 3. *Nature* 413(6857):732-738.
  37. Diebold SS, Kaisho T, Hemmi H, Akira S, & Reis e Sousa C (2004) Innate Antiviral Responses by Means of TLR7-Mediated Recognition of Single-Stranded RNA. *Science* 303(5663):1529.
  38. Yoneyama M, *et al.* (2005) Shared and Unique Functions of the DExD/H-Box

- Helicases RIG-I, MDA5, and LGP2 in Antiviral Innate Immunity. *The Journal of Immunology* 175(5):2851.
39. Wu B & Hur S (2015) How RIG-I like receptors activate MAVS. *Current Opinion in Virology* 12:91-98.
  40. Bruns AM & Horvath CM (2015) LGP2 synergy with MDA5 in RLR-mediated RNA recognition and antiviral signaling. *Cytokine* 74(2):198-206.
  41. Bruns Annie M, Leser George P, Lamb Robert A, & Horvath Curt M (2014) The Innate Immune Sensor LGP2 Activates Antiviral Signaling by Regulating MDA5-RNA Interaction and Filament Assembly. *Molecular Cell* 55(5):771-781.
  42. Poeck H, *et al.* (2010) Recognition of RNA virus by RIG-I results in activation of CARD9 and inflammasome signaling for interleukin 1[beta] production. *Nat Immunol* 11(1):63-69.
  43. Yoneyama M, *et al.* (2004) The RNA helicase RIG-I has an essential function in double-stranded RNA-induced innate antiviral responses. *Nat Immunol* 5(7):730-737.
  44. Hornung V, *et al.* (2006) 5'-Triphosphate RNA Is the Ligand for RIG-I. *Science* 314(5801):994.
  45. Wang Y, Zheng Y, & Beal PA (2017) Adenosine Deaminases That Act on RNA (ADARs). *Enzymes* 41:215-268.
  46. George CX, Gan Z, Liu Y, & Samuel CE (2011) Adenosine deaminases acting on RNA, RNA editing, and interferon action. *J Interferon Cytokine Res* 31(1):99-117.
  47. Bass BL (2002) RNA editing by adenosine deaminases that act on RNA. *Annu Rev Biochem* 71:817-846.
  48. Patterson JB & Samuel CE (1995) Expression and regulation by interferon of a double-stranded-RNA-specific adenosine deaminase from human cells: evidence for two forms of the deaminase. *Mol Cell Biol* 15(10):5376-5388.
  49. Kim U, Wang Y, Sanford T, Zeng Y, & Nishikura K (1994) Molecular cloning of cDNA for double-stranded RNA adenosine deaminase, a candidate enzyme for nuclear RNA editing. *Proceedings of the National Academy of Sciences of the United States of America* 91(24):11457-11461.
  50. Samuel CE (2011) Adenosine deaminases acting on RNA (ADARs) are both antiviral and proviral. *Virology* 411(2):180-193.
  51. Farrell PJ, *et al.* (1978) Interferon action: two distinct pathways for inhibition of protein synthesis by double-stranded RNA. *Proceedings of the National Academy of Sciences* 75(12):5893-5897.
  52. Nallagatla SR, Toroney R, & Bevilacqua PC (2011) Regulation of innate immunity through RNA structure and the protein kinase PKR. *Current Opinion in Structural Biology* 21(1):119-127.
  53. Williams BR (1999) PKR; a sentinel kinase for cellular stress. *Oncogene* 18(45):6112-6120.
  54. García MA, Meurs EF, & Esteban M (2007) The dsRNA protein kinase PKR: Virus and cell control. *Biochimie* 89(6-7):799-811.
  55. Clemens MJ & Elia A (1997) The double-stranded RNA-dependent protein kinase PKR: structure and function. *J Interferon Cytokine Res* 17(9):503-524.
  56. Sen GC, Taira H, & Lengyel P (1978) Interferon, double-stranded RNA, and

- protein phosphorylation. Characteristics of a double-stranded RNA-activated protein kinase system partially purified from interferon-treated Ehrlich ascites tumor cells. *Journal of Biological Chemistry* 253(17):5915-5921.
57. Huang H, *et al.* (2014) Dimeric structure of pseudokinase RNase L bound to 2-5A reveals a basis for interferon-induced antiviral activity. *Mol Cell* 53(2):221-234.
  58. Donovan J, Dufner M, & Korennykh A (2013) Structural basis for cytosolic double-stranded RNA surveillance by human oligoadenylate synthetase 1. *Proc Natl Acad Sci U S A* 110(5):1652-1657.
  59. Rebouillat D & Hovanessian AG (1999) The human 2',5'-oligoadenylate synthetase family: Interferon-induced proteins with unique enzymatic properties. *Journal of Interferon and Cytokine Research* 19(4):295-308.
  60. Yang K, *et al.* (1981) Interferons, double-stranded RNA, and RNA degradation. Isolation and characterization of homogeneous human (2'-5')(A)<sub>n</sub> synthetase. *Journal of Biological Chemistry* 256(17):9324-9328.
  61. Baglioni C, Minks MA, & Maroney PA (1978) Interferon action may be mediated by activation of a nuclease by pppA2[prime]p5[prime]A2[prime]p5[prime]A. *Nature* 273(5664):684-687.
  62. Chow J, Franz KM, & Kagan JC (2015) PRRs are watching you: Localization of innate sensing and signaling regulators. *Virology* 479-480:104-109.
  63. Gebhardt A, Laudenbach BT, & Pichlmair A (2017) Discrimination of Self and Non-Self Ribonucleic Acids. *J Interferon Cytokine Res* 37(5):184-197.
  64. Roers A, Hiller B, & Hornung V (2016) Recognition of Endogenous Nucleic Acids by the Innate Immune System. *Immunity* 44(4):739-754.
  65. Devarkar SC, *et al.* (2016) Structural basis for m7G recognition and 2'-O-methyl discrimination in capped RNAs by the innate immune receptor RIG-I. *Proc Natl Acad Sci U S A* 113(3):596-601.
  66. Nallagatla SR, Toroney R, & Bevilacqua PC (2008) A brilliant disguise for self RNA: 5'-end and internal modifications of primary transcripts suppress elements of innate immunity. *RNA Biol* 5(3):140-144.
  67. Nallagatla SR, *et al.* (2013) Native tertiary structure and nucleoside modifications suppress tRNA's intrinsic ability to activate the innate immune sensor PKR. *PLoS One* 8(3):e57905.
  68. Nallagatla SR & Bevilacqua PC (2008) Nucleoside modifications modulate activation of the protein kinase PKR in an RNA structure-specific manner. *Rna* 14(6):1201-1213.
  69. Kariko K, Buckstein M, Ni H, & Weissman D (2005) Suppression of RNA recognition by Toll-like receptors: the impact of nucleoside modification and the evolutionary origin of RNA. *Immunity* 23(2):165-175.
  70. Hull CM & Bevilacqua PC (2016) Discriminating Self and Non-Self by RNA: Roles for RNA Structure, Misfolding, and Modification in Regulating the Innate Immune Sensor PKR. *Acc Chem Res* 49(6):1242-1249.
  71. Roberts LO, Jopling CL, Jackson RJ, & Willis AE (2009) Viral strategies to subvert the mammalian translation machinery. *Prog Mol Biol Transl Sci* 90:313-367.
  72. Chan YK & Gack MU (2016) Viral evasion of intracellular DNA and RNA sensing. *Nat Rev Microbiol* 14(6):360-373.

73. Li Y, *et al.* (2017) Ribonuclease L mediates the cell-lethal phenotype of double-stranded RNA editing enzyme ADAR1 deficiency in a human cell line. *Elife* 6.
74. Silverman RH (2007) Viral encounters with 2',5'-oligoadenylate synthetase and RNase L during the interferon antiviral response. *J Virol* 81(23):12720-12729.
75. Rice GI, *et al.* (2012) Mutations in ADAR1 cause Aicardi-Goutieres syndrome associated with a type I interferon signature. *Nature genetics* 44(11):1243-1248.
76. Pokatayev V, *et al.* (2016) RNase H2 catalytic core Aicardi-Goutieres syndrome-related mutant invokes cGAS-STING innate immune-sensing pathway in mice. *The Journal of experimental medicine* 213(3):329-336.
77. Gray EE, Treuting PM, Woodward JJ, & Stetson DB (2015) Cutting Edge: cGAS Is Required for Lethal Autoimmune Disease in the Trex1-Deficient Mouse Model of Aicardi-Goutieres Syndrome. *J Immunol* 195(5):1939-1943.
78. Donnelly N, Gorman AM, Gupta S, & Samali A (2013) The eIF2 $\alpha$  kinases: their structures and functions. *Cell. Mol. Life Sci.* 70(19):3493-3511.
79. Lemaire PA, Anderson E, Lary J, & Cole JL (2008) Mechanism of PKR Activation by dsRNA. *Journal of Molecular Biology* 381(2):351-360.
80. Vattem KM, Staschke KA, & Wek RC (2001) Mechanism of activation of the double-stranded-RNA-dependent protein kinase, PKR. *European Journal of Biochemistry* 268(13):3674-3684.
81. Nanduri S, Carpick BW, Yang Y, Williams BRG, & Qin J (1998) Structure of the double-stranded RNA-binding domain of the protein kinase PKR reveals the molecular basis of its dsRNA-mediated activation. *EMBO J* 17(18):5458-5465.
82. Wu S & Kaufman RJ (1997) A Model for the Double-stranded RNA (dsRNA)-dependent Dimerization and Activation of the dsRNA-activated Protein Kinase PKR. *Journal of Biological Chemistry* 272(2):1291-1296.
83. Bevilacqua PC & Cech TR (1996) Minor-groove recognition of double-stranded RNA by the double-stranded RNA-binding domain from the RNA-activated protein kinase PKR. *Biochemistry* 35(31):9983-9994.
84. Lemaire PA, Lary J, & Cole JL (2005) Mechanism of PKR Activation: Dimerization and Kinase Activation in the Absence of Double-stranded RNA. *Journal of Molecular Biology* 345(1):81-90.
85. Manche L, Green SR, Schmedt C, & Mathews MB (1992) Interactions between double-stranded RNA regulators and the protein kinase DAI. *Mol Cell Biol* 12(11):5238-5248.
86. Zhang F, *et al.* (2001) Binding of double-stranded RNA to protein kinase PKR is required for dimerization and promotes critical autophosphorylation events in the activation loop. *J Biol Chem* 276(27):24946-24958.
87. Dar AC, Dever TE, & Sicheri F (2005) Higher-order substrate recognition of eIF2 $\alpha$  by the RNA-dependent protein kinase PKR. *Cell* 122(6):887-900.
88. Dey M, *et al.* (2005) PKR and GCN2 kinases and guanine nucleotide exchange factor eukaryotic translation initiation factor 2B (eIF2B) recognize overlapping surfaces on eIF2 $\alpha$ . *Mol Cell Biol* 25(8):3063-3075.
89. Majumdar R & Maitra U (2005) Regulation of GTP hydrolysis prior to ribosomal AUG selection during eukaryotic translation initiation. *The EMBO Journal* 24(21):3737-3746.
90. Sudhakar A, *et al.* (2000) Phosphorylation of serine 51 in initiation factor 2 alpha

- (eIF2 alpha) promotes complex formation between eIF2 alpha(P) and eIF2B and causes inhibition in the guanine nucleotide exchange activity of eIF2B. *Biochemistry* 39(42):12929-12938.
91. Yamasaki S & Anderson P (2008) Reprogramming mRNA translation during stress. *Curr Opin Cell Biol* 20(2):222-226.
  92. Holcik M & Sonenberg N (2005) Translational control in stress and apoptosis. *Nature reviews. Molecular cell biology* 6(4):318-327.
  93. Balachandran S, *et al.* (1998) Activation of the dsRNA-dependent protein kinase, PKR, induces apoptosis through FADD-mediated death signaling. *EMBO J* 17(23):6888-6902.
  94. Kim Y, *et al.* (2014) PKR is activated by cellular dsRNAs during mitosis and acts as a mitotic regulator. *Genes & Development* 28(12):1310-1322.
  95. Cohen-Chalamish S, *et al.* (2009) Dynamic refolding of IFN- $\gamma$  mRNA enables it to function as PKR activator and translation template. *Nature Chemical Biology* 5(12):896-903.
  96. Nussbaum JM (2002) The 3'-untranslated regions of cytoskeletal muscle mRNAs inhibit translation by activating the double-stranded RNA-dependent protein kinase PKR. *Nucleic Acids Research* 30(5):1205-1212.
  97. Li S, *et al.* (2006) Molecular basis for PKR activation by PACT or dsRNA. *Proceedings of the National Academy of Sciences* 103(26):10005-10010.
  98. Marchal JA, *et al.* (2014) The impact of PKR activation: from neurodegeneration to cancer. *FASEB J* 28(5):1965-1974.
  99. Chang HW, Watson JC, & Jacobs BL (1992) The E3L gene of vaccinia virus encodes an inhibitor of the interferon-induced, double-stranded RNA-dependent protein kinase. *Proc Natl Acad Sci U S A* 89(11):4825-4829.
  100. Bergmann M, *et al.* (2000) Influenza virus NS1 protein counteracts PKR-mediated inhibition of replication. *J Virol* 74(13):6203-6206.
  101. Feng Z, Cerveny M, Yan Z, & He B (2007) The VP35 protein of Ebola virus inhibits the antiviral effect mediated by double-stranded RNA-dependent protein kinase PKR. *J Virol* 81(1):182-192.
  102. Cassady KA (2005) Human cytomegalovirus TRS1 and IRS1 gene products block the double-stranded-RNA-activated host protein shutoff response induced by herpes simplex virus type 1 infection. *J Virol* 79(14):8707-8715.
  103. Imani F & Jacobs BL (1988) Inhibitory activity for the interferon-induced protein kinase is associated with the reovirus serotype 1 sigma 3 protein. *Proc Natl Acad Sci U S A* 85(21):7887-7891.
  104. Khoo D, Perez C, & Mohr I (2002) Characterization of RNA determinants recognized by the arginine- and proline-rich region of Us11, a herpes simplex virus type 1-encoded double-stranded RNA binding protein that prevents PKR activation. *J Virol* 76(23):11971-11981.
  105. Launer-Felty K, Wong CJ, & Cole James L (2015) Structural Analysis of Adenovirus VAI RNA Defines the Mechanism of Inhibition of PKR. *Biophysical Journal* 108(3):748-757.
  106. Wilson JL, Vachon VK, Sunita S, Schwartz SL, & Conn GL (2014) Dissection of the adenoviral VA RNAI central domain structure reveals minimum requirements for RNA-mediated inhibition of PKR. *J Biol Chem* 289(33):23233-23245.

107. McKenna SA, Lindhout DA, Shimoike T, Aitken CE, & Puglisi JD (2007) Viral dsRNA Inhibitors Prevent Self-association and Autophosphorylation of PKR. *Journal of Molecular Biology* 372(1):103-113.
108. McKenna SA, Kim I, Liu CW, & Puglisi JD (2006) Uncoupling of RNA binding and PKR kinase activation by viral inhibitor RNAs. *J Mol Biol* 358(5):1270-1285.
109. Jammi NV & Beal PA (2001) Phosphorylation of the RNA-dependent protein kinase regulates its RNA-binding activity. *Nucleic Acids Res* 29(14):3020-3029.
110. Elde NC, Child SJ, Geballe AP, & Malik HS (2009) Protein kinase R reveals an evolutionary model for defeating viral mimicry. *Nature* 457(7228):485-489.
111. Dar AC & Sicheri F (2002) X-ray crystal structure and functional analysis of vaccinia virus K3L reveals molecular determinants for PKR subversion and substrate recognition. *Mol Cell* 10(2):295-305.
112. Gale M, Jr., *et al.* (1998) Control of PKR protein kinase by hepatitis C virus nonstructural 5A protein: molecular mechanisms of kinase regulation. *Mol Cell Biol* 18(9):5208-5218.
113. Taylor DR, Shi ST, Romano PR, Barber GN, & Lai MM (1999) Inhibition of the interferon-inducible protein kinase PKR by HCV E2 protein. *Science* 285(5424):107-110.
114. Kazemi S, *et al.* (2004) Control of alpha subunit of eukaryotic translation initiation factor 2 (eIF2 alpha) phosphorylation by the human papillomavirus type 18 E6 oncoprotein: implications for eIF2 alpha-dependent gene expression and cell death. *Mol Cell Biol* 24(8):3415-3429.
115. He B, Gross M, & Roizman B (1997) The  $\gamma$ 134.5 protein of herpes simplex virus 1 complexes with protein phosphatase 1 $\alpha$  to dephosphorylate the  $\alpha$  subunit of the eukaryotic translation initiation factor 2 and preclude the shutoff of protein synthesis by double-stranded RNA-activated protein kinase. *Proceedings of the National Academy of Sciences* 94(3):843-848.
116. Mudhasani R, *et al.* (2016) Protein Kinase R Degradation Is Essential for Rift Valley Fever Virus Infection and Is Regulated by SKP1-CUL1-F-box (SCF)FBXW11-NSs E3 Ligase. *PLoS pathogens* 12(2):e1005437.
117. Domingo-Gil E, Toribio R, Najera JL, Esteban M, & Ventoso I (2011) Diversity in viral anti-PKR mechanisms: a remarkable case of evolutionary convergence. *PLoS One* 6(2):e16711.
118. White JP, Reineke LC, & Lloyd RE (2011) Poliovirus switches to an eIF2-independent mode of translation during infection. *J Virol* 85(17):8884-8893.
119. Pari M, *et al.* (2014) Enzymatically active 2',5'-oligoadenylate synthetases are widely distributed among Metazoa, including protostome lineage. *Biochimie* 97:200-209.
120. Kristiansen H, Gad HH, Eskildsen-Larsen S, Despres P, & Hartmann R (2011) The oligoadenylate synthetase family: an ancient protein family with multiple antiviral activities. *J Interferon Cytokine Res* 31(1):41-47.
121. Hovnanian A, *et al.* (1998) The human 2',5'-oligoadenylate synthetase locus is composed of three distinct genes clustered on chromosome 12q24.2 encoding the 100-, 69-, and 40-kDa forms. *Genomics* 52(3):267-277.
122. Martin G & Keller W (2007) RNA-specific ribonucleotidyl transferases. *Rna* 13(11):1834-1849.

123. Hancks DC, Hartley MK, Hagan C, Clark NL, & Elde NC (2015) Overlapping Patterns of Rapid Evolution in the Nucleic Acid Sensors cGAS and OAS1 Suggest a Common Mechanism of Pathogen Antagonism and Escape. *PLoS Genet* 11(5):e1005203.
124. Eskildsen S, Justesen J, Schierup MH, & Hartmann R (2003) Characterization of the 2'-5'-oligoadenylate synthetase ubiquitin-like family. *Nucleic Acids Res* 31(12):3166-3173.
125. Hartmann R, Justesen J, Sarkar SN, Sen GC, & Yee VC (2003) Crystal structure of the 2'-specific and double-stranded RNA-activated interferon-induced antiviral protein 2'-5'-oligoadenylate synthetase. *Mol Cell* 12(5):1173-1185.
126. Ibsen MS, *et al.* (2014) The 2'-5'-oligoadenylate synthetase 3 enzyme potentially synthesizes the 2'-5'-oligoadenylates required for RNase L activation. *J Virol* 88(24):14222-14231.
127. Donovan J, Whitney G, Rath S, & Korennykh A (2015) Structural mechanism of sensing long dsRNA via a noncatalytic domain in human oligoadenylate synthetase 3. *Proc Natl Acad Sci U S A* 112(13):3949-3954.
128. Kodym R, Kodym E, & Story MD (2009) 2'-5'-Oligoadenylate synthetase is activated by a specific RNA sequence motif. *Biochem Biophys Res Commun* 388(2):317-322.
129. Vachon VK & Conn GL (2016) Adenovirus VA RNA: An essential pro-viral non-coding RNA. *Virus Research* 212:39-52.
130. Vachon VK, Calderon BM, & Conn GL (2015) A novel RNA molecular signature for activation of 2'-5' oligoadenylate synthetase-1. *Nucleic Acids Res* 43(1):544-552.
131. Zhou A, Hassel BA, & Silverman RH (1993) Expression cloning of 2-5A-dependent RNAase: A uniquely regulated mediator of interferon action. *Cell* 72(5):753-765.
132. Han Y, Whitney G, Donovan J, & Korennykh A (2012) Innate immune messenger 2-5A tethers human RNase L into active high-order complexes. *Cell Rep* 2(4):902-913.
133. Rath S, *et al.* (2015) Human RNase L tunes gene expression by selectively destabilizing the microRNA-regulated transcriptome. *Proc Natl Acad Sci U S A* 112(52):15916-15921.
134. Banerjee S, *et al.* (2015) RNase L is a negative regulator of cell migration. *Oncotarget* 6(42):44360-44372.
135. Siddiqui MA, Mukherjee S, Manivannan P, & Malathi K (2015) RNase L Cleavage Products Promote Switch from Autophagy to Apoptosis by Caspase-Mediated Cleavage of Beclin-1. *Int J Mol Sci* 16(8):17611-17636.
136. Malathi K, Dong B, Gale M, Jr., & Silverman RH (2007) Small self-RNA generated by RNase L amplifies antiviral innate immunity. *Nature* 448(7155):816-819.
137. Luthra P, Sun D, Silverman RH, & He B (2011) Activation of IFN- $\beta$  expression by a viral mRNA through RNase L and MDA5. *Proc Natl Acad Sci U S A* 108(5):2118-2123.
138. Ibsen MS, *et al.* (2015) Structural and functional analysis reveals that human OASL binds dsRNA to enhance RIG-I signaling. *Nucleic Acids Res* 43(10):5236-

- 5248.
139. Zhu J, *et al.* (2014) Antiviral activity of human OASL protein is mediated by enhancing signaling of the RIG-I RNA sensor. *Immunity* 40(6):936-948.
  140. Taguchi T, *et al.* (2004) Hepatitis C virus NS5A protein interacts with 2',5'-oligoadenylate synthetase and inhibits antiviral activity of IFN in an IFN sensitivity-determining region-independent manner. *J Gen Virol* 85(Pt 4):959-969.
  141. Silverman RH & Weiss SR (2014) Viral Phosphodiesterases That Antagonize Double-Stranded RNA Signaling to RNase L by Degrading 2-5A. *J Interferon Cytokine Res* 34(6):455-463.
  142. Zhao L, *et al.* (2012) Antagonism of the Interferon-Induced OAS-RNase L Pathway by Murine Coronavirus ns2 Protein Is Required for Virus Replication and Liver Pathology. *Cell Host & Microbe* 11(6):607-616.
  143. Ogden KM, *et al.* (2015) Structural basis for 2'-5'-oligoadenylate binding and enzyme activity of a viral RNase L antagonist. *J Virol* 89(13):6633-6645.
  144. Cayley PJ, Davies JA, McCullagh KG, & Kerr IM (1984) Activation of the ppp(A2'p)nA system in interferon-treated, herpes simplex virus-infected cells and evidence for novel inhibitors of the ppp(A2'p)nA-dependent RNase. *Eur J Biochem* 143(1):165-174.
  145. Hersh CL, *et al.* (1984) Simian virus 40-infected, interferon-treated cells contain 2',5'-oligoadenylates which do not activate cleavage of RNA. *J Biol Chem* 259(3):1731-1737.
  146. Rice AP, Kerr SM, Roberts WK, Brown RE, & Kerr IM (1985) Novel 2',5'-oligoadenylates synthesized in interferon-treated, vaccinia virus-infected cells. *J Virol* 56(3):1041-1044.
  147. van Eyll O & Michiels T (2000) Influence of the Theiler's virus L\* protein on macrophage infection, viral persistence, and neurovirulence. *J Virol* 74(19):9071-9077.
  148. Han JQ, *et al.* (2007) A phylogenetically conserved RNA structure in the poliovirus open reading frame inhibits the antiviral endoribonuclease RNase L. *J Virol* 81(11):5561-5572.
  149. Lee K, *et al.* (2011) Precursor miR-886, a novel noncoding RNA repressed in cancer, associates with PKR and modulates its activity. *RNA* 17(6):1076-1089.
  150. Oler AJ, *et al.* (2010) Human RNA polymerase III transcriptomes and relationships to Pol II promoter chromatin and enhancer-binding factors. *Nature structural & molecular biology* 17(5):620-628.
  151. Canella D, Praz V, Reina JH, Cousin P, & Hernandez N (2010) Defining the RNA polymerase III transcriptome: Genome-wide localization of the RNA polymerase III transcription machinery in human cells. *Genome research* 20(6):710-721.
  152. Moqtaderi Z, *et al.* (2010) Genomic binding profiles of functionally distinct RNA polymerase III transcription complexes in human cells. *Nature structural & molecular biology* 17(5):635-640.
  153. DiDonato JA, Mercurio F, & Karin M (2012) NF-kappaB and the link between inflammation and cancer. *Immunol Rev* 246(1):379-400.
  154. Zamanian-Daryoush M, Mogensen TH, DiDonato JA, & Williams BRG (2000) NF-κB Activation by Double-Stranded-RNA-Activated Protein Kinase (PKR) Is

- Mediated through NF- $\kappa$ B-Inducing Kinase and I $\kappa$ B Kinase. *Molecular and Cellular Biology* 20(4):1278-1290.
155. Lee YS (2015) A Novel Type of Non-coding RNA, nc886, Implicated in Tumor Sensing and Suppression. *Genomics Inform* 13(2):26-30.
  156. Lee HS, *et al.* (2014) Epigenetic silencing of the non-coding RNA nc886 provokes oncogenes during human esophageal tumorigenesis. *Oncotarget* 5(11):3472-3481.
  157. Romanelli V, *et al.* (2014) Variable maternal methylation overlapping the nc886/vtRNA2-1 locus is locked between hypermethylated repeats and is frequently altered in cancer. *Epigenetics* 9(5):783-790.
  158. Lee KS, *et al.* (2014) nc886, a non-coding RNA of anti-proliferative role, is suppressed by CpG DNA methylation in human gastric cancer. *Oncotarget* 5(11):3944-3955.
  159. Kunkeaw N, *et al.* (2012) Cell death/proliferation roles for nc886, a non-coding RNA, in the protein kinase R pathway in cholangiocarcinoma. *Oncogene* 32(32):3722-3731.
  160. Jeon SH, *et al.* (2012) Characterization of the direct physical interaction of nc886, a cellular non-coding RNA, and PKR. *FEBS Lett* 586(19):3477-3484.
  161. Lee EK, *et al.* (2016) nc886, a non-coding RNA and suppressor of PKR, exerts an oncogenic function in thyroid cancer. *Oncotarget* 7(46):75000-75012.
  162. Kong L, *et al.* (2015) Regulation of p53 expression and apoptosis by vault RNA2-1-5p in cervical cancer cells. *Oncotarget* 6(29):28371-28388.

## Chapter 2

### **Human noncoding RNA 886 (nc886) adopts two structurally distinct conformers that are functionally opposing regulators of PKR**

Brenda M. Calderon and Graeme L. Conn

This research was originally published in *RNA* a publication of the RNA Society.

Calderon, B.M. and Conn, G.L. Human noncoding RNA 886 (nc886) adopts two structurally distinct conformers that are functionally opposing regulators of PKR. *RNA*. 2017 23: 557-566. © Cold Spring Harbor Laboratory Press for the RNA Society.

#### **2.1 Abstract**

The double-stranded RNA (dsRNA)-activated protein kinase (PKR) senses dsRNA produced during viral infection and halts cellular protein synthesis to block viral replication. How basal PKR activity is controlled in the absence of infection was unclear until the recent identification of a potential endogenous regulator, the cellular noncoding RNA 886 (nc886). However, nc886 adopts two distinct conformations for which the structural details and potential functional differences remain unclear. Here, we isolated and separately dissected the function of each form of nc886 to more clearly define the molecular mechanism of nc886-mediated PKR inhibition. We show that nc886 adopts two stable, noninterconverting RNA conformers that are functionally nonequivalent using complementary RNA structure probing and mutational analyses combined with PKR binding and activity assays. One conformer acts as a potent inhibitor, while the other is a

pseudoinhibitor capable of weakly activating the kinase. We mapped the nc886 region necessary for high affinity binding and potent inhibition of PKR to an apical stem-loop structure present in only one conformer of the RNA. This structural feature is not only critical for inhibiting PKR autophosphorylation, but also the phosphorylation of its cellular substrate, the eukaryotic translation initiation factor 2 $\alpha$  subunit. The identification of different activities of the nc886 conformers suggests a potential mechanism for producing a gradient of PKR regulation within the cell and reveals a way by which a cellular noncoding RNA can mask or present a structural feature to PKR for inhibition.

## **2.2 Introduction**

The innate immune response is an intrinsic cellular system that serves as the first defense against pathogens (1, 2). Pattern recognition receptors (PRRs) on the cell surface and in the cytosol detect pathogen-associated molecular patterns, such as viral proteins and nucleic acids, and initiate signaling cascades to prevent viral replication and to establish an antiviral state (3-5). One critical PRR is the double-stranded RNA (dsRNA)-activated protein kinase (PKR), which senses dsRNA in the cytoplasm and halts protein synthesis (4, 6, 7). Binding of viral dsRNA promotes PKR dimerization and autophosphorylation, activating the kinase to phosphorylate its substrate, the eukaryotic translation initiation factor 2 $\alpha$  subunit (eIF2 $\alpha$ ) on serine 51. Phosphorylation increases eIF2 affinity for its guanine nucleotide exchange factor eIF2B and thus sequesters the protein complex, effectively halting recycling of eIF2 to a GTP-bound form (8). As a result, general translation is attenuated, blocking viral replication while permitting enhanced translation

of specific transcripts including stress response genes (9).

The central importance of PKR to innate immunity is highlighted by the diverse array of mechanisms viruses have evolved to subvert this pathway (10-12). Due to its ubiquitous expression and functional roles outside of innate immunity, PKR activity must be tightly regulated so that it can recognize viral RNA, but not be spuriously activated by cellular RNA. Studies on the proliferative role of PKR in cancer cells recently led to the discovery of a potential endogenous RNA regulator, the noncoding RNA 886 (nc886) (Figure 2.1A) (13). nc886 is a ubiquitously expressed, cytosolic noncoding RNA that was found to interact with PKR (13). Additionally, expression of nc886 is down-regulated or completely absent in many cancer cells along with associated increased levels of PKR phosphorylation (14-21). Silencing of nc886 leads to increased basal kinase activity, as demonstrated by PKR autophosphorylation of threonine 446 and phosphorylation of eIF2 $\alpha$  in the absence of exogenous activating dsRNA (13, 16). These observations clearly point to the existence of cellular RNAs with the ability to activate PKR in the absence of nc886. Furthermore, reintroduction of nc886 to cells lacking the transcript resulted in reduced levels of phosphorylated PKR and eIF2 $\alpha$ , demonstrating that nc886 is necessary and sufficient to negatively regulate PKR activity (16).

Despite this significant advance in our understanding of endogenous regulation of PKR activity, many questions remain about the nature of nc886-mediated PKR inhibition. In particular, it remains unclear why nc886 behaves as an inhibitor rather than an activator of PKR activity and what specific RNA features confer its potency of inhibition. Notably, although nc886 was found to exist in two conformations, all analyses performed to date used a mixture of these two different forms. We therefore set out to

isolate and separately dissect the functions of these two conformers to clearly define the molecular mechanisms of nc886-mediated PKR inhibition.

Our results demonstrate that nc886 RNA does indeed exist in two structurally and functionally nonequivalent forms. One conformer, which exhibits slower migration on native polyacrylamide gels, has higher binding affinity for PKR and potently inhibits both PKR and downstream eIF2 $\alpha$  phosphorylation. In contrast, the second conformer is a weak activator that behaves as a pseudoinhibitor of PKR in competition with other dsRNAs, and may serve as a more transient regulator of PKR activity. This work emphasizes the importance of RNA folding in regard to noncoding RNA function and highlights a potential mechanism for regulating the activity of nc886 RNA independent of its transcript level through the presentation or masking of a critical structural element.

## **2.3 Results**

### **2.3.1 nc886 RNA adopts two noninterconverting conformers with distinct stabilities**

nc886 RNA (101 nucleotides) was *in vitro* transcribed using T7 RNA polymerase from a linearized plasmid DNA template producing nc886 fused at its 3'-end to a self-cleaving hepatitis delta virus (HDV) ribozyme (Figure 2.1A). The *in vitro* transcription reaction was analyzed by native polyacrylamide gel electrophoresis (PAGE) revealing two nc886 RNA bands of differing mobility, as previously reported (22), in addition to the cleaved HDV ribozyme (Figure 2.1B). These distinct nc886 structural conformers are referred to as “Conformer 1” (slower migrating form) and “Conformer 2” (faster migrating form).

Purification of nc886 by denaturing PAGE results in a mixture of both conformers (22). We therefore used preparative native PAGE to isolate the individual nc886 RNA

conformers and found through reanalysis of the purified conformers that both structures are stable and do not interconvert under nondenaturing conditions (Figure 2.1B). We next analyzed the thermal stability of each isolated nc886 RNA conformer by UV melting analysis in the same 0.5× TBE buffer as used in native PAGE (Figure 2.2A). The melting profile (first derivative of the raw UV melting curve) for nc886 Conformer 2 revealed that this RNA structure unfolds in a single apparent transition with a  $T_m$  of  $\sim 40^\circ\text{C}$ . In contrast, Conformer 1 exhibits much greater stability with a final major apparent unfolding transition with a  $T_m > 70^\circ\text{C}$ . Unfolding of each nc886 conformer was also assessed in 20 mM HEPES buffer (pH 7.5) containing 100 mM NaCl yielding essentially identical melting profiles, but with apparent  $T_m$  values shifted to higher temperatures (data not shown and Table 2.1). Thus, a dramatic difference in stability between the two conformers of nc886 ( $\Delta T_m > 30^\circ\text{C}$ ) was observed under both the lower and higher ionic strength conditions. A mixture of the conformers, purified using standard denaturing PAGE, was also analyzed under both solution conditions and had a melting profile consistent with a combination of the profiles for the two individual conformers (Figure 2.2A).

Collectively, these observations demonstrate that the purified nc886 conformers retain their conformational identity under native conditions and adopt structures with very different stabilities. Interestingly, however, upon complete thermal denaturation (heating to  $>90^\circ\text{C}$ ) and refolding, a subsequent analysis reveals that Conformer 1 can either re-adopt its original structure or can refold as Conformer 2. In contrast, Conformer 2 exclusively re-adopts its original structure (Figure 2.2B,C).

### 2.3.2 nc886 RNA conformers have opposing activities against PKR

To begin characterizing the activities of the nc886 conformers, we first tested the ability of each isolated RNA to bind to PKR using an electrophoretic mobility shift assay (EMSA). Each individual purified conformer (300 nM) was incubated with a range of PKR concentrations (0–3  $\mu$ M) and free and bound RNA resolved by native PAGE (Figure 2.3A). Both conformers bind to PKR, but with starkly different affinities: while nc886 Conformer 1 readily forms a PKR–RNA complex, with shifted RNA observed at the lowest protein concentration, nc886 Conformer 2 does so only at the highest concentrations of PKR.

Each isolated nc886 conformer appears to result in a PKR–nc886 complex with similar native gel mobility (Figure 2.3A). We therefore considered the possibility that PKR binding might induce a structural conversion in one or both of the nc886 conformers such that the final bound structure is the same regardless of the original nc886 conformation. Each nc886 conformer (1  $\mu$ M) was treated in an equivalent manner as for the EMSA analysis, either in the absence or presence of a twofold excess of PKR, except that the RNA was subsequently phenol:chloroform extracted and ethanol precipitated prior to analysis by native PAGE. Following this process, the original mobility of each nc886 RNA conformer was fully retained (Figure 2.3B), indicating that PKR binding does not induce a conformational interconversion in either nc886 conformer.

We next tested the effect that these differences in PKR binding had on the ability of each nc886 conformer to inhibit PKR autophosphorylation in the presence of a dsRNA activator using an established slot-blot radiometric kinase assay (23). PKR autophosphorylation was measured in the presence of a fixed concentration of poly(rI:rC)

dsRNA and increasing amounts of each nc886 RNA conformer. Both conformers cause a dose-dependent decrease in PKR autophosphorylation, but to markedly different extents (Figure 2.3C). nc886 Conformer 1 is a potent, dose-dependent inhibitor of PKR, capable of completely abolishing PKR autophosphorylation. In contrast, with Conformer 2 partial inhibition was only observed at the highest RNA concentration tested. Surprisingly, at the mid-range concentrations of nc886 RNA, where Conformer 1 fully inhibits PKR, Conformer 2 appears to modestly increase the extent of PKR autophosphorylation compared to poly(rI:rC) dsRNA alone. This prompted us to test whether nc886 Conformer 2 is capable of weakly activating PKR in the absence of dsRNA. Using an autophosphorylation assay in which PKR was incubated with increasing concentrations of nc886 Conformer 2 (0.001–10  $\mu$ M) alone, a dose-dependent increase in PKR autophosphorylation was indeed observed (Figure 2.3D). Further, the extent of autophosphorylation was comparable to the amount of additional activation we observed in the inhibition assay (Figure 2.3C,D). These results demonstrate that rather than simply being a poorer PKR inhibitor, nc886 RNA Conformer 2 behaves as a pseudoinhibitor. This contributes to overall PKR activation at lower concentrations, but competes for PKR binding with the more potent poly(rI:rC) dsRNA activator at the highest concentration in the inhibition assay.

### **2.3.3 Differences in apical stem-loop structure distinguish the two nc886 RNA conformers**

To understand the basis for the stark differences in activity between nc886 conformers, we used selective 2'-hydroxyl acylation analyzed by primer extension (SHAPE) with N-

methylisotoic anhydride (NMIA) to experimentally assess the secondary structure of each isolated RNA. A 5'-end  $^{32}\text{P}$ -labeled DNA oligonucleotide complementary to the 3'-end of nc886 RNA was used for reverse transcription (RT) following incubation of each individual nc886 conformer with or without NMIA, and the products resolved on denaturing polyacrylamide sequencing gels (Figure 2.4).

The SHAPE reactivity for Conformer 2 correlates well with the predicted secondary structure for nc886 RNA, with strong modification of most nucleotides within predicted loops and essentially none in predicted base-paired regions (Figure 2.4A,C). The most significant deviation between SHAPE reactivity and the predicted structure occurs for the 5'-side of Loop 3 (nucleotides 25–28), which exhibits lower than expected reactivity, indicative of a more base-paired or rigid structure. Probing of nc886 Conformer 1 revealed an essentially identical pattern for the 3'-half of the RNA, with high reactivity within the 3'-side of Loop 3 and within Loop 4. However, in sharp contrast to Conformer 2, Loop 5 reactivity is absent in Conformer 1 except at the single, strongly reactive nucleotide A47 (Figure 2.4C). Additionally, unique to Conformer 1, a series of remarkably strong, NMIA-independent stops was observed corresponding to the nucleotides immediately preceding Loop 5 in the structure (nucleotides 36–40; Figure 2.4B,C), indicative of a stable structure resistant to unfolding during the RT reaction. The remainder of the 5'-half of Conformer 1 was examined using a second, internal primer (complementary to nucleotides 36–54) and found to have similar reactivity as Conformer 2 in this region, including the strong reactivity in the 5'-sides of Loop 1 and lower than expected reactivity for Loop 3.

These results demonstrate that each nc886 conformer adopts a common structure

within its terminal and central regions, but that they differ dramatically in the apical stem–loop. The reduced reactivity of Loop 5 and the adjacent RT-read-through resistant sequence suggest that the apical stem–loop adopts a stable, higher order structure unique to nc886 Conformer 1. As the only significant structural difference between the two nc886 conformers, these data strongly suggest that the absence (Conformer 2) or presence (Conformer 1) of this additional structural element is responsible for their different native gel motilities, thermal stabilities, and activities against PKR.

### **2.3.4 The unique Conformer 1 apical stem–loop structure is critical for PKR repression**

We next sought to fully define which regions of nc886 are critical for binding and inhibition of PKR. Based on the SHAPE probing data, we created nc886 variants with a truncation of either the terminal stem (nc886 $\Delta$ TS) or the apical stem–loop (nc886 $\Delta$ AS) (Figure 2.5A). The nc886 $\Delta$ TS variant exists as two conformers that possess similar relative stability to each full-length nc886 conformer as determined by UV thermal melting analysis (Table 2.1; Figure 2.5B). These observations are consistent with the nc886 $\Delta$ TS conformers retaining a common central stem organization but distinct structures in the apical stem–loop as for the wild-type RNA. In contrast, nc886 $\Delta$ AS folds into a single conformer with an apparent  $T_m$  for unfolding most similar to Conformer 2 of full-length nc886 and nc886 $\Delta$ TS. Again, this result is consistent with the apical stem–loop containing the structure that distinguishes the two nc886 RNA conformers. The nc886 $\Delta$ TS conformers and nc886 $\Delta$ AS were native PAGE purified as previously described and the isolated RNAs tested for binding to PKR. The nc886 $\Delta$ TS conformers

were found to have similar binding properties as their full-length nc886 equivalents (Figure 2.5C), with nc886 $\Delta$ TS Conformer 1 binding PKR with higher affinity than Conformer 2. In contrast, nc886 $\Delta$ AS-PKR binding was significantly reduced, comparable to the level of full-length nc886 and nc886 $\Delta$ TS Conformer 2.

We next tested the ability of each RNA variant to inhibit PKR autophosphorylation. Again, the activity of each nc886 $\Delta$ TS conformer closely resembled that of the equivalent full-length nc886 conformer, whereas nc886 $\Delta$ AS was a poor PKR inhibitor, comparable to nc886 $\Delta$ TS Conformer 2 (Figure 2.5D). Both nc886 $\Delta$ AS and nc886 $\Delta$ TS Conformer 2 were additionally tested in the kinase activation assay to determine whether these RNAs weakly activate PKR as for full-length nc886 Conformer 2. However, neither of these RNAs activated PKR at any of the concentrations tested (Figure 2.5E). These results suggest that in the presence of poly(rI:rC) dsRNA, the similarly weak inhibition of PKR observed at the highest concentration of full-length nc886 Conformer 2, nc886 $\Delta$ TS Conformer 2, and nc886 $\Delta$ AS RNAs arises due to their comparable weak PKR binding affinities. However, unlike full-length nc886 Conformer 2 which weakly activates PKR in the absence of other dsRNA, nc886 $\Delta$ TS Conformer 2 has lost this ability. This result suggests that the nc886 terminal stem contributes significantly to this activity in the context of the structure of Conformer 2, which lacks the high affinity apical stem-loop PKR binding site.

The cellular impact of PKR activation is the downstream phosphorylation of its substrate eIF2 $\alpha$ . We therefore tested the effect of full-length and each variant nc886 RNA on PKR's ability to phosphorylate eIF2 $\alpha$  using the same radiometric kinase assay, except that the phosphorylated protein products were resolved by SDS-PAGE prior to

autoradiography. After a preincubation in the absence or presence of each nc886 RNA (10  $\mu$ M), the extent of PKR and eIF2 $\alpha$  phosphorylation was measured following incubation with poly(rI:rC) dsRNA activator (Figure 2.6A). Full-length nc886 Conformer 1 and nc886 $\Delta$ TS Conformer 1 both potently inhibit PKR and downstream eIF2 $\alpha$  phosphorylation (Figure 2.6B). In contrast, nc886 Conformer 2, nc886 $\Delta$ TS Conformer 2, and nc886 $\Delta$ AS only partially inhibit PKR autophosphorylation and, as a result, confer almost no inhibition of eIF2 $\alpha$  phosphorylation.

Collectively, the combined structural and functional analyses of wild-type and variant nc886 conformers point to a unique structure, present only in Conformer 1, being responsible for potent PKR inhibition. To this end, we created a final variant RNA (nc886 $\Delta$ L5) with a minimally altered Loop 5 sequence designed to specifically disrupt this apical stem-loop structure. SHAPE probing and native PAGE analysis demonstrates that this variant RNA exists as a single conformer that adopts a secondary structure similar to wild-type Conformer 2 (Figure 2.7A,B). UV thermal melting analysis indicates the stability of the RNA to be similar to that of wild-type Conformer 2 (Table 2.1). We next tested for PKR binding using the same electrophoretic mobility shift assay and found that nc886 $\Delta$ L5 binds PKR weakly, similar to both wild-type nc886 Conformer 2 and the larger  $\Delta$ AS truncation variant (Figure 2.7C). Finally, we tested nc886 $\Delta$ L5 for its ability to inhibit PKR autophosphorylation in the presence of the synthetic dsRNA poly(rI:rC) using the radiometric kinase assay. nc886 $\Delta$ L5 is a poor PKR inhibitor (Figure 2.7D), consistent with Loop 5 being critical for forming the apical stem-loop structure essential for potent PKR inhibition. Contrary to our expectation, however, nc886 $\Delta$ L5 did not retain the capacity of wild-type Conformer 2 to weakly activate PKR. This suggests

the full apical stem–loop structure of the RNA is required in addition to the terminal stem for this activity.

## 2.4 Discussion

PKR binds to and is activated by RNAs containing a variety of structural elements, including internal bulges, stem–loops, and single-stranded regions, or RNAs which may only be sufficiently double-stranded through tertiary interactions (24-31). With our growing appreciation that cellular RNAs adopt complex secondary and tertiary folds, the number of potential PKR activators in a cell is high. The identification that nc886 RNA functions as a negative regulator of PKR (13) thus provides a cellular mechanism to repress spurious inhibition of translation in the absence of viral infection.

In this study, we have demonstrated that nc886 RNA can adopt two nonequivalent structures that modulate PKR activity in distinct and opposing manners. Our SHAPE structure probing studies revealed that Conformer 2 adopts an apical stem–loop structure consistent with the predicted secondary structure for nc886, specifically, high reactivity of all Loop 5 nucleotides and low reactivity for the nucleotides of the adjacent four base pair helix. In contrast, the Loop 5 nucleotides of nc886 Conformer 1 had predominantly low reactivity, and the 5'-half of the adjacent helix was found to block reverse transcriptase, independent of the presence of SHAPE probing reagent. RNA dimerization is known to influence PKR–RNA interaction, resulting in increased PKR activation (28, 32). Dimerization could potentially give rise to the relative native gel mobilities of the two nc886 conformers and result in the changes in SHAPE reactivity we observed for Conformer 1. Dimerization-based generation of a PKR-inhibitory structure would be an

unexpected mechanism of PKR regulation. However, the significantly greater stability of Conformer 1 and the equivalent native gel mobility of the PKR complexes with each conformer argue against nc886 dimerization as the difference between the two forms. Further, we have found that while neither nc886 conformer is formed in a concentration-dependent manner, both conformers form slower migrating bands on native gel at higher concentrations and both these dimeric/oligomeric forms can be disrupted by annealing at temperatures below the unfolding of Conformer 1 (data not shown). Thus, while dimerization cannot be definitively excluded, we propose based on our results that Conformer 1 adopts a higher order structure involving nucleotides of Loop 5 within its apical stem-loop and that this tertiary structure distinguishes the two monomeric forms of nc886.

nc886 Conformer 1 binds with higher affinity resulting in potent inhibition of PKR whereas Conformer 2 binds more weakly and, surprisingly, behaves as a pseudoinhibitor. As such, nc886 Conformer 2 can weakly activate the kinase but becomes inhibitory at high concentrations against a more potent activator, such as poly(rI:rC) dsRNA. These opposing functions also impact phosphorylation of PKR's substrate eIF2 $\alpha$ : nc886 Conformer 1 effectively inhibits the downstream phosphorylation of eIF2 $\alpha$ , while Conformer 2 results in no loss of eIF2 $\alpha$  phosphorylation. The two nc886 conformers adopt common terminal and central stem structures, and deletion of the terminal stem has no impact on the formation of distinct RNA conformers or the PKR binding and inhibitory potential of each compared to the wild-type RNA. In contrast, deletion of the entire apical stem-loop or just Loop 5 results in a single conformer with the same functional properties as Conformer 2. These observations demonstrate the critical

importance of the unique apical stem–loop structure of Conformer 1 for potent nc886-mediated inhibition of PKR. However, high-resolution structural analysis will be required to fully define the nc886 Conformer 1 apical stem–loop structure and thus reveal the basis for its specific ability to potently inhibit PKR. Furthermore, the nature of the two nc886 conformers has direct functional consequences for PKR regulation, and it may not be appropriate to simply consider them as active and inert forms, as previously suggested (22).

Aside from its central importance to innate immunity, PKR plays diverse roles in cell signaling pathways and during mitosis, cell differentiation, and transcriptional regulation (6, 33-37). Thus, there is a clear need for tight regulation of PKR activity in the uninfected cell in a manner which still allows for appropriate activation by cellular RNAs and proteins. Identification of opposing PKR-regulatory activities for the two nc886 conformers suggests a potential mechanism that would allow for a gradient of regulation rather than all-or-nothing PKR inhibition. We speculate that by tuning the levels of each nc886 conformer, the cell would be able to prevent basal activation of PKR in the absence of infection while still allowing for specific and timed activation in response to diverse cellular needs. The nc886 conformer levels and/or ratio could be shifted either transcriptionally or through refolding of nc886, similar to the autoregulation of IFN- $\gamma$  mRNA translation via refolding of its 5'-untranslated region into a PKR-activating structure (27). During viral infection, either conformer of nc886 RNA could be easily displaced by viral RNAs through greater binding affinity or through excess viral dsRNA, thus allowing PKR to mount an immune response. Indeed, in cells stably expressing nc886, poly(rI:rC) dsRNA transfection still elicits PKR activation (22). The

questions of if, how, and when the levels or ratios of the nc886 conformers may change during the life of the cell remain to be answered.

The importance of nc886 in the regulation of PKR activity is highlighted by both its implication in disease and by the perturbation of its function by a range of viruses (6, 10, 38, 39). Addressing what other cellular binding partners nc886 RNA may have and whether these would be shared or distinct between the two conformers would reveal potential mechanisms by which nc886 dysregulation might contribute to disease.

Moreover, viruses also inhibit PKR activity through the actions of nc886. For example, Epstein-Barr virus infection stimulated a three- to fourfold increase in the level of nc886 RNA (then named CBL3) (40) and Influenza A virus infection increased levels of nc886 (then named vtRNA 2-1) by 25-fold (41). However, whether viruses may also influence the relative expression of the nc886 conformers to promote their replication by masking detection for survival is unknown.

In summary, the current study has revealed new insights into how nc886 RNA adopts multiple conformers that are critical for its function as a regulator of PKR activity, as well as elucidating the differences both in their structure and function. Future studies building on this work would contribute to our understanding of this critical regulator of innate immunity and could potentially inform therapeutic approaches to inhibit or to stimulate the immune response through the actions of this noncoding RNA.

## **2.5 Material and Methods**

### **2.5.1 RNA *in vitro* transcription and purification**

Full-length and variant nc886 RNAs were *in vitro* transcribed from linearized plasmid

DNA templates using T7 RNA polymerase as previously described (42). nc886 variants were produced in the same way from plasmids encoding sequences with the following changes: deletion of nucleotides 1–12 and 88–101 (nc886 $\Delta$ TS), deletion of nucleotides 36–63 (nc886 $\Delta$ AS), and deletion of nucleotides 44–48 with additional U50 to G mutation (nc886 $\Delta$ L5). Following dialysis against 1 $\times$  Tris–EDTA (TE) buffer, RNAs were purified by polyacrylamide gel electrophoresis (PAGE) on denaturing (50% urea, 1 $\times$  Tris–Borate–EDTA [TBE]) or native (0.5 $\times$  TBE) gels. RNA bands were identified by UV shadowing, excised, eluted from the gel by crushing and soaking in 0.3 M sodium acetate, and ethanol precipitated as previously described (42).

### **2.5.2 PKR and eIF2 $\alpha$ protein expression and purification**

For PKR expression, *E. coli* Rosetta 2 (DE3) cells were transformed with the pET-PKR/PPase plasmid encoding full-length human PKR (43). Single colonies were used to inoculate large-scale cultures in Terrific Broth. PKR expression was induced with 0.1 mM isopropyl  $\beta$ -D-1-thiogalactopyranoside (IPTG) at mid-log phase growth (OD<sub>600</sub> ~0.5) and growth continued overnight at 20°C. PKR was purified by sequential heparin-affinity (HiPrep Heparin 16/10), poly(rI:rC) dsRNA-affinity, and gel filtration (Superdex 200 10/300) chromatographies on an ÄKTApurifier10 system (GE Healthcare). PKR was eluted from the gel filtration column in 20 mM HEPES buffer (pH 7.5) containing 150 mM NaCl, 0.1 mM EDTA, 10% glycerol, and 10 mM  $\beta$ -mercaptoethanol (BME).

For eIF2 $\alpha$  expression, *E. coli* BL21 (DE3) cells were transformed with a plasmid encoding an amino-terminal hexa-histidine-tagged human eIF2 $\alpha$ . Single colonies were

used to inoculate large-scale cultures in Lysogeny Broth. eIF2 $\alpha$  expression was induced with 0.1 mM IPTG at mid-log phase growth ( $OD_{600} \sim 0.5$ ) and growth continued overnight at 18°C. eIF2 $\alpha$  was purified using a bench-top HisSpinTrap column (GE Healthcare). Fractions containing the protein were pooled and further purified by gel filtration chromatography (Superdex 200 10/300) on an ÄKTApurifier10 system. eIF2 $\alpha$  was eluted from the gel filtration column in 20 mM HEPES buffer (pH 7.5) containing 150 mM NaCl, 0.1 mM EDTA, 10% glycerol, and 10 mM BME.

### **2.5.3 RNA UV thermal melting analysis**

RNA UV melting curves were collected at 260 and 280 nm on a Cary400 UV-visible spectrophotometer (Varian). Samples contained 20–25  $\mu$ g of RNA in a solution of either 0.5 $\times$  TBE or 20 mM HEPES buffer (pH 7.5) containing 100 mM NaCl. To simplify comparisons between RNA constructs, the first derivative of each UV absorbance curve (the “melting profile”) was calculated for each RNA in GraphPad Prism6 software after normalization using the following equation:  $(Abs_T - Abs_{Tmin})/Abs_{Tmin}$ .

### **2.5.4 Electrophoretic mobility shift assays (EMSA)**

A range of PKR concentrations, from 0–3  $\mu$ M, was incubated with 300 nM full-length or variant nc886 RNA for 30 min on ice in 20 mM HEPES (pH 7.5) 150 mM NaCl, 10% glycerol, and 2 mM EDTA. After incubation, free and bound RNAs were resolved by native PAGE (10% acrylamide, 0.5 $\times$  TBE). Gels were stained with SYBR Green gel stain for 20 min and visualized on a Typhoon FLA 7000 (GE Healthcare) using the fluorescence setting and a 520 nm emission filter. EMSAs were repeated at least two

times producing essentially identical results.

### **2.5.5 PKR inhibition assays**

PKR (0.1  $\mu\text{g}$ ) was preincubated with 0–10  $\mu\text{M}$  of full-length or variant nc886 RNA for 10 min at 25°C in 50 mM Tris buffer (pH 7.8) containing 50 mM KCl, 2.5 mM DTT, and 10% glycerol. Reactions were initiated by the addition of 0.05  $\mu\text{g}/\text{mL}$  poly(rI:rC) dsRNA, 20  $\mu\text{M}$  ATP, 1  $\mu\text{Ci}$  [ $\gamma$ <sup>32</sup>P]-ATP, and 2 mM  $\text{MgCl}_2$ . After incubation at 25°C for 10 min, reactions were quenched with excess ice-cold phosphate buffered saline containing 200  $\mu\text{M}$  ATP and applied to a Bio-Dot SF (Bio-Rad) microfiltration system as described previously (23). Membranes were exposed to a phosphor storage screen and the extent of phosphorylation was determined by analysis on a Typhoon FLA 7000 PhosphorImager and ImageQuant software (GE Healthcare). Assays were repeated at least two times for each RNA and normalized to a control lacking nc886 RNA after background subtraction. Assays of inhibition of eIF2 $\alpha$  phosphorylation were carried out as described above but at a single nc886 RNA concentration (10  $\mu\text{M}$ ) and with the additional inclusion of 0.25  $\mu\text{g}$  eIF2 $\alpha$  in the reaction initiation mixture. Reactions were quenched by the addition of gel loading dye for SDS-PAGE analysis. Gels were dried and exposed to a phosphor storage screen and analyzed as above. Assays of PKR and eIF2 $\alpha$  inhibition were repeated at least three times for each RNA. Phosphorylation intensity for each protein was normalized to a reaction lacking nc886 after background subtraction from a control reaction lacking both poly(rI:rC) dsRNA and nc886.

### **2.5.6 PKR activation assays**

PKR (0.1  $\mu\text{g}$ ) was incubated with 0–10  $\mu\text{M}$  of full-length or variant nc886 RNA for 10 min at 25°C in 50 mM Tris buffer (pH 7.8) containing 50 mM KCl, 2.5 mM DTT, 10% glycerol, 20  $\mu\text{M}$  ATP, 1  $\mu\text{Ci}$  [ $\gamma^{32}\text{P}$ ]-ATP, and 2 mM  $\text{MgCl}_2$ . After incubation, reactions were quenched with excess ice-cold phosphate buffered saline containing 200  $\mu\text{M}$  ATP and applied to a Bio-Dot SF (Bio-Rad) microfiltration system as described previously (23). Membranes were exposed to a phosphor storage screen and the extent of phosphorylation was determined using analysis by a Typhoon FLA 7000 PhosphorImager and ImageQuant software (GE Healthcare). Values were normalized to a poly(rI:rC) (0.1  $\mu\text{g}/\text{mL}$ ) reaction performed in parallel, following background subtraction from a control reaction without nc886 RNA. Assays were repeated at least three times for each RNA.

#### **2.5.7 Selective 2'-hydroxyl acylation analyzed by primer extension (SHAPE)**

SHAPE RNA probing with NMIA was carried out as described previously (44) with the following modifications: Reactions were initiated using 1  $\mu\text{L}$  of 130 mM NMIA for 45 min at 37°C. Reverse transcription was carried out with a 5'-end labeled [ $\gamma^{32}\text{P}$ ]-ATP DNA primer corresponding to the sequence of the 3'-end of the RNA (nucleotides 84–101 for both conformers) or to an internal sequence (nucleotides 36–54 for Conformer 1 only). To determine the position of each SHAPE reactive nucleotide, dideoxy nucleotide (ddNTP) sequencing was carried out using the radiolabeled primer and untreated RNA. All reactions were run on sequencing gels, dried, and exposed to a phosphor storage screen. The intensity of bands was analyzed on a Typhoon Trio Imager and quantified using ImageQuant software (GE Healthcare). Following subtraction of background reactivity in the no NMIA lanes, reactivity at each nucleotide was normalized and the

values from at least two replicates were averaged and classified as 5.5%–11%, 11%–22%, and >22% (44). SHAPE reactivity for nc886 Conformer 1 was separately normalized to highest reactivity in each data set for the external and internal primers.

## **2.6 Acknowledgments**

We thank Dr. Christine M. Dunham and Samantha L. Schwartz for their comments on the manuscript and the members of the Conn and Dunham groups for useful discussions during the course of this work. This work was supported by a Bridge Funding Award from the Emory University School of Medicine and the Department of Biochemistry, and by the Biochemistry, Cell and Molecular Biology (BCMB) National Institutes of Health/National Institute of General Medical Sciences training grant T32-GM008367.

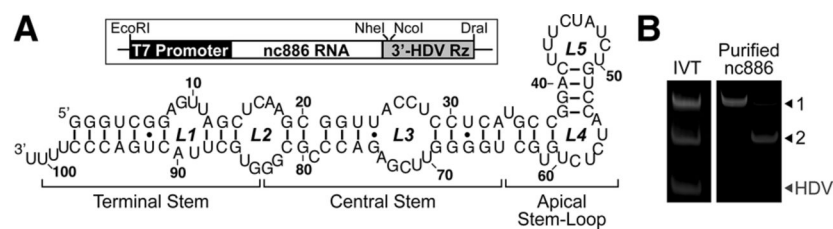


**Figure 2.1 nc886 RNA forms two distinct, noninterconverting conformers that can be isolated and characterized separately.** A. The predicted secondary structure of nc886 derived using Mfold software (45), with the three regions of the RNA referred to in the main text indicated below. *Inset*, schematic of the construct used to produce the nc886-HDV ribozyme *in vitro* transcript. B. Native PAGE analysis of the *in vitro* transcription reaction (IVT) and purified nc886 conformers stained with ethidium bromide.

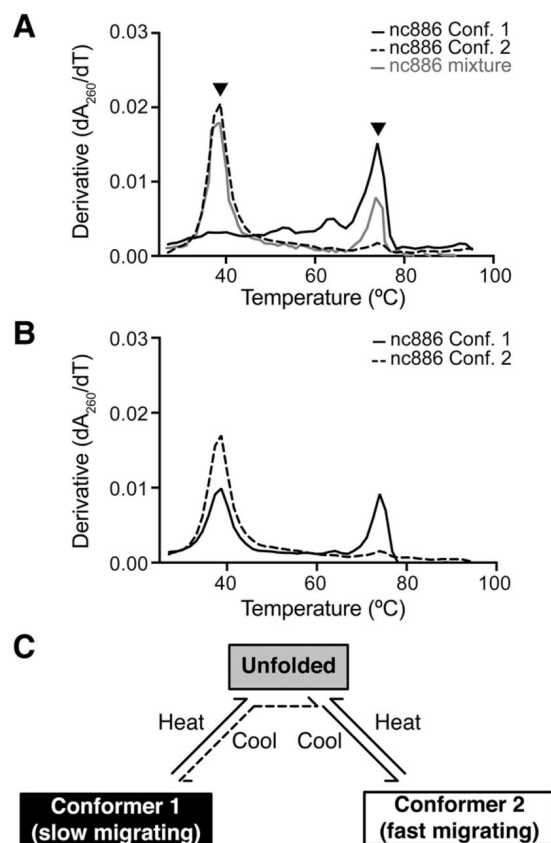


**Figure 2.2 nc886 conformer stability and refolding.** A. UV melting profiles of each isolated native PAGE purified nc886 RNA conformer, and of a mixture of the two produced by denaturing PAGE purification. Melting temperatures ( $T_m$ ) for the major apparent unfolding transitions (marked with arrowheads) are listed in Table 1. B. UV melting profiles for each conformer of nc886 after complete thermal denaturation ( $>90^{\circ}\text{C}$ ) and refolding. C. Schematic illustrating the observed interconversion properties of each nc886 conformer. Under native conditions both conformers are stable and do not interconvert (*lower boxes*). Following denaturation (Heat) and refolding (Cool), Conformer 1 can re-adopt its original structure or refold as Conformer 2 (dashed double arrow), while in contrast Conformer 2 only refolds into its original form.

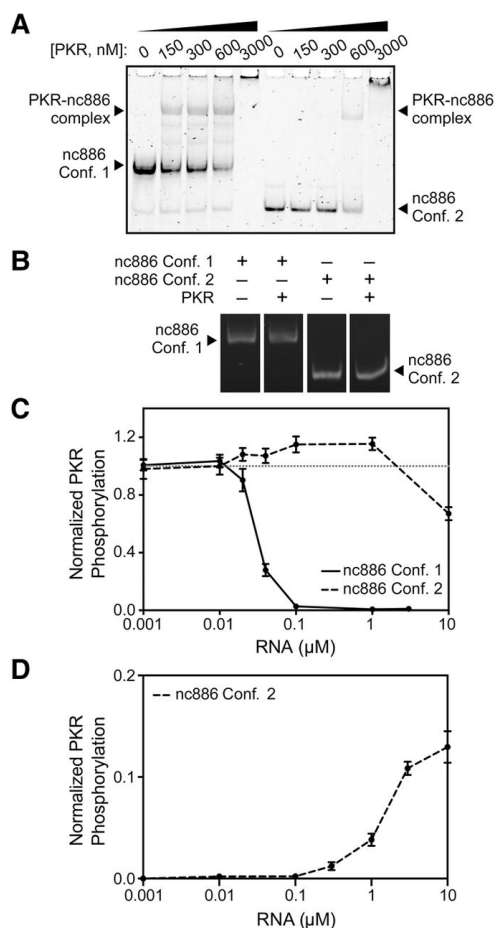


**Figure 2.3 The individual nc886 conformers have distinct activities against PKR. A.**

EMSA analysis of binding of each individual nc886 conformer to PKR. Native PAGE gels were stained with SYBR Green to identify free and PKR-bound RNA. B. Native PAGE analysis of purified conformers extracted following incubation with or without PKR demonstrating that nc886 conformers do not undergo PKR binding-induced conformational interconversion. C. Quantification of slot-blot radiometric PKR autophosphorylation inhibition assays with each individual isolated nc886 conformer. The dotted line represents the extent of PKR phosphorylation, in the absence of any nc886 RNA, at the fixed concentration of poly(rI:rC) dsRNA activator used in all samples. D. Radiometric PKR autophosphorylation activation assay demonstrating the capacity of nc886 Conformer 2 to weakly activate PKR.

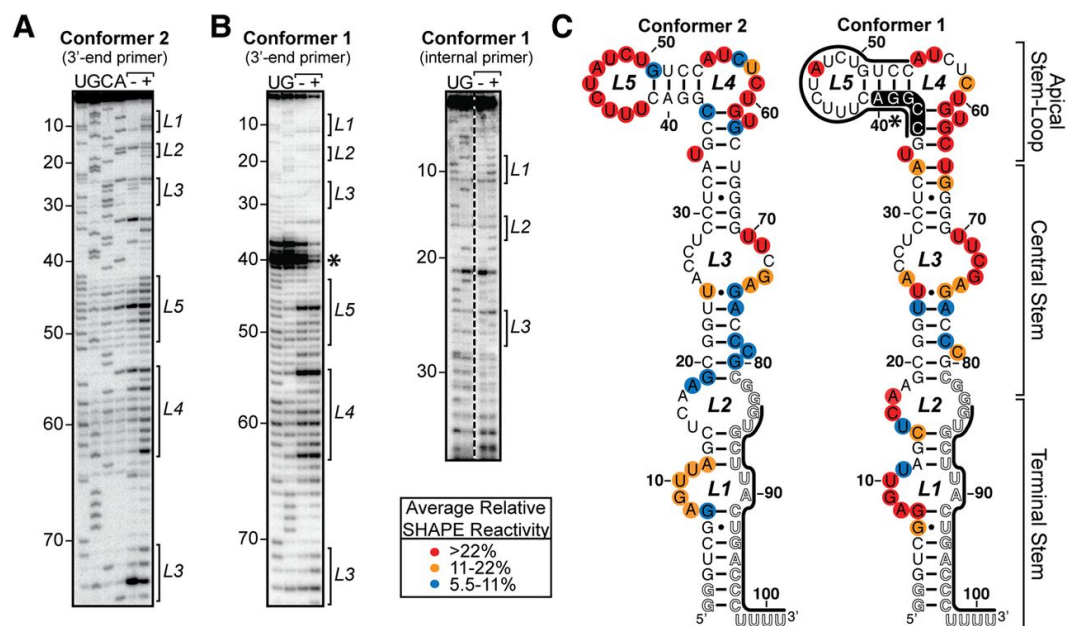


**Figure 2.4** The apical stem–loop of nc886 distinguishes the two RNA conformers. **A.**

Example autoradiogram of sequencing gel analysis of nc886 Conformer 2 SHAPE probing. Lanes are: –, mock treated (no NMIA); +, NMIA treated; and, U/G/C/A, sequencing lanes containing the complementary dideoxy NTP. Brackets on the *right* of the gel image denote the loop regions (L1–L5) in the predicted nc886 RNA secondary structure. **B.** Example autoradiogram of sequencing gel analysis of nc886 Conformer 1 SHAPE probing using either the 3'-end (*left*) or internal (*right*) primer. Lane labels are the same as Panel *A*. **C.** Categorized average nucleotide SHAPE reactivity for each conformer mapped onto the predicted nc886 secondary structure. Also noted are the sequences complementary to the 3'-end and internal primers (thick black lines), nucleotides for which reactivity could not be determined (outline font), and the strong structure-induced RT stops (nucleotides 36–40) observed only for nc886 Conformer 1 (black shading and region marked by an asterisk in panels *B* and *C*).

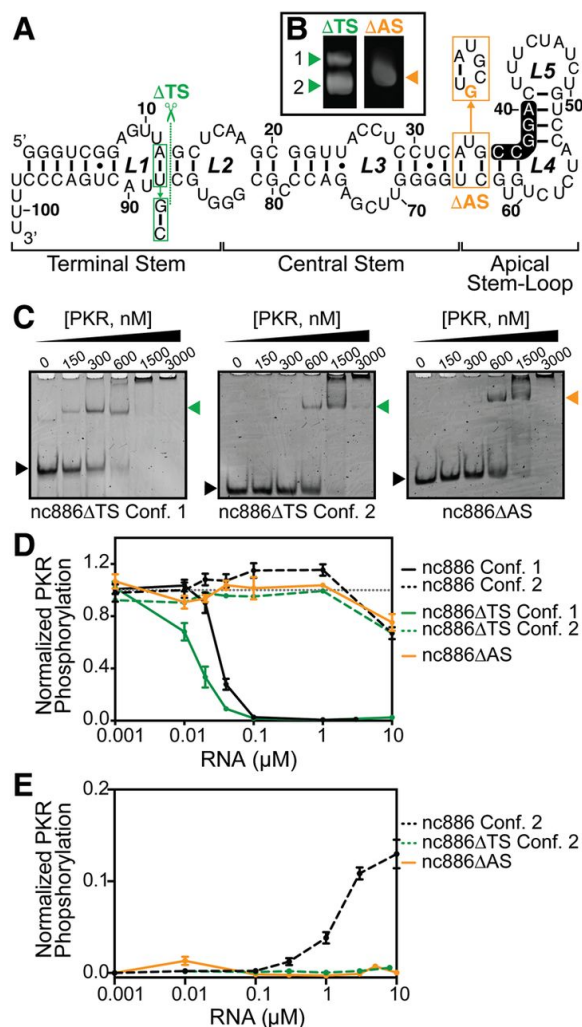


**Figure 2.5 Binding and inhibition of PKR by terminal stem and apical stem–loop deletion variants of nc886 RNA.** A. Schematic showing the RNA regions and sites of truncation for the nc886 terminal stem and the apical stem–loop to create variants nc886ΔTS (deletion of nucleotides 1–12 and 88–101) and nc886ΔAS (deletion of nucleotides 36–63), respectively. One additional sequence alteration (G insertion) in nc886ΔAS is highlighted within the orange dashed line boxes. B. Native PAGE analysis of *in vitro* transcribed variant nc886 RNAs. nc886ΔTS, but not nc886ΔAS, maintains formation of two conformers. C. EMSA analysis of RNA variants binding to PKR for nc886ΔTS Conformer 1, nc886ΔTS Conformer 2, and nc886ΔAS RNAs. Native PAGE

gels were stained with SYBR Green to identify free (black arrows) and PKR-bound RNA (green or orange). D. Quantification of slot-blot radiometric PKR autophosphorylation inhibition assays with nc886 $\Delta$ TS Conformer 1 (solid green line), nc886 $\Delta$ TS Conformer 2 (dashed green line), and nc886 $\Delta$ AS (solid orange line). Full-length nc886 data (black lines) shown for comparison are the same as those shown in Figure 2.3C. The dotted line represents the extent of PKR phosphorylation, in the absence of any nc886 RNA, at the fixed concentration of poly(rI:rC) dsRNA activator used in all samples. E. Radiometric PKR autophosphorylation activation assay demonstrating the loss of PKR activation in nc886 $\Delta$ AS (solid orange line) and nc886 $\Delta$ TS Conformer 2 (dashed green line), as compared to full-length nc886 Conformer 2 (dashed black line). nc886 Conformer 2 data are the same as those shown in Figure 2.3D.

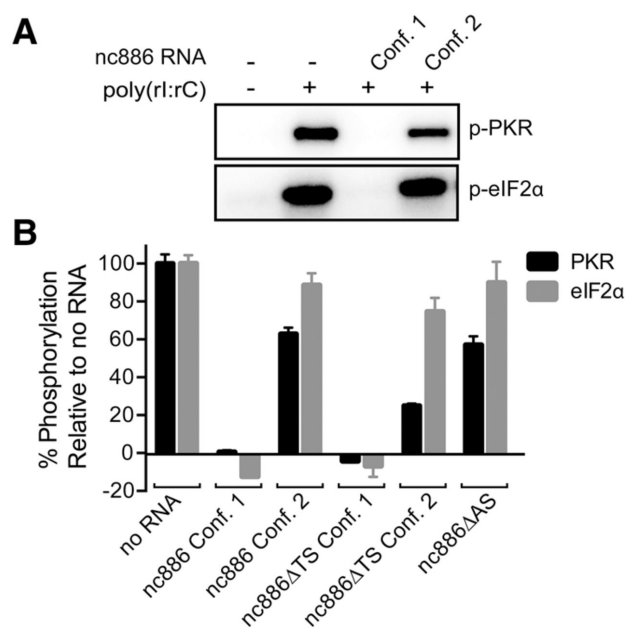


**Figure 2.6 Inhibition of PKR phosphorylation of eIF2 $\alpha$  substrate by wild-type and nc886 RNA variants.** A. Example SDS-PAGE analysis of a radiometric kinase inhibition assay containing both PKR and eIF2 $\alpha$  substrate. B. Quantification of PKR and eIF2 $\alpha$  phosphorylation in the presence of fixed concentrations of poly(rI:rC) RNA (0.05  $\mu$ g/mL) and the indicated nc886 RNA variant (10  $\mu$ M) normalized to a no RNA control after background subtraction.

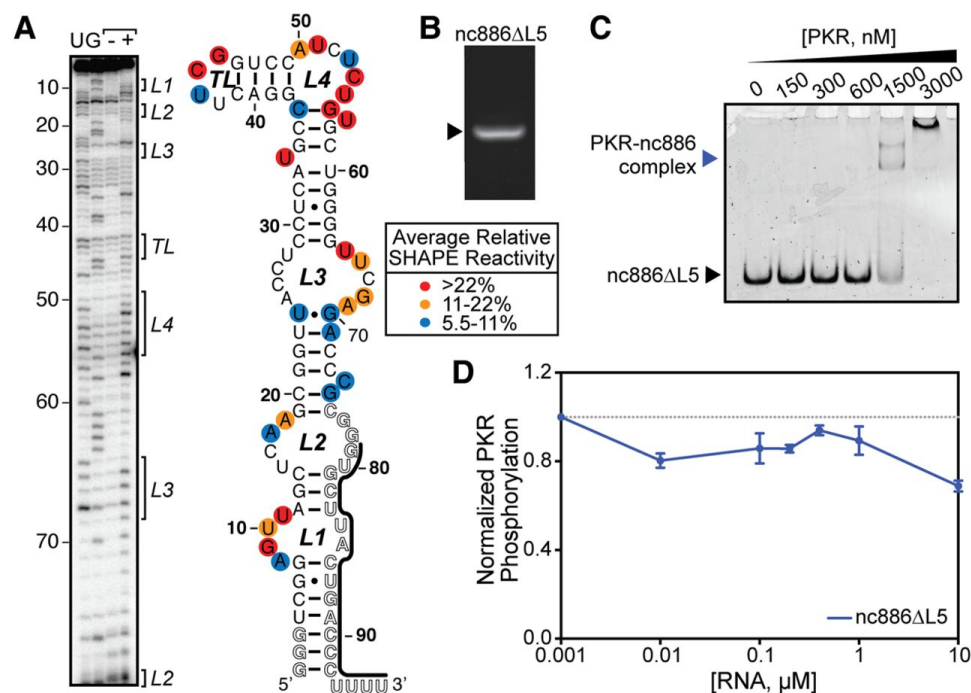


**Figure 2.7** Alteration of loop 5 (nucleotides 44–48; nc886ΔL5) disrupts the structure specific to nc886 Conformer 1 and abrogates PKR inhibition. **A.** *Left*, example autoradiogram of sequencing gel analysis of nc886ΔL5 SHAPE probing. Lanes are: –, mock treated (no NMIA); +, NMIA treated; and, U/G, sequencing lanes containing the complementary dideoxy NTP. Brackets on the *right* of the gel image denote the loop regions (L1 to TL) in the predicted nc886 RNA secondary structure. *Right*, categorized average nucleotide SHAPE reactivity mapped onto the predicted secondary structure. **B.** Native PAGE analysis of nc886ΔL5 RNA. **C.** EMSA analysis of nc886ΔL5 RNA binding to PKR using SYBR Green staining to identify free (black arrow) and PKR-bound RNA (blue arrow). **D.** Quantification of slot-blot radiometric PKR autophosphorylation inhibition assays with nc886ΔL5. The dotted line represents the extent of PKR phosphorylation, in the absence of any nc886 RNA, at the fixed concentration of poly(rI:rC) dsRNA activator used in all samples.

**TABLE 1.** Apparent melting temperatures ( $T_m$ ) for wild-type and variant nc886 unfolding

RNA	Apparent $T_m$ ( $^{\circ}\text{C}$ ) <sup>a</sup>	
	0.5 $\times$ TBE	HEPES/NaCl
nc886 Conf. 1	73.8	92.2
nc886 Conf. 2	38.2	58.4
nc886 $\Delta$ TS Conf. 1	71.7	87.7
nc886 $\Delta$ TS Conf. 2	31.8	52.8
nc886 $\Delta$ AS	44.4	61.6
nc886 $\Delta$ L5	37.6	59.4

<sup>a</sup>Value is for the major peak in the melting profile under each condition (0.5  $\times$  Tris–Borate–EDTA buffer or 20 mM HEPES buffer pH 7.5 containing 100 mM NaCl). Estimated error for  $T_m$  values  $\pm 0.5^{\circ}\text{C}$ .

**Table 2.1 Apparent melting temperatures ( $T_m$ ) for wild-type and variant nc886 unfolding**

## 2.7 References

1. Schoggins JW & Rice CM (2011) Interferon-stimulated genes and their antiviral effector functions. *Current Opinion in Virology* 1(6):519-525.
2. Iwasaki A (2012) A Virological View of Innate Immune Recognition. *Annual Review of Microbiology* 66(1):177-196.
3. Yoneyama M & Fujita T (2010) Recognition of viral nucleic acids in innate immunity. *Rev. Med. Virol.* 20(1):4-22.
4. Dalet A, Gatti E, & Pierre P (2015) Integration of PKR-dependent translation inhibition with innate immunity is required for a coordinated anti-viral response. *FEBS Lett* 589(14):1539-1545.
5. Schlee M & Hartmann G (2016) Discriminating self from non-self in nucleic acid sensing. *Nat Rev Immunol* 16(9):566-580.
6. Garcia MA, *et al.* (2006) Impact of Protein Kinase PKR in Cell Biology: from Antiviral to Antiproliferative Action. *Microbiology and Molecular Biology Reviews* 70(4):1032-1060.
7. Balachandran S & Barber GN (2007) PKR in innate immunity, cancer, and viral oncolysis. *Methods Mol Biol* 383:277-301.
8. Sudhakar A, *et al.* (2000) Phosphorylation of serine 51 in initiation factor 2 alpha (eIF2 alpha) promotes complex formation between eIF2 alpha(P) and eIF2B and causes inhibition in the guanine nucleotide exchange activity of eIF2B. *Biochemistry* 39(42):12929-12938.
9. Yamasaki S & Anderson P (2008) Reprogramming mRNA translation during stress. *Curr Opin Cell Biol* 20(2):222-226.
10. Langland JO, Cameron JM, Heck MC, Jancovich JK, & Jacobs BL (2006) Inhibition of PKR by RNA and DNA viruses. *Virus Research* 119(1):100-110.
11. McKenna SA, Lindhout DA, Shimoike T, Aitken CE, & Puglisi JD (2007) Viral dsRNA Inhibitors Prevent Self-association and Autophosphorylation of PKR. *Journal of Molecular Biology* 372(1):103-113.
12. Domingo-Gil E, Toribio R, Najera JL, Esteban M, & Ventoso I (2011) Diversity in viral anti-PKR mechanisms: a remarkable case of evolutionary convergence. *PLoS One* 6(2):e16711.
13. Lee K, *et al.* (2011) Precursor miR-886, a novel noncoding RNA repressed in cancer, associates with PKR and modulates its activity. *RNA* 17(6):1076-1089.
14. Treppendahl MB, *et al.* (2011) Allelic methylation levels of the noncoding VTRNA2-1 located on chromosome 5q31.1 predict outcome in AML. *Blood* 119(1):206-216.
15. Xiong Y, *et al.* (2011) MiR-886-3p regulates cell proliferation and migration, and is dysregulated in familial non-medullary thyroid cancer. *PLoS One* 6(10):e24717.
16. Kunkeaw N, *et al.* (2012) Cell death/proliferation roles for nc886, a non-coding RNA, in the protein kinase R pathway in cholangiocarcinoma. *Oncogene* 32(32):3722-3731.
17. Cao J, *et al.* (2013) DNA Methylation-Mediated Repression of miR-886-3p Predicts Poor Outcome of Human Small Cell Lung Cancer. *Cancer Research* 73(11):3326-3335.

18. Lee HS, *et al.* (2014) Epigenetic silencing of the non-coding RNA nc886 provokes oncogenes during human esophageal tumorigenesis. *Oncotarget* 5(11):3472-3481.
19. Lee KS, *et al.* (2014) nc886, a non-coding RNA of anti-proliferative role, is suppressed by CpG DNA methylation in human gastric cancer. *Oncotarget* 5(11):3944-3955.
20. Romanelli V, *et al.* (2014) Variable maternal methylation overlapping the nc886/vtRNA2-1 locus is locked between hypermethylated repeats and is frequently altered in cancer. *Epigenetics* 9(5):783-790.
21. Lee YS (2015) A Novel Type of Non-coding RNA, nc886, Implicated in Tumor Sensing and Suppression. *Genomics Inform* 13(2):26-30.
22. Jeon SH, *et al.* (2012) Characterization of the direct physical interaction of nc886, a cellular non-coding RNA, and PKR. *FEBS Lett* 586(19):3477-3484.
23. Sunita S, Schwartz SL, & Conn GL (2015) The Regulatory and Kinase Domains but Not the Interdomain Linker Determine Human Double-stranded RNA-activated Kinase (PKR) Sensitivity to Inhibition by Viral Non-coding RNAs. *J Biol Chem* 290(47):28156-28165.
24. Osman F, Jarrous N, Ben-Asouli Y, & Kaempfer R (1999) A cis-acting element in the 3'-untranslated region of human TNF-alpha mRNA renders splicing dependent on the activation of protein kinase PKR. *Genes & Development* 13(24):3280-3293.
25. Nussbaum JM (2002) The 3'-untranslated regions of cytoskeletal muscle mRNAs inhibit translation by activating the double-stranded RNA-dependent protein kinase PKR. *Nucleic Acids Research* 30(5):1205-1212.
26. Kim I, Liu CW, & Puglisi JD (2006) Specific Recognition of HIV TAR RNA by the dsRNA Binding Domains (dsRBD1–dsRBD2) of PKR. *Journal of Molecular Biology* 358(2):430-442.
27. Cohen-Chalamish S, *et al.* (2009) Dynamic refolding of IFN- $\gamma$  mRNA enables it to function as PKR activator and translation template. *Nature Chemical Biology* 5(12):896-903.
28. Heinicke LA, *et al.* (2009) RNA Dimerization Promotes PKR Dimerization and Activation. *Journal of Molecular Biology* 390(2):319-338.
29. Nallagatla SR, Toroney R, & Bevilacqua PC (2011) Regulation of innate immunity through RNA structure and the protein kinase PKR. *Current Opinion in Structural Biology* 21(1):119-127.
30. Džananović E, *et al.* (2013) Recognition of viral RNA stem-loops by the tandem double-stranded RNA binding domains of PKR. *RNA* 19(3):333-344.
31. Mayo CB, Wong CJ, Lopez PE, Lary JW, & Cole JL (2016) Activation of PKR by short stem-loop RNAs containing single-stranded arms. *RNA* 22(7):1065-1075.
32. Hull CM & Bevilacqua PC (2016) Discriminating Self and Non-Self by RNA: Roles for RNA Structure, Misfolding, and Modification in Regulating the Innate Immune Sensor PKR. *Acc Chem Res* 49(6):1242-1249.
33. García MA, Meurs EF, & Esteban M (2007) The dsRNA protein kinase PKR: Virus and cell control. *Biochimie* 89(6-7):799-811.
34. Kang R & Tang D (2012) PKR-Dependent Inflammatory Signals. *Science Signaling* 5(247):pe47-pe47.

35. Liu S, *et al.* (2013) MAVS recruits multiple ubiquitin E3 ligases to activate antiviral signaling cascades. *eLife* 2:e00785.
36. Kim Y, *et al.* (2014) PKR is activated by cellular dsRNAs during mitosis and acts as a mitotic regulator. *Genes & Development* 28(12):1310-1322.
37. Youssef OA, *et al.* (2015) Potential role for snoRNAs in PKR activation during metabolic stress. *Proc Natl Acad Sci U S A* 112(16):5023-5028.
38. Roberts LO, Jopling CL, Jackson RJ, & Willis AE (2009) Viral strategies to subvert the mammalian translation machinery. *Prog Mol Biol Transl Sci* 90:313-367.
39. Marchal JA, *et al.* (2014) The impact of PKR activation: from neurodegeneration to cancer. *FASEB J* 28(5):1965-1974.
40. Nandy C, *et al.* (2009) Epstein-barr virus-induced expression of a novel human vault RNA. *J Mol Biol* 388(4):776-784.
41. Li F, *et al.* (2015) Robust expression of vault RNAs induced by influenza A virus plays a critical role in suppression of PKR-mediated innate immunity. *Nucleic Acids Res* 43(21):10321-10337.
42. Linpinsel JL & Conn GL (2012) General Protocols for Preparation of Plasmid DNA Template, RNA In Vitro Transcription, and RNA Purification by Denaturing PAGE. in *Recombinant and In Vitro RNA Synthesis* (Springer Science + Business Media), pp 43-58.
43. Lemaire PA, Anderson E, Lary J, & Cole JL (2008) Mechanism of PKR Activation by dsRNA. *Journal of Molecular Biology* 381(2):351-360.
44. Wilkinson KA, Merino EJ, & Weeks KM (2006) Selective 2'-hydroxyl acylation analyzed by primer extension (SHAPE): quantitative RNA structure analysis at single nucleotide resolution. *Nat Protoc* 1(3):1610-1616.
45. Zuker M (2003) Mfold web server for nucleic acid folding and hybridization prediction. *Nucleic Acids Research* 31(13):3406-3415.

## Chapter 3

### Activation of the OAS/ RNase L pathway by a human cellular non-coding RNA

Brenda M. Calderon and Graeme L. Conn

A version of this manuscript is in preparation for submission for publication.

#### 3.1 Abstract

The 2'-5'-oligoadenylate synthetase (OAS) family of enzymes sense double-stranded RNA (dsRNA) in the cytosol, a potent signal of viral infection. In response to dsRNA-binding, OAS proteins synthesize 2'-5'-linked oligoadenylate second messengers that activate the latent ribonuclease L (RNase L). Degradation of viral and cellular RNA by RNase L effectively halts viral replication and further induces innate immune responses by induction of Type I Interferon. The OAS/RNase L pathway is thus central in innate immune recognition and promotion of host antiviral responses. The specific RNA features that drive potent OAS1 activation are currently not fully understood. Moreover, cellular regulators of OAS activity are not well defined. Here, we demonstrate that the cellular non-coding RNA 886 (nc886) potently activates OAS *in vitro* and in human A549 cells. We show that a unique structure present only in one of the two conformers adopted by nc886 is responsible for potentiating OAS1 activity. Formation of this structural motif is dependent on the nucleotides in the apical-most loop of nc886 and the adjacent helix. These findings represent the discovery of a cellular RNA capable of activating the OAS/RNase L pathway in cells and illustrate the importance of structural

elements, and their context, in potentiating OAS1 activity.

### 3.2 Introduction

The innate immune response serves as a critical first line of defense against pathogens, comprising membrane-bound and cytosolic pattern recognition receptors (PRRs) that detect bacterial or viral pathogen-associated molecular patterns (1, 2). For example, accumulation of double-stranded RNA (dsRNA) in the cell cytoplasm is a potent signal of viral infection and is detected by PRRs including Toll-like receptors 3, 7, and 8, dsRNA-activated protein kinase (PKR), and the retinoic acid-inducible gene I (RIG-I)-like and 2'-5'-oligoadenylate synthetase (OAS) families of enzymes (3, 4).

OAS enzymes are activated by dsRNA and initiate signaling cascades to halt viral replication and establish an antiviral state in the cell. The OAS family includes three catalytically active, 2'-specific nucleotidyl transferases, OAS1/2/3, whose action is effected by the latent ribonuclease L (RNase L), and a catalytically inactive form, OASL, which acts in the RIG-I pathway (5, 6). The catalytically active OAS proteins differ by the number of copies of the 2'-5'-oligoadenylate synthetase domain although only one copy is catalytically active in each protein (7). In OAS1, binding of short dsRNA ( $\geq 17$  base pairs) drives a conformational change that organizes the enzyme active site, resulting in synthesis of 2'-5'-linked oligoadenylate (2-5A) second messengers that in turn activate RNase L (8-10). In OAS3, the N-terminal 2'-5'-oligoadenylate synthetase domain serves as a dsRNA-binding module, while the third C-terminal domain carries out 2-5A synthesis, thus making OAS3 selective for longer dsRNA ( $\geq 50$  base pairs) (11). The immediate consequence of OAS/RNase L pathway activation is the degradation of

viral and cellular messenger RNA (mRNA) and ribosomal RNA (rRNA) to halt protein synthesis and thus prevent viral replication (12-16). More recent evidence also suggests that OAS/RNase L-mediated translational arrest arises, in part, via specific cleavage of cellular transfer RNAs (tRNA) and Y RNAs (17).

Precisely how PRRs distinguish “self” from “non-self” and how basal activity of constitutively expressed PRRs is regulated in the absence of infection are important areas of current investigation. PKR, for example, is well established as a critical sensor of dsRNA during viral infection and effector of other important cellular processes (18-22). Recent evidence suggests that basal PKR activity is specifically regulated by the ubiquitously expressed, 101-nucleotide cellular non-coding RNA 886 (nc886) to ensure the proper detection of foreign dsRNA while preventing spurious activation in the uninfected cell (23-25).

Our previous work has demonstrated that nc886 RNA adopts two structurally distinct conformers, distinguished by their apical stem-loop structures (Figure 3.1A), which possess opposing activities in the regulation of PKR activity (26). We also previously reported that the mixture of nc886 conformers appeared to strongly activate OAS1 and that this activity was only modestly reduced by deletion of the 3'-end single-stranded pyrimidine-rich (3'-ssPy) motif that more significantly potentiates activity by viral non-coding RNAs (27). Here, we show that, as is the case for PKR regulation, the two nc886 conformers exhibit starkly differing capacities to activate the OAS/RNase L pathway: while one nc886 conformer is a potent activator of OAS1 *in vitro* and in human lung adenocarcinoma A549 cells, the other activates only very weakly. We further show that potent activation is dependent on an intact nc886 apical stem structure revealing

distinct, but overlapping requirements for nc886-mediated regulation of PKR and OAS/RNase L. Thus, nc886 may serve as a key regulator of these two arms of the innate immune response at distinct times depending on the needs of the cell.

### 3.3 Results and Discussion

#### 3.3.1 OAS1 is potently activated by a single nc886 RNA conformer

To discern the capacity of each individual nc886 conformer to activate OAS1, each conformer was purified by native polyacrylamide gel electrophoresis (PAGE) and tested using an established *in vitro* OAS1 assay (27, 28). nc886 Conformer 1 potently activates OAS1, with activity near that measured for the synthetic dsRNA poly(rI:rC) under the standard conditions used (Figure 3.1B). In stark contrast, nc886 Conformer 2 has dramatically attenuated activity. This limited capacity to activate OAS1 is, however, still comparable to that of structured viral ncRNAs (27).

Next, we quantified the differing ability of each nc886 conformer to promote OAS1 activity using a complete *in vitro* kinetic analysis of 2-5A synthesis by OAS1 over a range of nc886 Conformer 1 or nc886 Conformer 2 concentrations (Figure 3.1C). The presence of the apical stem-loop structure of nc886 Conformer 1 increases the  $V_{\max}$  more than 8-fold ( $11.6 \pm 0.7$  and  $1.3 \pm 1.4$  nmol/min for Conformer 1 and Conformer 2, respectively). The most significant impact, however, is observed for the interaction of OAS1 and nc886 with a ~30-fold difference in apparent binding affinity ( $K_{\text{app}}$ ) when the tertiary structure is present ( $0.23 \pm 0.0$  and  $7.4 \pm 10.7$   $\mu\text{M}$  for Conformer 1 and Conformer 2, respectively).

### 3.3.2 nc886 Conformer 1 activates the OAS/RNase L pathway in human A549 cells

We next assessed the ability of nc886 conformers to activate the OAS/RNase L pathway in human A549 cells, which basally express OAS1 and OAS3 without interferon treatment (29). A549 cells were transfected with nc886 Conformer 1, nc886 Conformer 2, or a truncated version of adenoviral VA RNA<sub>1</sub> (TSA $\Delta$ 21), an RNA of comparable size (99 nts) to nc886 previously shown to very weakly activate OAS1 (30-32). Prior to each transfection, native PAGE analysis was used to confirm the conformational identity of nc886 RNAs used for transfections (Figure 3.2A). At 3 hours post-transfection, total cellular RNA was extracted and analyzed by agarose gel electrophoresis to monitor rRNA cleavage by RNase L (Figure 3.2B). nc886 Conformer 1 drives significant rRNA degradation, comparable to poly(rI:rC) dsRNA and consistent with strong activation of the OAS/RNase L pathway. In contrast, nc886 Conformer 2 shows no detectable rRNA degradation, with rRNA integrity remaining identical to untransfected and mock-transfected controls. Finally, consistent with its known *in vitro* activity (32), transfection with VA RNA<sub>1</sub> (TSA $\Delta$ 21) resulted in a small amount of rRNA cleavage. These results thus mirror the activity seen for each nc886 conformer in our *in vitro* chromogenic assay (Figure 3.1B). Further, nc886-mediated rRNA cleavage activity is completely absent in A549 cells lacking RNase L (RNASEL KO), confirming that the observed rRNA cleavage results exclusively from activation of the OAS/RNase L pathway by nc886 Conformer 1 (Figure 3.2C).

### 3.3.3 The nc886 terminal stem is dispensable for activation of OAS1

To test the contributions of different regions of the RNA to OAS1 activation, four nc886

variants were prepared (Figure 3.3A) with truncations of the terminal stem ( $\Delta$ T<sub>S</sub>, deletion of nts 1-12 and 88-101; and,  $\Delta$ T<sub>S</sub>2, deletion of nts 1-18 and 82-101), the terminal stem and central stem ( $\Delta$ C<sub>S</sub>, deletion of nts 1-28 and 70-101), or the apical stem-loop ( $\Delta$ A<sub>S</sub>, deletion of nts 36-63). The  $\Delta$ T<sub>S</sub> and  $\Delta$ A<sub>S</sub> variants are the same constructs as previously described in our analysis of PKR regulation by nc886 (26). As previously reported, the  $\Delta$ A<sub>S</sub> variant adopts a single conformer as expected since this region forms the structure that distinguishes the two nc886 conformers. In contrast, each of the terminal and central stem deletion variants ( $\Delta$ T<sub>S</sub>,  $\Delta$ T<sub>S</sub>2 and  $\Delta$ C<sub>S</sub>) retains the ability to form two conformers like the wild-type RNA since the apical stem-loop structure remains intact.

We tested the capacity of each nc886 variant, and each individual RNA conformer where applicable, to activate OAS1 *in vitro* at a single fixed RNA concentration (as used for wild-type nc886 in Figure 3.1B). nc886 $\Delta$ A<sub>S</sub> fails to activate OAS1, with activity comparable to the control reaction with no RNA (Figure 3.3B). This result indicates that the apical stem-loop of nc886 is essential for activation of OAS1 by either conformer and, in particular, for potent activation by Conformer 1. Consistent with this interpretation, Conformer 1 of both the  $\Delta$ T<sub>S</sub> and  $\Delta$ T<sub>S</sub>2 variants retains near wild-type activity suggesting that in the context of Conformer 1, the terminal stem is largely dispensable for OAS1 activation. In contrast, Conformer 1 of the  $\Delta$ C<sub>S</sub> variant has lost most of its ability to activate OAS1. Finally, similar to the  $\Delta$ A<sub>S</sub> variant and in contrast to the weakly activating wild-type nc886 Conformer 2, Conformer 2 of each terminal or central stem deletion completely fails to activate OAS1 (Figure 3.3B). The initial rates of reaction were also calculated for ease of comparison of relative OAS1 activation by each nc886 variant (Figure 3.3C). Collectively, these data reveal that deletion of the nc886

terminal stem fully ablates OAS1 activation in the context of the Conformer 2 apical stem-loop structure but has only a very minor impact on the activity of Conformer 1 RNAs. Only the largest deletion ( $\Delta$ CS) significantly impacts OAS1 activation in the context of Conformer 1 suggesting that this region forms a critical part of the OAS1 binding site required for potent OAS1 activation.

The differential effects of the various deletions on each nc886 conformer suggest that there are multiple OAS1 interaction sites in nc886 that are not equivalent. OAS1 may bind along the terminal stem or apical stem-loop of nc886 RNA, and the tertiary interaction present in the apical stem-loop region of nc886 Conformer 1 would then potentiate the activity of OAS1. The loss of activity observed in  $\Delta$ CS Conformer 1 suggests that the central stem of the RNA is important for OAS1 binding, and loss of this binding site prevents correct positioning of the nc886 Conformer 1 tertiary structure to exert its effect on OAS1 activation. This would be similar to the potentiation in activity conferred to simple duplex RNAs or viral non-coding RNAs by the 3'-ssPy motif (27).

### **3.3.4 OAS1 activation requires an intact nc886 apical stem-loop**

To determine which regions of the apical stem-loop of nc886 Conformer 1 are critical to potentiate OAS1 activity, we created specific variants to define the minimally functional apical stem-loop of nc886. Guided by experimentally defined RNA secondary structures from selective 2'-hydroxyl acylation analyzed by primer extension (SHAPE) analyses of the wild-type nc886 RNA conformers (26), we created targeted variants of the apical stem-loop-region. These included smaller deletions of the apical stem-loop ( $\Delta$ AS2 and  $\Delta$ L5) and a Loop 4 deletion ( $\Delta$ L4) to create more perfectly duplex dsRNA (Figure 3.4A).

Each of these new variants adopted a single conformation as determined by native gel analysis and their secondary structures were confirmed by SHAPE RNA probing to be as expected (Figure 3.4A,B and Figure 3.6). The stability of each RNA was assessed by UV thermal melting analysis revealing that these variants more closely resemble wild-type nc886 Conformer 2 than Conformer 1 (Table 3.1). We next tested each isolated RNA for its ability to activate OAS1 *in vitro* and found that all variants failed to activate OAS1 above the level of the control lacking RNA. This result suggests that OAS1 requires all of the apical stem-loop structure of nc886 in the context of both conformers. The complete loss of activity in  $\Delta L5$ , compared to wild-type nc886 Conformer 2, further points to a specific interaction of OAS1 with Loop 5 of the RNA. The  $\Delta AS2$  and  $\Delta L5$  variants demonstrate the critical role Loop 5 nucleotides play in forming this unique structure. In contrast, SHAPE reactivity was observed for Loop 4 nucleotides in both full-length nc886 Conformer 1 and nc886 Conformer 2, which suggested that Loop 4 did not play a role in forming this structure. However, the loss of  $\Delta L4$ 's ability to form the tertiary structure suggests that Loop 4 is important in nc886 to create the L4-L5 helix junction and that this adjacent helix is critical in formation of the tertiary structure and, additionally, the tertiary structure in Conformer 1 provides stability to the RNA, shifting the  $T_m$  higher.

### **3.4 Conclusions**

The OAS/ RNase L pathway halts viral replication through translational control in response to viral infection. In this study, we demonstrate that a cellular non-coding RNA, nc886, regulates OAS1 activity *in vitro* and in A549 cells. nc886 was previously shown

to regulate another viral dsRNA sensor, PKR, and this activity was dependent on the nc886 conformer involved (26). While nc886 Conformer 1 and 2 share the same sequence and the majority of their structure, the different folding of the apical stem-loop of each greatly impacts their ability to activate OAS1. Despite both conformers containing more than the 18 bp required by OAS1 for activation, they have stark differences in their respective levels of OAS1 activation. Furthermore, the structural motif in nc886 Conformer 1 requires the nucleotides of Loop 5 and the adjacent helix for formation. In addition, this putative tertiary interaction present in the apical stem-loop of nc886 Conformer 1 potentiates the activity of the RNA. OAS1 activation can thus be affected by specific RNA structural elements in addition to dsRNA length or the presence of motifs such as the 3'-ssPy or a consensus sequence (27, 33, 34). Moreover, we show that multiple OAS1 binding sites exist within nc886 RNA that are not equivalent and this highlights the importance of context with regards to the effects of specific RNA structural elements. Furthermore, the nature of an overlapping, but distinct, requirement for the apical stem of nc886 in the regulation of OAS1 versus PKR suggests a model in which PKR and OAS1 may compete for binding to nc886 basally and during infection. This may implicate nc886 RNA as mediating a synergistic response in innate immunity if it were to be displaced from PKR during infection, allowing it to bind and potentially activate OAS1 (Figure 3.5).

### **3.5 Materials and Methods**

#### **3.5.1 RNA *in vitro* transcription and purification**

RNAs were *in vitro* transcribed from linearized plasmid DNA templates using T7 RNA

polymerase as previously described (35). Completed transcription reactions were dialyzed against 1× TE (10 mM Tris, pH 8 and 1 mM EDTA) buffer and RNA purified by native polyacrylamide gel electrophoresis (PAGE) on 0.5× TBE (44.5 mM Tris, pH 8.3, 44.5 mM boric acid and 1 mM EDTA) gels. RNA bands were identified by UV shadowing, excised from the gel, eluted by crushing and soaking in 0.3 M sodium acetate (pH 5.2), and recovered by ethanol precipitation. All RNAs were analyzed by native PAGE after purification and prior to use in assays.

### **3.5.2 OAS1 expression and purification**

Human OAS1 (p41/E16 isoform) was expressed in *E. coli* BL21 (DE3) as an amino-terminal hexa-histidine tagged SUMO-OAS1 fusion protein (27). Cells were grown in Lysogeny Broth at 37 °C and expression was induced with 0.1 mM isopropyl- $\beta$ -D-1-thiogalactopyranoside (IPTG) at mid-log phase growth ( $OD_{600} \sim 0.5$ ). Growth was continued overnight at 20 °C. Cells were lysed in 50 mM Tris-HCl buffer (pH 8) containing 150 mM NaCl, 10% (v/v) glycerol, 10 mM imidazole, and 1 mM DTT. SUMO-OAS1 fusion protein was purified by sequential Ni<sup>2+</sup>-affinity and heparin-affinity chromatographies on an ÄKTApurifier 10 system (GE Healthcare). The fusion protein was dialyzed against SUMO cleavage buffer (50 mM Tris-HCl buffer (pH 8) containing 150 mM NaCl, 10% (v/v) glycerol and 2 mM DTT) and cleaved with SUMO Protease 1 (LifeSensors) leaving a native OAS1 amino-terminus.

### **3.5.3 *In vitro* chromogenic assay of OAS1 activity**

2'-5'-oligoadenylate synthesis was monitored by detection of the reaction by-product

pyrophosphate (PPi) in an established chromogenic assay of OAS1 activity (27). OAS1 (300 nM) was incubated at 37 °C with 20 µg/mL poly(rI:rC) or 300 nM wild-type or variant nc886 RNA in solution containing 20 mM Tris HCl buffer (pH 7.4), 7 mM MgCl<sub>2</sub>, 1 mM DTT and 1.5 mM ATP. Aliquots (10 µL) were removed at time points between 0 and 120 minutes, and quenched with 2.5 µL of 250 mM EDTA pre-dispensed into the wells of a 96-well plate. At completion of the time course, 10 µL of 2.5% ammonium molybdate in 2.5 M H<sub>2</sub>SO<sub>4</sub>, 10 µL of 0.5 M β-mercaptoethanol, and water to 100 µL total volume were added to each well. Absorbance at 580 nm was measured using a Synergy4 plate reader (Biotek) and readings were converted to PPi produced by comparison with PPi standards after background subtraction from a blank reaction (containing all components of the reaction except for OAS1 and RNA).

Complete kinetic analyses were performed similarly, but using RNA in the range of 0.01-1 µM (nc886 Conformer 1) or 0.1-3 µM (nc886 Conformer 2), and only measuring the first 10-20 minutes of the reaction. Linear regression analysis was used to obtain the nmols PPi produced/minute for each RNA concentration and the values plotted using Prism 6 (GraphPad). The curves were then fit using non-linear regression analysis using the Michaelis-Menten model to obtain OAS1 V<sub>max</sub> and RNA K<sub>app</sub> values. For each RNA, two replicate experiments were carried out using two different preps of protein.

### **3.5.4 OAS/RNase L activation in A549 cells**

Human wild-type A549 and RNase L knockout A549 cells, constructed using CRISPR-Cas9 gene editing technology as reported previously (36), were cultured in F-12K medium (Gibco/Invitrogen) supplemented with 10% fetal bovine serum (FBS), 100

U/mL penicillin and 100 µg/mL streptomycin. Both cell lines tested negative for mycoplasma. For analysis of OAS/RNase L pathway activation, A549 cells ( $0.3 \times 10^6$ ) were seeded into six-well plates in media lacking antibiotics and after 24 hours were transfected with 1 µg/mL RNA (nc886 Conformer 1, nc886 Conformer 2, poly(rI:rC), or VA RNA<sub>1</sub> TSA21 variant) using Lipofectamine 2000 reagent (Invitrogen) for 3 hours. Cells were harvested in 350 µL RLT lysis buffer (Qiagen) and the total RNA extracted using the RNeasy Kit (Qiagen). Total RNA was resolved on 1.5% agarose gels, stained with ethidium bromide, to determine integrity of 28S and 18S rRNA.

### **3.5.5 RNA UV thermal melting analysis**

RNA UV melting curves were collected at 260 and 280 nm on a Cary400 UV-visible spectrophotometer (Varian). Samples contained 20-25 µg RNA in a solution of 0.5× TBE or 20 mM HEPES buffer (pH 7.5) containing 100 mM NaCl. The first derivative of each UV absorbance curve ("melting profile") was calculated for each RNA in GraphPad Prism6 software after normalization to simplify comparisons between RNA variants.

### **3.5.6 Selective 2'-hydroxyl acylation analyzed by primer extension (SHAPE)**

SHAPE RNA probing with N-methyl isatoic anhydride (NMIA) was carried out as previously described (26, 37) with the following modifications: reactions were initiated with 1 µL of 130 mM NMIA and run for 45 min at 37 °C. Reverse transcription was carried out with a 5'-end labeled [ $\gamma$ <sup>32</sup>P]-ATP DNA primer corresponding to the sequence of the 3' end of the full-length nc886 RNA (nucleotides 84-101) or to an internal sequence for full-length nc886 Conformer 1 (nucleotides 36-54). The primer used for the apical

stem variants was the same as that corresponding to the 3' end of the full-length nc886 RNA. To determine the position of each SHAPE reactive nucleotide, dideoxy nucleotide (ddNTP) sequencing was carried out using the radiolabeled primer and untreated RNA. All reactions were resolved on denaturing (urea) sequencing-style polyacrylamide gels, dried, and exposed to a phosphor storage screen. The intensity of bands was analyzed on a Typhoon Trio Imager (GE Healthcare) and quantified using ImageQuant software (GE Healthcare). Following subtraction of background corresponding to reactions without NMIA, reactivity at each nucleotide was normalized and the values from at least two replicates were averaged and classified as low (5.5-11%), medium (11-22%), and high (>22%) (37). Previously reported SHAPE reactivities for full-length nc886 Conformer 1, nc886 Conformer 2, and nc886 $\Delta$ L5 (26) are shown for comparison with the variant RNAs generated in this study.

### **3.6 Acknowledgements**

We thank Dr. Anice Lowen (Emory University) and Dr. Susan Wiess (University of Pennsylvania) for providing the human A549 cells and human A549 RNASE L K/O cells, respectively. We thank Dr. Anice Lowen, Dr. John Steel, and Shamika Danzy at Emory University for assistance with cell culture. We thank Samantha Schwartz (Emory University) for providing purified OAS1 for some of the kinetic experiments. This work was supported by an award from the Emory University Research Council, a scholarship from the ARCS Foundation, and by the Biochemistry, Cell and Molecular Biology (BCMB) National Institutes of Health/National Institute of General Medical Sciences training grant T32-GM008367.

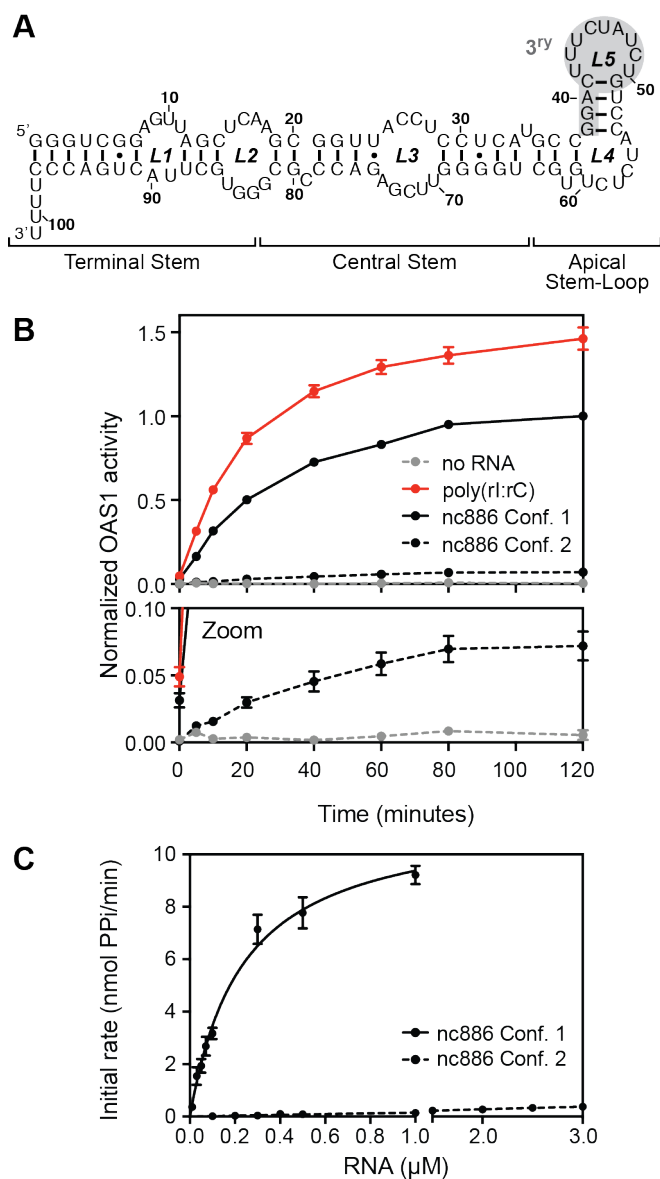


**Figure 3.1 Differential activation of OAS1 by the two nc886 conformers.** A. nc886 secondary structure and domain organization. The region of predicted tertiary structure present only in Conformer 1 is highlighted by gray shading. B. Chromogenic assay of OAS1 activity performed under previously established conditions (27) demonstrating that the nc886 conformers activate OAS1 to starkly different levels. nc886 Conformer 1 (solid black line) potently activates OAS1, near the levels of activation for the synthetic dsRNA poly(rI:rC) (red line), whereas Conformer 2 (dashed black line) only weakly activates

OAS1. The lower panel is a zoomed in view of the plot showing that nc886 Conformer 2 activates OAS1 at a low level but above the background control lacking RNA (dashed gray line). Data are normalized to nc886 Conformer 1. Error bars represent the SEM. C. Kinetic analysis of OAS1 activation by nc886 RNA conformers. OAS1 activity over a range of nc886 Conformer 1 and Conformer 2 concentrations. Data were fit using non-linear regression to obtain the kinetic parameters ( $V_{\max}$  and  $K_{\text{app}}$ ) as described in the main text. Error bars represent the SEM.

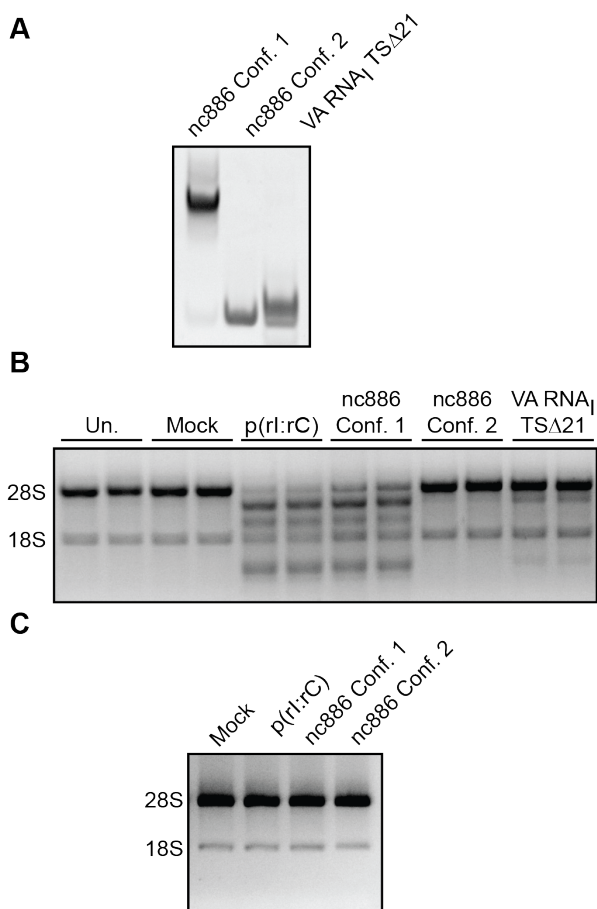


**Figure 3.2 nc886 Conformer 1 activates the OAS/RNase L pathway in human A549 cells.** A. Native PAGE analysis of purified nc886 conformers and the adenoviral VA RNA<sub>I</sub> (TSAΔ21) variant used to transfect A549 cells. B. Agarose gel analysis of total RNA extracted from cells at 3 hours post-transfection with the indicated RNA (1 μg/mL) or other treatment: untransfected (Un.) or mock-transfected (Mock). A representative gel is shown for one independent set of experiments. rRNA degradation, based on 28S and 18S rRNA integrity, is only induced by treatment with nc886 Conformer 1 and poly(rI:rC). C. Analysis of total RNA extracted from A549 cells lacking RNase L treated as in panel B, demonstrating that rRNA degradation observed with nc886 Conformer 1 and poly(rI:rC) treatment is specifically dependent on activation of the OAS/RNase L pathway.

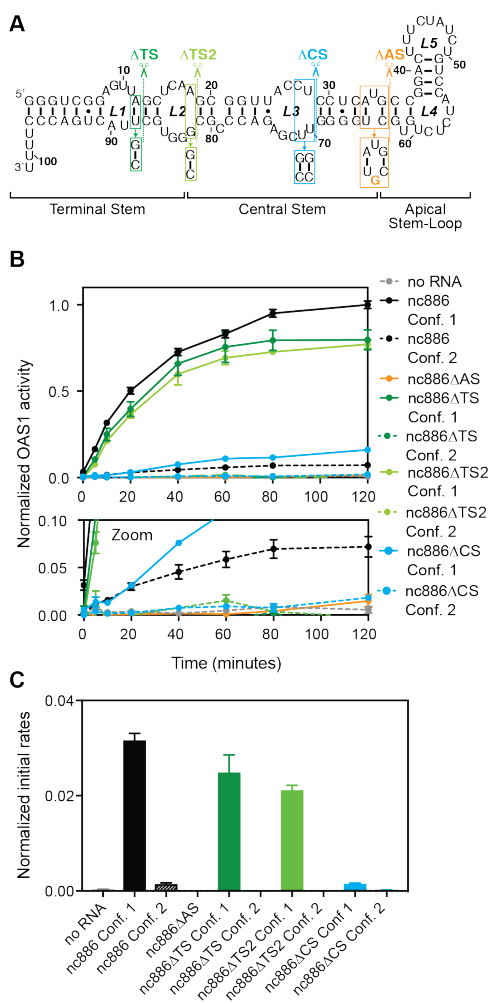


**Figure 3.3 The apical stem-loop of nc886, but not the terminal stem, is critical for OAS1 activation.** A. nc886 secondary structure and domain organization with truncations of the terminal stem (TS), central stem (CS), or apical stem (AS) highlighted. B. Chromogenic assay of OAS1 activity demonstrating that the terminal stem of nc886 stem is largely dispensable for activity towards OAS1. The lower panel is a zoomed in view of the plot to show that nc886 $\Delta$ TS Conformer 2, nc886 $\Delta$ TS2 Conformer 2, nc886 $\Delta$ CS Conformer 2, and nc886 $\Delta$ AS all completely fail to activate OAS1. C. Initial rates are shown for the first 10 minutes of the reactions in panel B. Data in panels B and C are normalized to nc886 Conformer 1. Error bars represent the SEM.

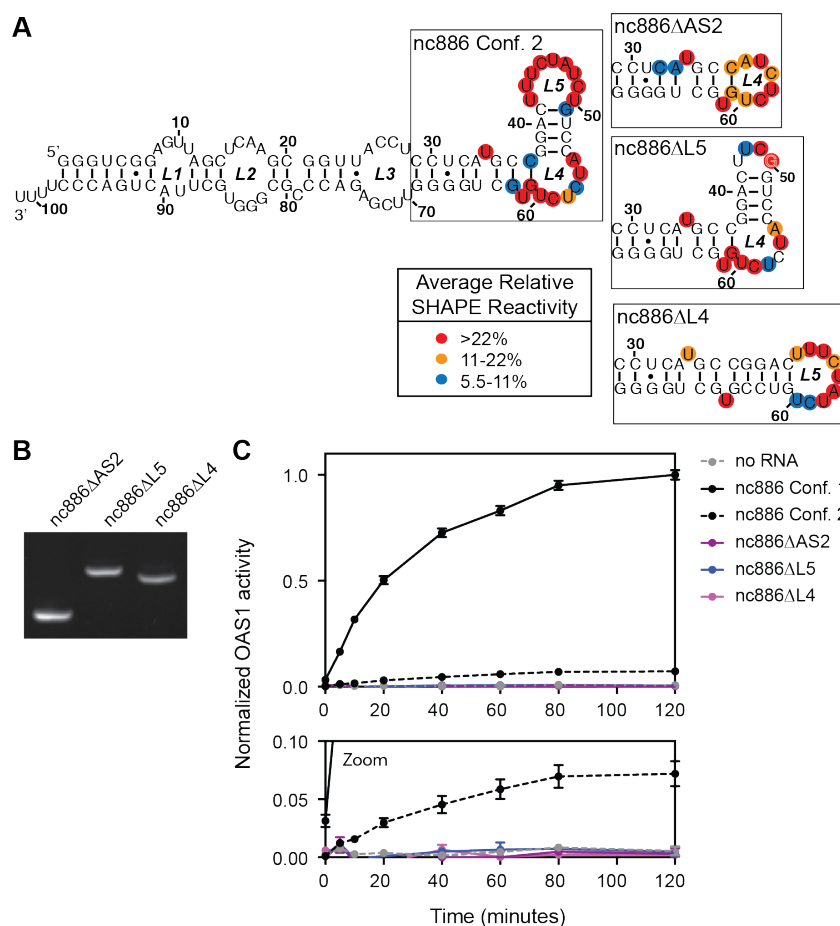


**Figure 3.4 Activation of OAS1 is dependent on an intact apical stem of nc886 RNA.**

A. Sequence and secondary structure of wild-type nc886 and apical stem variants with experimental SHAPE reactivities mapped onto the secondary structure of the apical stem-loop region of each variant. B. Native PAGE analysis of purified variant RNAs. C. Chromogenic assay of OAS1 activity demonstrating that AS variants fail to activate OAS1. nc886 Conformer 1 (solid black line) potently activates OAS1, whereas Conformer 2 (dashed black line) only weakly activates OAS1. nc886ΔAS2 (solid purple line), nc886ΔL5 (solid blue line), and nc886ΔL4 (solid pink line) all fail to activate OAS1. The lower panel is a zoomed in view of the plot showing that the AS mutants all have activity that overlaps with the background control lacking RNA (dashed gray line). Data are normalized to nc886 Conformer 1. Error bars represent the SEM.

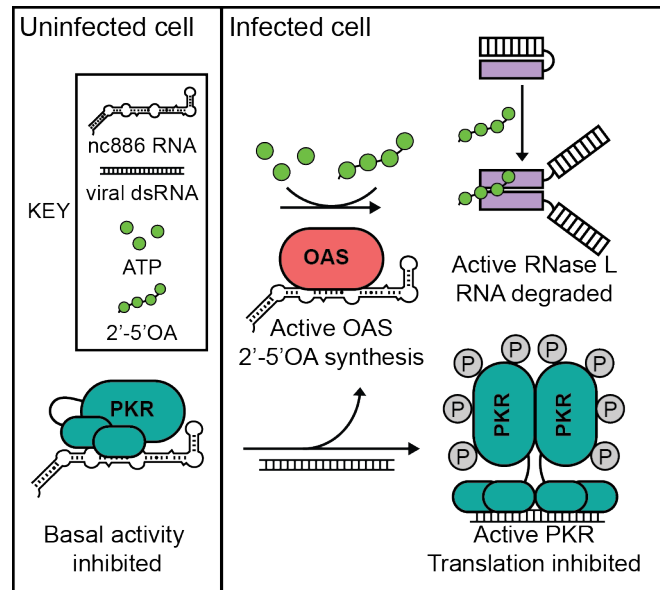


**Figure 3.5 Model for coordinated nc886-mediated regulation of the viral dsRNA sensors PKR and OAS.** In the uninfected cell, nc886 binds to and inhibits basal PKR activity. Upon infection, nc886 is displaced by viral dsRNA, which then activates PKR leading to translation inhibition. nc886 is then free to bind to and activate OAS, leading to production of 2'-5'-OA second messengers that activate RNase L resulting in RNA cleavage further halting translation and inhibiting viral replication.

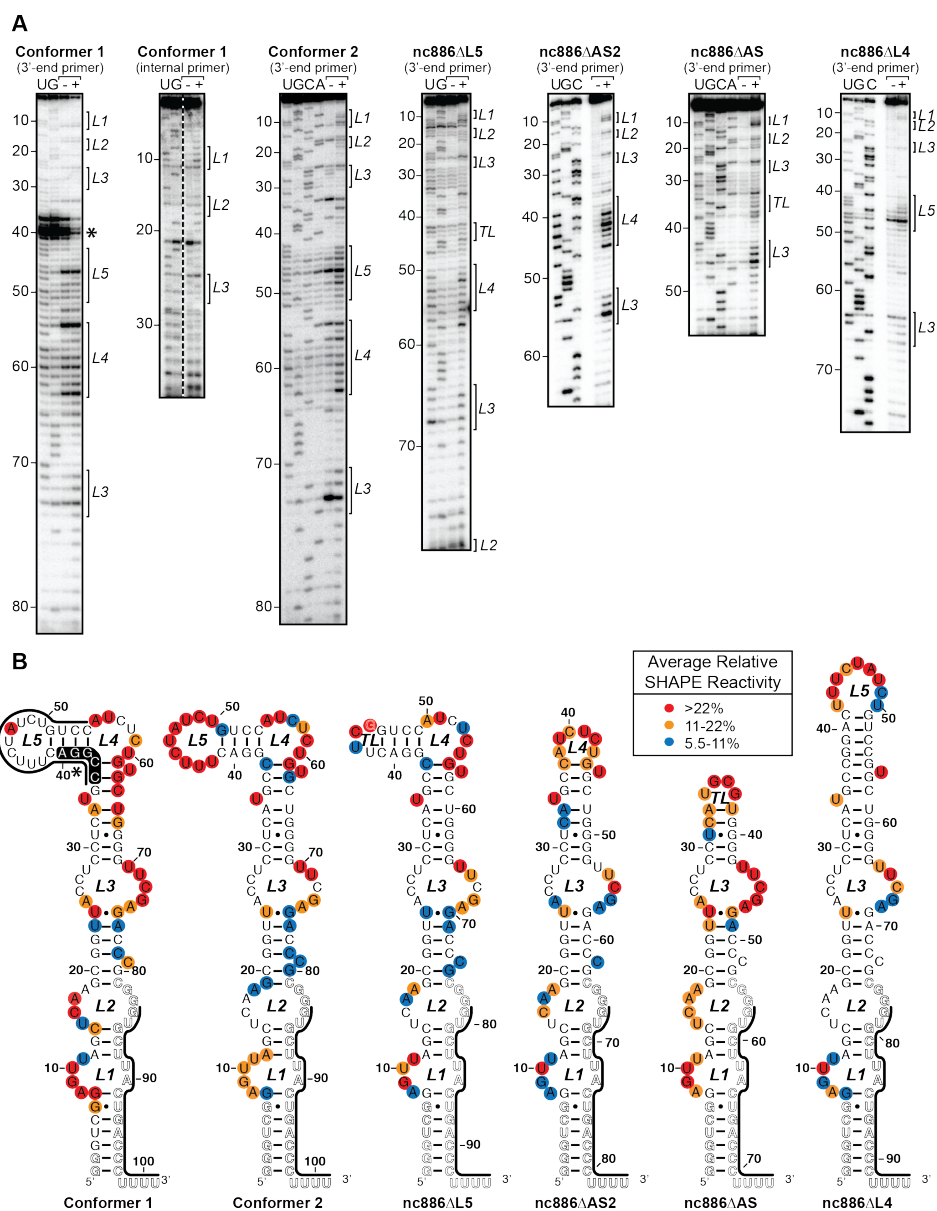


**Figure 3.6 SHAPE probing of nc886 variants.** A. Example autoradiograms of sequencing gel analysis of SHAPE probing of wild-type nc886 and apical stem variants. Lanes are -, mock treated (no NMIA); +, NMIA treated; and U/G/C/A, sequencing lanes containing the complementary dideoxy-NTP. Brackets on the right of gel images denote the loop regions (L1-L5) in the predicted secondary structures. B. Expected secondary structures of wild-type nc886 and apical stem variants with experimental SHAPE reactivity mapped onto these structures.

RNA	Apparent $T_m$ (°C)	
	0.5 × TBE	HEPES/NaCl
nc886 Conf. 1	73.8	92.2
nc886 Conf. 2	38.2	58.4
nc886ΔAS2	40.9	61.2
nc886ΔL4	43.6	63.9
nc886ΔL5	39	59.4

**Table 3.1** Apparent melting temperatures ( $T_m$ ) for wild-type and variant nc886 unfolding.

### 3.7 References

1. Chow J, Franz KM, & Kagan JC (2015) PRRs are watching you: Localization of innate sensing and signaling regulators. *Virology* 479-480:104-109.
2. Schneider WM, Chevillotte MD, & Rice CM (2014) Interferon-stimulated genes: a complex web of host defenses. *Annu Rev Immunol* 32:513-545.
3. Schlee M & Hartmann G (2016) Discriminating self from non-self in nucleic acid sensing. *Nat Rev Immunol* 16(9):566-580.
4. Tsutsui-Takeuchi M, *et al.* (2015) Roles of retinoic acid-inducible gene-I-like receptors (RLRs), Toll-like receptor (TLR) 3 and 2'-5' oligoadenylate synthetase as viral recognition receptors on human mast cells in response to viral infection. *Immunol Res* 61(3):240-249.
5. Kristiansen H, Gad HH, Eskildsen-Larsen S, Despres P, & Hartmann R (2011) The oligoadenylate synthetase family: an ancient protein family with multiple antiviral activities. *J Interferon Cytokine Res* 31(1):41-47.
6. Eskildsen S, Justesen J, Schierup MH, & Hartmann R (2003) Characterization of the 2'-5'-oligoadenylate synthetase ubiquitin-like family. *Nucleic Acids Res* 31(12):3166-3173.
7. Martin G & Keller W (2007) RNA-specific ribonucleotidyl transferases. *Rna* 13(11):1834-1849.
8. Donovan J, Dufner M, & Korennykh A (2013) Structural basis for cytosolic double-stranded RNA surveillance by human oligoadenylate synthetase 1. *Proc Natl Acad Sci U S A* 110(5):1652-1657.
9. Huang H, *et al.* (2014) Dimeric structure of pseudokinase RNase L bound to 2-5A reveals a basis for interferon-induced antiviral activity. *Mol Cell* 53(2):221-234.
10. Han Y, Whitney G, Donovan J, & Korennykh A (2012) Innate immune messenger 2-5A tethers human RNase L into active high-order complexes. *Cell Rep* 2(4):902-913.
11. Donovan J, Whitney G, Rath S, & Korennykh A (2015) Structural mechanism of sensing long dsRNA via a noncatalytic domain in human oligoadenylate synthetase 3. *Proc Natl Acad Sci U S A* 112(13):3949-3954.
12. Rath S, *et al.* (2015) Human RNase L tunes gene expression by selectively destabilizing the microRNA-regulated transcriptome. *Proc Natl Acad Sci U S A* 112(52):15916-15921.
13. Brennan-Laun SE, Ezelle HJ, Li XL, & Hassel BA (2014) RNase-L control of cellular mRNAs: roles in biologic functions and mechanisms of substrate targeting. *J Interferon Cytokine Res* 34(4):275-288.
14. Banerjee S, *et al.* (2015) RNase L is a negative regulator of cell migration. *Oncotarget* 6(42):44360-44372.
15. Siddiqui MA, Mukherjee S, Manivannan P, & Malathi K (2015) RNase L Cleavage Products Promote Switch from Autophagy to Apoptosis by Caspase-Mediated Cleavage of Beclin-1. *Int J Mol Sci* 16(8):17611-17636.
16. Banerjee S, Chakrabarti A, Jha BK, Weiss SR, & Silverman RH (2014) Cell-type-specific effects of RNase L on viral induction of beta interferon. *MBio* 5(2):e00856-00814.
17. Donovan J, Rath S, Kolet-Mandrikov D, & Korennykh A (2017) Rapid RNase L-

- Driven Arrest of Protein Synthesis in the dsRNA Response without Degradation of Translation Machinery. *Rna*.
18. Yim HC, *et al.* (2016) The kinase activity of PKR represses inflammasome activity. *Cell Res* 26(3):367-379.
  19. Youssef OA, *et al.* (2015) Potential role for snoRNAs in PKR activation during metabolic stress. *Proc Natl Acad Sci U S A* 112(16):5023-5028.
  20. Dalet A, Gatti E, & Pierre P (2015) Integration of PKR-dependent translation inhibition with innate immunity is required for a coordinated anti-viral response. *FEBS Lett* 589(14):1539-1545.
  21. Kim Y, *et al.* (2014) PKR is activated by cellular dsRNAs during mitosis and acts as a mitotic regulator. *Genes & Development* 28(12):1310-1322.
  22. Marchal JA, *et al.* (2014) The impact of PKR activation: from neurodegeneration to cancer. *FASEB J* 28(5):1965-1974.
  23. Kunkeaw N, *et al.* (2012) Cell death/proliferation roles for nc886, a non-coding RNA, in the protein kinase R pathway in cholangiocarcinoma. *Oncogene* 32(32):3722-3731.
  24. Jeon SH, *et al.* (2012) Characterization of the direct physical interaction of nc886, a cellular non-coding RNA, and PKR. *FEBS Lett* 586(19):3477-3484.
  25. Lee K, *et al.* (2011) Precursor miR-886, a novel noncoding RNA repressed in cancer, associates with PKR and modulates its activity. *RNA* 17(6):1076-1089.
  26. Calderon BM & Conn GL (2017) Human noncoding RNA 886 (nc886) adopts two structurally distinct conformers that are functionally opposing regulators of PKR. *RNA* 23(4):557-566.
  27. Vachon VK, Calderon BM, & Conn GL (2015) A novel RNA molecular signature for activation of 2'-5' oligoadenylate synthetase-1. *Nucleic Acids Res* 43(1):544-552.
  28. Justesen J & Kjeldgaard NO (1992) Spectrophotometric pyrophosphate assay of 2',5'-oligoadenylate synthetase. *Anal Biochem* 207(1):90-93.
  29. Kwon YC, Kang JI, Hwang SB, & Ahn BY (2013) The ribonuclease L-dependent antiviral roles of human 2',5'-oligoadenylate synthetase family members against hepatitis C virus. *FEBS Lett* 587(2):156-164.
  30. Wahid AM, Coventry VK, & Conn GL (2008) Systematic Deletion of the Adenovirus-associated RNAI Terminal Stem Reveals a Surprisingly Active RNA Inhibitor of Double-stranded RNA-activated Protein Kinase. *Journal of Biological Chemistry* 283(25):17485-17493.
  31. Wilson JL, Vachon VK, Sunita S, Schwartz SL, & Conn GL (2014) Dissection of the adenoviral VA RNAI central domain structure reveals minimum requirements for RNA-mediated inhibition of PKR. *J Biol Chem* 289(33):23233-23245.
  32. Meng H, *et al.* (2012) Regulation of the interferon-inducible 2'-5'-oligoadenylate synthetases by adenovirus VA(I) RNA. *Journal of Molecular Biology* 422(5):635-649.
  33. Kodym R, Kodym E, & Story MD (2009) 2'-5'-Oligoadenylate synthetase is activated by a specific RNA sequence motif. *Biochem Biophys Res Commun* 388(2):317-322.
  34. Hartmann R, *et al.* (1998) Activation of 2'-5' oligoadenylate synthetase by single-stranded and double-stranded RNA aptamers. *J Biol Chem* 273(6):3236-3246.

35. Linpinsel JL & Conn GL (2012) General Protocols for Preparation of Plasmid DNA Template, RNA In Vitro Transcription, and RNA Purification by Denaturing PAGE. in *Recombinant and In Vitro RNA Synthesis* (Springer Science + Business Media), pp 43-58.
36. Li Y, *et al.* (2016) Activation of RNase L is dependent on OAS3 expression during infection with diverse human viruses. *Proc Natl Acad Sci U S A* 113(8):2241-2246.
37. Wilkinson KA, Merino EJ, & Weeks KM (2006) Selective 2'-hydroxyl acylation analyzed by primer extension (SHAPE): quantitative RNA structure analysis at single nucleotide resolution. *Nat Protoc* 1(3):1610-1616.

## Chapter 4

### Conclusion

The work presented in this thesis has deepened our understanding of non-coding RNA-mediated regulation of the innate immune proteins PKR and OAS. These proteins exert their antiviral activity through distinct mechanisms of translational control. Such viral dsRNA sensors play a critical role in innate immunity and must achieve a balance between accurate detection of foreign nucleic acids and prevention of spurious activation by host nucleic acids, which could have deleterious effects for the cell. Deregulation of their activity can leave cells susceptible to viral infections or contribute to human disease. As such, the precise regulation of innate immune sensors by specific recognition of pathogen-associated molecular patterns or by endogenous factors is required for proper cell function. For example, the non-coding RNA nc886 is proposed to play this latter role, regulating PKR activity to prevent basal activation by host nucleic acids.

Our work has elucidated molecular details of nc886-mediated PKR regulation. nc886 inhibits basal PKR activity and this role is crucial for proper cell function; loss of nc886 and concomitant upregulation of PKR activity is observed in several different cancer cell lines and tissues. We have shown that nc886 adopts two distinct structural conformations with opposing function towards PKR. These nc886 conformers share the majority of their central and terminal stem structure, but differ in their apical region. There, nc886 Conformer 1 forms a unique RNA tertiary structure that is critical for potent inhibition of PKR activity. Conformer 2, in contrast, lacks this tertiary structure

and acts as a weak activator of PKR. We have demonstrated that nc886 also possesses the ability to regulate OAS1 activity through potent activation *in vitro* and in human A549 cells. This activity is again dependent on an intact apical stem forming the tertiary structure present only in nc886 Conformer 1. Thus, nc886 serves as a non-coding RNA regulator with opposing activities against two arms of the innate immune response that function in translational control during viral infection. The overlapping, but distinct requirements for nc886-mediated regulation of each dsRNA sensor suggests that PKR and OAS may compete for nc886 binding. Finally, we expand our analyses of non-coding RNA regulators to include another human non-coding RNA, the Gas5 lincRNA, capable of regulating PKR activity in a sequence and structural motif-independent manner. In the following sections I highlight the larger implications of this work and open questions that need to be addressed to more fully complete our knowledge of non-coding RNA-mediated regulation of innate immunity.

#### **4.1 Structural differences in nc886 conformers have functional consequences**

In Chapter 2, the secondary structures of nc886 Conformer 1 and 2 were elucidated using SHAPE RNA probing, revealing that the terminal and central stem secondary structure is largely shared between the two forms. However, there are stark differences in the folding of the apical stem region with nc886 Conformer 2 adopting the predicted apical stem-loop resulting in high reactivity to NMIA for the nucleotides in Loop 5. In contrast, nc886 Conformer 1 exhibits significantly lower reactivity in Loop 5, except for a single nucleotide A47. Furthermore, multiple NMIA-independent stops are observed for nc886 Conformer 1, indicating a stable structure resistant to unfolding during the reverse

transcription reaction in the helix adjacent to Loop 5. Based on these two observations, we propose that this apical stem-loop forms a higher order tertiary structure that distinguishes the nc886 Conformer 1 structure.

The presence or absence of this nc886 apical stem-loop tertiary structure greatly impacts nc886 function towards PKR and OAS1. The presence of this tertiary structure in Conformer 1 confers potent inhibitory activity towards PKR. This structural motif is not required for binding as nc886 Conformer 2 and an apical stem deletion variant (nc886 $\Delta$ AS) all bind PKR albeit with lower affinity than nc886 Conformer 1. Surprisingly, nc886 Conformer 2 is able to weakly activate PKR suggesting that the tertiary structure masks what would otherwise be an activating RNA structure. Furthermore, in Chapter 3 we demonstrate that the presence or absence of the same structural motif dictates the potency of nc886-mediated OAS1 activation with Conformer 1 being a potent activator and Conformer 2 activating weakly.

While the molecular details of the unique nc886 Conformer 1 structure are unknown, we speculate that it may arise from a different organization of base pairing that is very stable but which must be kinetically trapped during transcription. Alternatively, adoption of a unique fold around a buried ion could help explain the properties of each conformer, as described in Chapter 2. However, the lack of experimental determination of this nc886 motif remains a significant gap in our understanding of its function. Although we know this structural motif requires Loop 4, Loop 5, and the junction between them, the elucidation of the three-dimensional structure of nc886, for example by x-ray crystallography, is required in order to determine the molecular details of this motif fold. This additional structural information would also provide insight into both

how nc886 Conformer 1 can potently inhibit PKR activity and potentiate OAS1 activation, though structural studies of the RNA-protein complex would be most informative. Such structures would reveal important new details of the mechanisms of nc886-mediated regulation of PKR and OAS1. Along with structural information already available on dsRNA-mediated activation of PKR and OAS1 (1, 2), such studies would reveal why nc886 is so potent in regards to both proteins. Furthermore, these structures could provide insights that lead to novel avenues for modulating the activity of these viral dsRNA sensors through their interaction with nc886.

While the differences in nc886 structure have large impacts on its function, the ability of nc886 to fold into multiple structures from the same sequence is not unique. In fact, at least one cellular mRNA, the interferon-gamma (IFN- $\gamma$ ) mRNA, regulates its own translation through dynamic refolding of its 5'-untranslated region (5'-UTR) (3). The IFN- $\gamma$  mRNA 5'-UTR forms three short helices that align with a pseudoknot stem in the RNA, allowing it to transition from a translation template to PKR activator, and thus a specific translational repressor. For nc886, it remains to be addressed if both conformers exist *in vivo* and what conditions may favor one form or the other. In order to address the first part of this question it is important to use primary cell culture, as nc886 is deficient in many cancer cell lines and is expected to also be downregulated in other immortalized or cancer cell lines. Furthermore, whether the total levels of nc886 or the ratio of the conformers change in the cell during infection or under other cellular stresses must still be determined. We speculate that the ratio of the conformers in the cell has the potential to dictate the nature and extent of regulation of PKR and OAS activity in response to diverse cell needs both during and in the absence of infection.

Changes in total nc886 RNA levels could occur through changes in transcription or decay of the RNA. Transcriptional changes could potentially affect the folding of the RNA, favoring formation of one conformer or the other. Changes in the ratio of the two forms could also occur through refolding of the RNA, such as seen with IFN- $\gamma$  mRNA (3). While nc886 conformers maintain their structural identity under non-denaturing conditions, binding to other proteins may induce structural changes. Although we tested and found no PKR binding-induced changes *in vitro*, this observation does not rule out the possibility of other protein or RNA binding partners being able to induce nc886 conformational changes within the cell. To more fully address this, Northern Blot analysis in uninfected and virally infected cells could be compared to address differences in steady-state levels of nc886 RNA. Native Northern Blot analysis could be used to determine if both conformers are expressed in human cells and if the ratio of the two conformers changes upon viral infection.

#### **4.2 PKR and OAS interact with overlapping segments of nc886 RNA**

Through combined mutational and functional analyses, we established that the nc886 tertiary structure, present only in Conformer 1, is required for both potent inhibition of PKR and potent activation of OAS1. This suggests that both proteins interact with the tertiary structure, located in the apical region of nc886 RNA, and thus may have overlapping binding regions. An important implication of this finding is therefore that nc886 may be bound to only one protein at a time. Thus, nc886 might serve as a mediator of communication between these two arms of the innate immune response.

Downregulation of nc886 in cancer cells leads to unregulated basal PKR activity

illustrating the important role nc886 plays in keeping PKR activity under control (4-8). Further, artificial downregulation of nc886 using siRNAs leads to activation of PKR in the absence of exogenous dsRNA and results in the downstream activation of nuclear factor kappa-light-chain-enhancer of activated B cells (NF- $\kappa$ B) (5). NF- $\kappa$ B is oncogenic and activates survival genes allowing for proliferation of cancer cells (9). Thus, the literature supports a model in which the primary role of nc886 in the cell is to inhibit basal PKR activity (Figure 4.1). During infection, nc886 should be displaced from PKR by viral dsRNA, either through higher binding affinity or sheer excess, thus allowing for an appropriate immune response. The discovery here of nc886's potent activation of OAS *in vitro* and in human A549 cells highlights a potential avenue for nc886 to stimulate the immune response during infection by activating the OAS/ RNase L pathway after release from PKR.

An important question that needs to be addressed is whether nc886 can be released from PKR during infection to activate OAS. An experimental way to test this *in vitro* would be to use competition assays in which activating dsRNA is added to a PKR-nc886 complex and measuring release of nc886 RNA. Filter binding assays could be used to test for release of nc886 from PKR, exploiting the property of nitrocellulose membranes to only bind protein thus capturing only PKR-bound RNA. To test whether nc886 could activate OAS, similar competition assays could be used, but measuring OAS activity rather than RNA release from PKR. A caveat of this work, however, is the need to use an RNA that binds PKR but does not activate OAS. Cell based assays could also be used to test if OAS activation occurs, by measuring RNase L cleavage of rRNA, after transfection of an RNA that interacts with PKR, but does not activate OAS. Repeating

such experiments in cells where nc886 is naturally or artificially deleted would help confirm this synergistic response.

### **4.3 Gas5 lincRNA activates PKR**

We additionally demonstrated the ability of Gas5 (described in the Appendix), a long intergenic non-coding RNA (lincRNA), to activate PKR and the downstream phosphorylation of eIF2 $\alpha$  both *in vitro* and in HEK293T cells. This activation was RNA length-dependent, but not dependent on any particular sequence or structural motif. Two small truncation variants of Gas5, 187-253 and 471-531, had significantly reduced ability to activate PKR likely due to their small size, 68 and 62 nucleotides, respectively. PKR requires a minimum of 33 base pairs for activation making both variants potentially too small to accommodate two PKR double-stranded RNA-binding domains. However, the remaining larger truncation variants that were able to activate PKR at near wild-type levels (Figure 4.2) had no obvious conserved sequence or structure.

Unlike nc886, Gas5 lincRNA positively regulates PKR activity by inducing autophosphorylation *in vitro* and in HEK293T cells. These two examples add to a growing body of literature highlighting RNA-mediated regulation of PKR activity by structurally diverse cellular RNAs (Figure 4.3). Thus, an open question that remains is whether there are other non-coding RNA regulators of PKR or OAS activity and what cellular functions these may control. With increased RNA sequencing capabilities we can envision experiments aimed at isolating RNA binding partners of these and other dsRNA sensors in innate immunity. An important step moving forward with studies aimed at understanding the role of Gas5 and other non-coding RNAs on PKR activity is validation

in cells. While Gas5 acts in both growth arrest and apoptosis, both cellular processes that are also regulated by PKR-mediated translation inhibition, it remains to be addressed if endogenous Gas5 activates PKR and under what circumstances it does this. Given our work with nc886-mediated repression of PKR activity, it also remains to be addressed how Gas5 and nc886 may compete for PKR binding.

#### **4.4 Roles for nucleic acid sensors outside of immunity**

The discovery of novel cellular RNA-mediated regulation of PKR and OAS begs the question of what additional cellular functions PKR and OAS may possess outside of immunity. Studies have identified numerous PKR functions outside of immunity including roles in regulating gene expression, cell differentiation, cell division, and response to other cell stresses (10-12). The cellular functions of the OAS/RNase L pathway, however, are less well understood. Recently, RNase L has been implicated in regulating cell proliferation, differentiation, and adhesion (13-16). Both proteins have conserved functions that suggest roles outside of innate immunity. For example, PKR belongs to the family of eIF2 $\alpha$  kinases, which includes HRI, GCN2, and PERK. These kinases all inhibit general translation in response to different stimuli including dsRNA, heme deficiency, amino acid starvation, and ER stress, respectively. This downstream response is thus a conserved mechanism for responding to cell stress. Interestingly, OAS is evolutionarily conserved and found even in organisms lacking an interferon system, such as sponges (17, 18). This suggests that the OAS/RNase L pathway may have played other cellular roles prior to acting in the interferon-inducible antiviral system. Taken together, discovery of new RNAs capable of regulating the activity of these sensors and

thus their downstream responses may hint at other important biological roles these sensors play in uninfected cells. OAS and PKR may thus be thought of as evolutionarily conserved stress response pathways whose activities are regulated by cellular RNAs for diverse cell needs. In addition, this highlights a potential avenue that viruses might use to subvert the innate immune response through manipulation of endogenous regulators of these immune sensors in order to evade detection or alternatively activating these sensors for the purposes of turning on specific cellular functions downstream that may benefit the virus. For example, it has been shown that Epstein-Barr virus and Influenza A virus upregulate nc886 expression leading to PKR inhibition although the mechanistic details are unknown (19, 20). Long-term implications of this work, and studies building upon it, can be focused on the identification of other RNAs or structural motifs, such as that seen in nc886, with the ability to selectively stimulate or inhibit these sensors for therapeutic approaches.

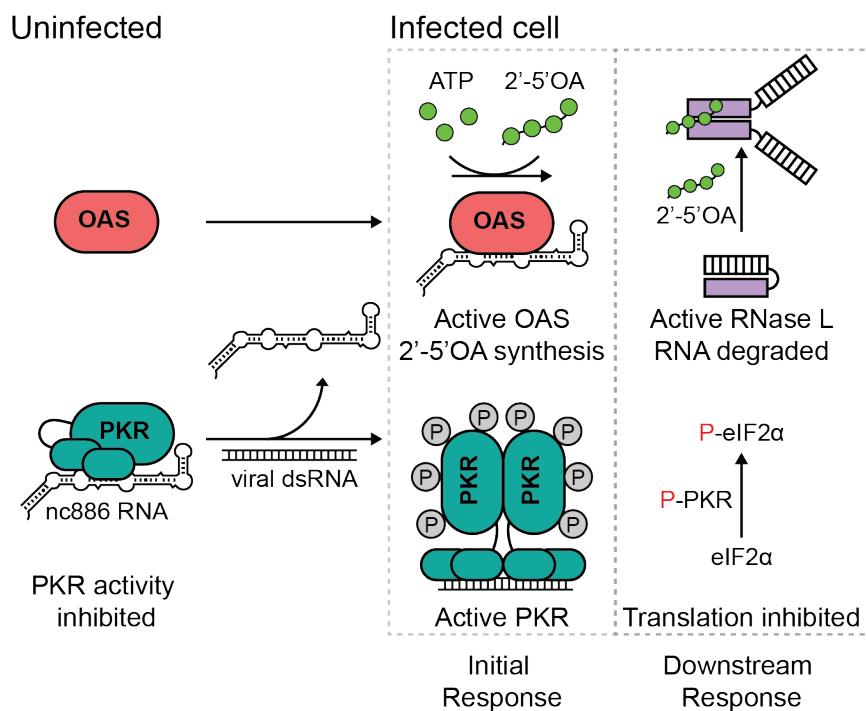


**Figure 4.1 Model for coordinated nc886-mediated regulation of the viral dsRNA sensors PKR and OAS.** In the uninfected cell, nc886 primarily binds to and inhibits basal PKR activity. During infection, nc886 RNA is displaced from PKR by viral dsRNA resulting in activation of PKR and the downstream phosphorylation of its substrate eIF2 $\alpha$  thus halting protein synthesis. Free nc886 can bind to and activate OAS, leading to production of 2'-5'-oligoadenylate second messenger that drives RNase L dimerization and activation, resulting in the degradation of viral and cellular RNA.

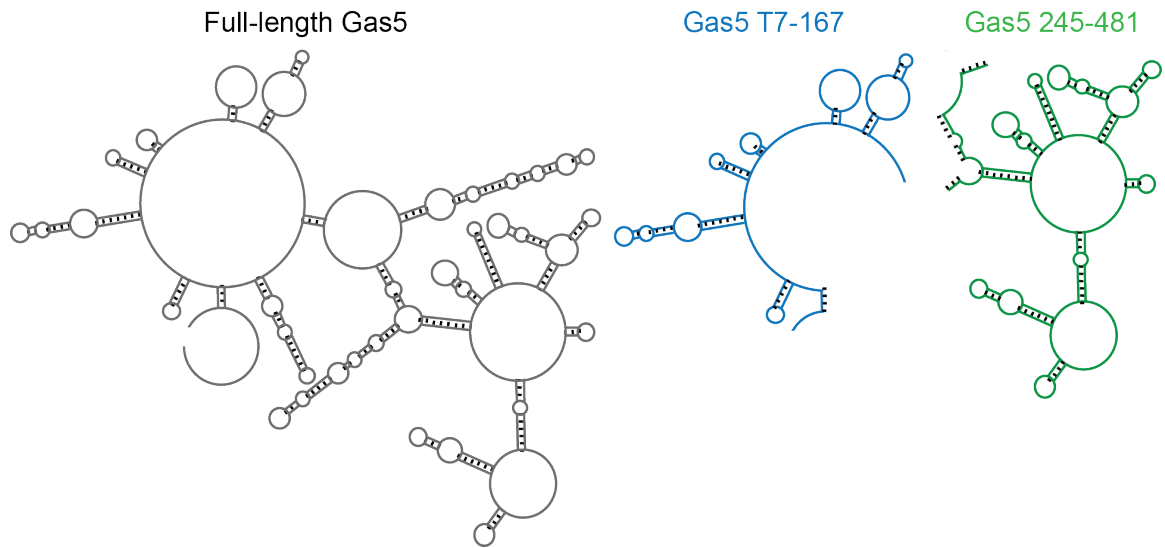


**Figure 4.2** PKR is activated by a variety of Gas5 secondary structures. Secondary structure maps of full-length Gas5 and the truncation variants T7-167 and 245-481.

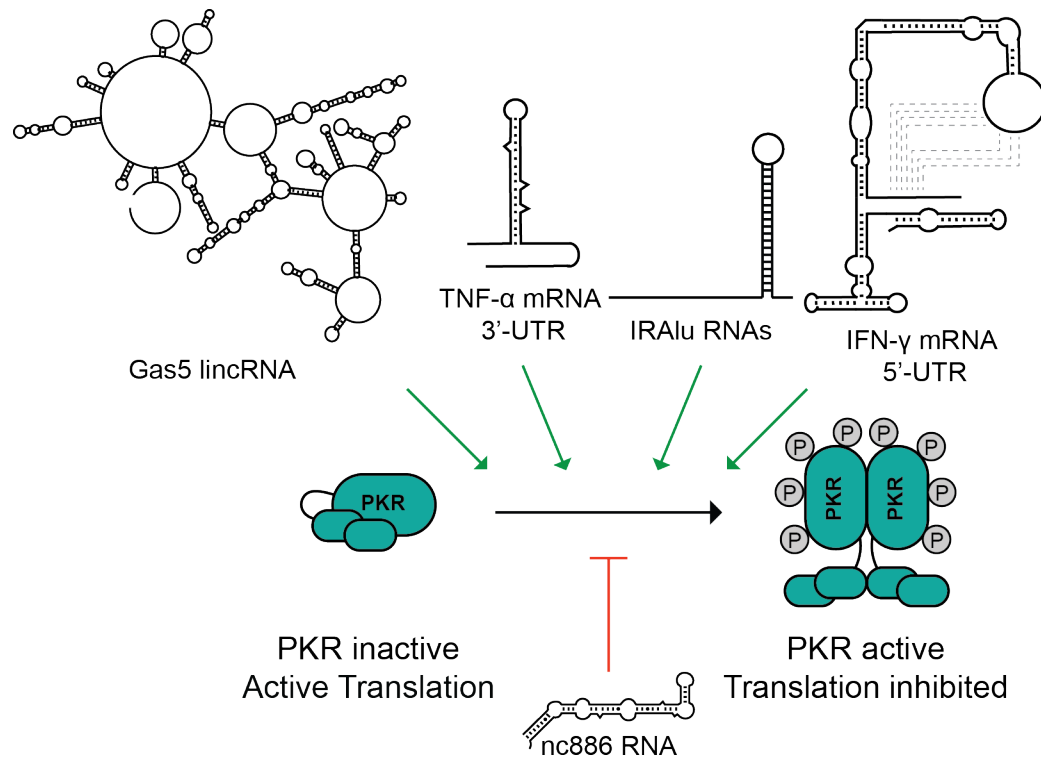


**Figure 4.3 PKR regulation by cellular RNAs with varied structures.** RNA secondary structure maps of PKR interacting RNAs including the positive (green arrows) regulators Gas5 lincRNA, TNF- $\alpha$  mRNA, Inverted Repeat Alu (IRAlu) containing RNAs, and IFN- $\gamma$  mRNA. The secondary structure of the only known cellular RNA that negatively (red inhibition) regulates PKR activity, nc886, is also shown. The positive regulators cytoskeletal mRNAs are not shown, as their secondary structures are not experimentally determined.

#### 4.5 References

1. Donovan J, Dufner M, & Korennykh A (2013) Structural basis for cytosolic double-stranded RNA surveillance by human oligoadenylate synthetase 1. *Proc Natl Acad Sci U S A* 110(5):1652-1657.
2. Nanduri S, Carpick BW, Yang Y, Williams BR, & Qin J (1998) Structure of the double-stranded RNA-binding domain of the protein kinase PKR reveals the molecular basis of its dsRNA-mediated activation. *Embo j* 17(18):5458-5465.
3. Cohen-Chalamish S, *et al.* (2009) Dynamic refolding of IFN- $\gamma$  mRNA enables it to function as PKR activator and translation template. *Nature Chemical Biology* 5(12):896-903.
4. Lee EK, *et al.* (2016) nc886, a non-coding RNA and suppressor of PKR, exerts an oncogenic function in thyroid cancer. *Oncotarget* 7(46):75000-75012.
5. Lee HS, *et al.* (2014) Epigenetic silencing of the non-coding RNA nc886 provokes oncogenes during human esophageal tumorigenesis. *Oncotarget* 5(11):3472-3481.
6. Romanelli V, *et al.* (2014) Variable maternal methylation overlapping the nc886/vtRNA2-1 locus is locked between hypermethylated repeats and is frequently altered in cancer. *Epigenetics* 9(5):783-790.
7. Lee KS, *et al.* (2014) nc886, a non-coding RNA of anti-proliferative role, is suppressed by CpG DNA methylation in human gastric cancer. *Oncotarget* 5(11):3944-3955.
8. Kunkeaw N, *et al.* (2012) Cell death/proliferation roles for nc886, a non-coding RNA, in the protein kinase R pathway in cholangiocarcinoma. *Oncogene* 32(32):3722-3731.
9. DiDonato JA, Mercurio F, & Karin M (2012) NF-kappaB and the link between inflammation and cancer. *Immunol Rev* 246(1):379-400.
10. Kim Y, *et al.* (2014) PKR is activated by cellular dsRNAs during mitosis and acts as a mitotic regulator. *Genes & Development* 28(12):1310-1322.
11. Liu X, *et al.* (2013) PKR regulates proliferation, differentiation, and survival of murine hematopoietic stem/progenitor cells. *Blood* 121(17):3364-3374.
12. Garcia MA, *et al.* (2006) Impact of Protein Kinase PKR in Cell Biology: from Antiviral to Antiproliferative Action. *Microbiology and Molecular Biology Reviews* 70(4):1032-1060.
13. Rath S, *et al.* (2015) Human RNase L tunes gene expression by selectively destabilizing the microRNA-regulated transcriptome. *Proc Natl Acad Sci U S A* 112(52):15916-15921.
14. Banerjee S, *et al.* (2015) RNase L is a negative regulator of cell migration. *Oncotarget* 6(42):44360-44372.
15. Siddiqui MA, Mukherjee S, Manivannan P, & Malathi K (2015) RNase L Cleavage Products Promote Switch from Autophagy to Apoptosis by Caspase-Mediated Cleavage of Beclin-1. *Int J Mol Sci* 16(8):17611-17636.
16. Brennan-Laun SE, Ezelle HJ, Li XL, & Hassel BA (2014) RNase-L control of cellular mRNAs: roles in biologic functions and mechanisms of substrate targeting. *J Interferon Cytokine Res* 34(4):275-288.
17. Pari M, *et al.* (2014) Enzymatically active 2',5'-oligoadenylate synthetases are

- widely distributed among Metazoa, including protostome lineage. *Biochimie* 97:200-209.
18. Kjaer KH, *et al.* (2009) Evolution of the 2'-5'-oligoadenylate synthetase family in eukaryotes and bacteria. *J Mol Evol* 69(6):612-624.
  19. Nandy C, *et al.* (2009) Epstein-barr virus-induced expression of a novel human vault RNA. *J Mol Biol* 388(4):776-784.
  20. Li F, *et al.* (2015) Robust expression of vault RNAs induced by influenza A virus plays a critical role in suppression of PKR-mediated innate immunity. *Nucleic Acids Res* 43(21):10321-10337.

## Appendix

### Gas5 lincRNA is a novel, cellular non-coding RNA activator of PKR

#### A.1 Abstract

The double-stranded RNA (dsRNA)-activated protein kinase (PKR) senses dsRNA in the cytosol, produced during viral infection, and blocks viral replication through translational control. Outside of innate immunity, PKR plays roles in diverse cellular processes including regulation of gene expression, cell division, cell differentiation, and apoptosis. As such, deregulation of PKR activity is implicated in myriad human diseases ranging from neurodegeneration to cancer. Clearly defining the mechanisms of PKR regulation in the cell and the factors involved is crucial for our understanding of PKR's impact on cell function and disease. Long intergenic non-coding RNAs (lincRNAs) are a class of non-coding RNAs that play essential roles in diverse biological processes. Their deregulation is also associated with many human diseases. The growth arrest-specific 5 (Gas5) lincRNA is one such RNA, and its roles in inhibition of cell proliferation and promotion of apoptosis result in its downregulation in multiple cancers. Here we demonstrate that Gas5 activates PKR *in vitro* and in HEK293T cells in a length-dependent manner. Gas5 activation of PKR serves as another example of cellular RNA-mediated regulation of PKR activity and has potential implications for modulating PKR activity for diverse cell needs.

#### A.2 Introduction

The human genome is comprised mostly of non-coding DNA, with only 2% coding for protein (1). However, the discovery of many new classes of non-coding transcripts has led to a growing appreciation for the roles of non-coding RNA (ncRNA) in diverse cell functions (2). While the roles of ribosomal RNA, transfer RNA, small nucleolar RNA, and micro RNAs are well established, there are many classes of ncRNAs with less understood structures and functions. These include PIWI-interacting RNAs, promoter-associated RNAs, small non-coding RNAs, and long non-coding RNAs (3). In particular, long intergenic non-coding RNAs (lincRNAs) represent a large component of the human transcriptome with poorly defined functions.

The growth arrest-specific 5 (*Gas5*) lincRNA regulates gene expression by binding to and repressing steroid hormone receptors including the glucocorticoid receptor, androgen receptor, progesterone receptor and mineralocorticoid receptor (4, 5). The human *GAS5* gene consists of 12 exons and encodes C/D box snoRNA genes within its introns (6). The *GAS5* gene yields two mature lincRNAs, *Gas5a* and *Gas5b*, and is expressed in all tissues (7). *Gas5* lincRNA has established roles in cell growth and arrest as well as apoptosis, functions that can be independent of steroid receptor signaling. As such, *Gas5* lincRNA expression is downregulated in several cancers (5, 8, 9). Our recent work highlighting the role of a small non-coding RNA in regulating the activity of an innate immune response protein implicated in cancer, the double-stranded RNA-activated protein kinase (PKR) (10), led us to ask if *Gas5* could also interact with and regulate PKR activity. PKR halts protein synthesis in response to viral infection and other cell stresses, through phosphorylation of the eukaryotic translation initiation factor 2 alpha subunit (eIF2 $\alpha$ ) and initiates the integrated stress response (11). PKR has been proposed

to act as both a tumor suppressor and as an oncogene depending on which of its downstream pathways are activated (12). While PKR can be anti-proliferative through inhibition of general translation, its role in activating nuclear factor kappa-light chain-enhancer of activated B cells (NF- $\kappa$ B) can confer proliferative properties on PKR. Here we show that Gas5 lincRNA activates PKR *in vitro* and in HEK293T cells, leading to autophosphorylation and activation of the kinase, resulting in the subsequent phosphorylation of eIF2 $\alpha$ . We propose that because Gas5 is anti-proliferative, Gas5-mediated PKR activation could also drive growth arrest and apoptosis through PKR's inhibition of general translation.

### **A.3 Results**

#### **A.3.1 Gas5 activates PKR *in vitro***

To test if Gas5 lincRNA directly interacts with PKR, Gas5 was *in vitro* transcribed, PAGE-purified, and annealed prior to use in a radiometric assay to measure RNA-binding induced PKR dimerization and autophosphorylation. Phosphorylation was measured by the transfer of a radioactive phosphate from [ $\gamma$ <sup>32</sup>P]-ATP. The biological substrate of PKR, eIF2 $\alpha$ , was also included in the radiometric assay and the two proteins were resolved by SDS-PAGE to determine the extent of phosphorylation of each protein. Gas5 lincRNA activates PKR leading to autophosphorylation of PKR and phosphorylation of its substrate eIF2 $\alpha$  (Figure A.1A), producing a bell-shaped dependence on RNA concentration typical of other PKR activators (Figure A.1B). PKR activation follows this profile as increasing concentrations of RNA induce successively greater PKR dimerization and autophosphorylation until higher concentrations of RNA

become inhibitory due to increased binding of isolated PKR monomers to RNA and thus dilution of the active dimeric form. Importantly, neither PKR nor eIF2 $\alpha$  phosphorylation was observed in a control reaction with no RNA. The peak of the activation curve was observed between 250 and 500 nM Gas5, suggesting that small changes in cellular concentrations of Gas5 can dramatically affect its ability to activate PKR.

### **A.3.2 Gas5 induces PKR T446 phosphorylation in HEK293T cells**

We next asked if Gas5 lincRNA could activate PKR and induce the downstream phosphorylation of eIF2 $\alpha$  in cells. HEK293T cells were transfected with Gas5 lincRNA or poly(rI:rC), a known activator of PKR, and PKR activation measured by immunoblotting for phosphorylated T446 of PKR and phosphorylated S51 of eIF2 $\alpha$ . Threonine 446 is located in the activation loop of PKR and is the only phosphorylated residue required for PKR kinase activity on eIF2 $\alpha$ . Transfection of poly(rI:rC) or Gas5 lincRNA induced PKR T446 phosphorylation (Figure A.2A), which was not observed in untransfected or mock-transfected controls. While poly(rI:rC) induced phosphorylation more than 2-fold higher compared to Gas5 at the low (0.005  $\mu$ M) or high (0.05  $\mu$ M) concentration, the Gas5-induced phosphorylation was still increased > 100-fold compared to untransfected controls. The changes observed in eIF2 $\alpha$  phosphorylation levels were comparable between transfection with poly(rI:rC) and low (0.005  $\mu$ M) concentration of Gas5, increasing 2- to 3-fold compared to mock-transfected controls. Importantly, differences in phosphorylation levels are not a result of dramatic differences in total levels of PKR and eIF2 $\alpha$  proteins (Figure A.2B).

### **A.3.3 PKR recognition of Gas5 is length but not sequence dependent**

Previous published work (5) demonstrated that Gas5 lincRNA interacts with steroid receptors in cells in a sequence-specific manner dependent on its nucleotides G549 and G559. PKR is a sensor of dsRNA in the cell, typically viral dsRNA in the infected cell and thus acts in a non-sequence-specific manner to detect dsRNA from a broad range of pathogens. PKR activation is, however, length-dependent due to the requirement of dsRNA to bind two PKR monomers driving their dimerization and thus autophosphorylation. We created a series of truncation variants based on unpublished SHAPE probing data on full-length Gas5 lincRNA (Figure A.3A,B) and tested each variant separately in the same radiometric activation assay (Figure A.3C). Two variants, corresponding to Gas5 nts 187-253 and 471-531 did not produce high levels of PKR autophosphorylation at the peak of their respective curves, suggesting that these RNAs are not sufficiently double-stranded. PKR requires 30-33 bp of dsRNA for RNA-induced dimerization/autophosphorylation, which these variants might fall short of due to their size. We selected the next two smallest variants corresponding to non-overlapping segments of Gas5, and tested these in the same radiometric activation assay along with full-length Gas5 lincRNA for comparison (Figure A.3D). Both truncation variants display similar activation curves but shifted to the right (i.e. higher RNA concentration) compared to full-length Gas5. Thus, more RNA is required to activate PKR in the case of the variants, suggesting that there are at least two distinct PKR binding sites in Gas5 lincRNA that are capable of activating the kinase.

### **A.4 Discussion**

Gas5 levels change in response to cell stress in order to allow for Gas5-mediated growth arrest and apoptosis. Serum starvation, rapamycin stimulation, and cortisol are just some of the cell stresses that induce an increase in Gas5 lincRNA levels (6, 13). Thus, changes in Gas5 levels in response to stress could allow for the activation of PKR and subsequent translational control as a potential stress response pathway. Using biochemical approaches we show that Gas5 lincRNA activates PKR *in vitro* and in HEK293T cells. This activation is length-dependent, but sequence-independent, distinct from the mechanism of Gas5 interaction with steroid receptors. Through creation of RNA truncation variants we show that Gas5 contains at least two, and potentially multiple, binding sites within its 651 nucleotide length. Despite large differences in their sequence and secondary structures, the two fragments tested here activate PKR to similar extents. The full-length Gas5 lincRNA activates PKR at lower RNA concentrations than each truncation variant likely due to the accumulated action of the multiple binding sites facilitating in PKR dimerization and activation.

Gas5-mediated activation of PKR highlights the broad range of RNA structures recognized by PKR. While PKR requires a minimum of 30-33 bp of dsRNA in order to accommodate the dsRNA-binding domains of two separate PKR monomers for dimerization-induced activation, this is not constrained to perfectly duplex RNA. Interferon gamma (IFN- $\gamma$ ) mRNA, for example, activates PKR through refolding of its 5'-untranslated region, which results in a tertiary structure composed of four adjoining helices stacking with a pseudoknot capable of activating PKR (14). Furthermore, the 3'-untranslated regions of cytoskeletal mRNAs and tumor necrosis factor- $\alpha$  have also been shown to activate PKR (15, 16). Gas5 lincRNA thus belongs to a growing list of cellular

RNAs capable of activating PKR though the biological significance of Gas5-mediated PKR activation, however, requires further study. Gas5 functions in growth arrest and apoptosis; these activities are clearly compatible with PKR's known roles in halting protein synthesis and inducing apoptosis.

Gas5 is one of the most abundantly expressed lincRNAs in humans, and as such it remains to be determined what regulates the Gas5-PKR interaction. While Gas5 levels are high, binding to endogenous protein partners may limit interaction with PKR. Furthermore, Gas5 levels change in response to different cell stresses, with an increase observed under serum starvation, rapamycin stimulation, and cortisol stimulation. Rapid changes in Gas5 levels can thus also add a layer of regulation to Gas5-mediated PKR activation with this interaction more likely to happen under conditions of cell stress when both PKR and Gas5 levels are elevated. In addition, localization can regulate PKR-mediated activation by other RNAs, for example, inverted Alu repeat containing RNAs are segregated in the nucleus of interphase cells, but are released into the cytosol during mitosis allowing for activation of PKR and resulting in suppression of general translation and regulation of mitotic factors (17). Here we have shown that Gas5 can activate PKR to elicit downstream eIF2 $\alpha$  phosphorylation, adding to the known non-coding RNAs capable of regulating PKR, in addition to the established role played by non-coding RNA 886. With our growing appreciation of non-coding RNA structure and function this highlights new avenues for RNA-mediated regulation of proteins in a post-transcriptional manner.

## **A.5 Material and Methods**

### **A.5.1 RNA *in vitro* transcription and purification**

Full-length (Gas5, sequence corresponding to Ensembl transcript 221, 651 bases) and variant Gas5 RNAs were *in vitro* transcribed (by F. Frank, Emory University) from linearized plasmid DNA templates using T7 RNA polymerase as previously described (18). Following dialysis against 1× Tris–EDTA (TE) buffer, RNAs were purified by polyacrylamide gel electrophoresis (PAGE) on denaturing (50% urea, 1× Tris–Borate–EDTA [TBE]) gels. RNA bands were identified by UV shadowing, excised, eluted from the gel by crushing and soaking in 0.3 M sodium acetate, and ethanol precipitated as previously described (18).

### **A.5.2 PKR protein expression and purification**

*E. coli* Rosetta 2 (DE3) cells were transformed with the pET-PKR/PPase plasmid encoding full-length human PKR (19). Single colonies were used to inoculate large-scale cultures in Terrific Broth. PKR expression was induced with 0.1 mM isopropyl β-D-1-thiogalactopyranoside (IPTG) at mid-log phase growth ( $OD_{600} \sim 0.5$ ) and growth continued overnight at 20°C. PKR was purified by sequential heparin-affinity (HiPrep Heparin 16/10), poly(rI:rC) dsRNA-affinity, and gel filtration (Superdex 200 10/300) chromatographies on an ÄKTApurifier10 system (GE Healthcare). PKR was eluted from the gel filtration column in 20 mM HEPES buffer (pH 7.5) containing 150 mM NaCl, 0.1 mM EDTA, 10% glycerol, and 10 mM β-mercaptoethanol (BME).

### **A.5.3 eIF2α protein expression and purification**

*E. coli* BL21 (DE3) cells were transformed with a plasmid encoding an amino-terminal

hexa-histidine-tagged human eIF2 $\alpha$ . Single colonies were used to inoculate large-scale cultures in Lysogeny Broth. eIF2 $\alpha$  expression was induced with 0.1 mM IPTG at mid-log phase growth ( $OD_{600} \sim 0.5$ ) and growth continued overnight at 18°C. eIF2 $\alpha$  was purified using a bench-top HisSpinTrap column (GE Healthcare). Fractions containing the protein were pooled and further purified by gel filtration chromatography (Superdex 200 10/300) on an ÄKTApurifier10 system. eIF2 $\alpha$  was eluted from the gel filtration column in 20 mM HEPES buffer (pH 7.5) containing 150 mM NaCl, 0.1 mM EDTA, 10% glycerol, and 10 mM BME.

#### **A.5.4 PKR activation assays**

PKR (0.1  $\mu$ g) was incubated with 0–10  $\mu$ M of full-length or variant Gas 5 RNA for 10 min at 25°C in 50 mM Tris buffer (pH 7.8) containing 50 mM KCl, 2.5 mM DTT, 10% glycerol, 20  $\mu$ M ATP, 1  $\mu$ Ci [ $\gamma$ <sup>32</sup>P]-ATP, and 2 mM MgCl<sub>2</sub>. After incubation, reactions were quenched with excess ice-cold phosphate buffered saline containing 200  $\mu$ M ATP and applied to a Bio-Dot SF (Bio-Rad) microfiltration system as described previously (20). Membranes were exposed to a phosphor storage screen and the extent of phosphorylation was determined using analysis by a Typhoon FLA 7000 PhosphorImager and ImageQuant software (GE Healthcare). Values were normalized to a poly(rI:rC) (0.1  $\mu$ g/mL) reaction performed in parallel, following background subtraction from a control reaction without RNA. Assays were repeated at least three times for each RNA.

#### **A.5.5 Cell lines, transfections and immunoblotting**

Human HEK293T cells, obtained from Dr. Richard A. Kahn (Emory University), were

cultured in Dulbecco's Modified Eagle's medium (DMEM) (Gibco/Invitrogen) supplemented with 10% fetal bovine serum (FBS). HEK293T cells ( $0.1 \times 10^6$ ) were seeded into twelve-well plates and after 24 hours were transfected with 1  $\mu\text{g}/\text{mL}$  poly(rI:rC), 0.005  $\mu\text{M}$  Gas5, or 0.05  $\mu\text{M}$  Gas5 using Lipofectamine 2000 reagent (Invitrogen) for 4 hours. Cells were harvested in radioimmunoprecipitation assay (RIPA) buffer (50 mM Tris, pH 8, 150 mM NaCl, 0.5% sodium deoxycholate, 0.1% SDS, 1% NP40, 1 mM NaF, 1 mM  $\text{Na}_3\text{VO}_4$ ) supplemented with a protease inhibitor tablet (Sigma-Aldrich). The protein concentration of the soluble lysate was measured using a BCA assay (ThermoFisher). Protein was resolved by SDS-PAGE, transferred to a nitrocellulose membrane (Bio-Rad), and probed with antibodies against total PKR (Abcam, 28934), total eIF2 $\alpha$  (Cell Signalling, D7D3), PKR phosphor-T446 (Abcam, 32036), eIF2 $\alpha$  phosphor-S51 (Abcam, 32157), or  $\alpha$ -Tubulin (Abcam, 15246). A peroxidase-conjugated secondary antibody Goat anti-Rabbit IgG (Jackson Laboratories, 111-035-003) was used for detection of all primary antibodies. Membranes were developed with Clarity Western ECL Substrate (Bio-Rad) and exposed to film. Densitometric analysis of bands were quantified with Image Quant Software (GE Healthcare), background subtracted, normalized to tubulin levels and fold-change compared to untransfected controls.

#### **A.6. Acknowledgements**

We thank Dr. Eric Ortlund and Dr. Filipp Frank for useful discussions during the course of this work. We thank Dr. Filipp Frank for providing the RNA used in these experiments.

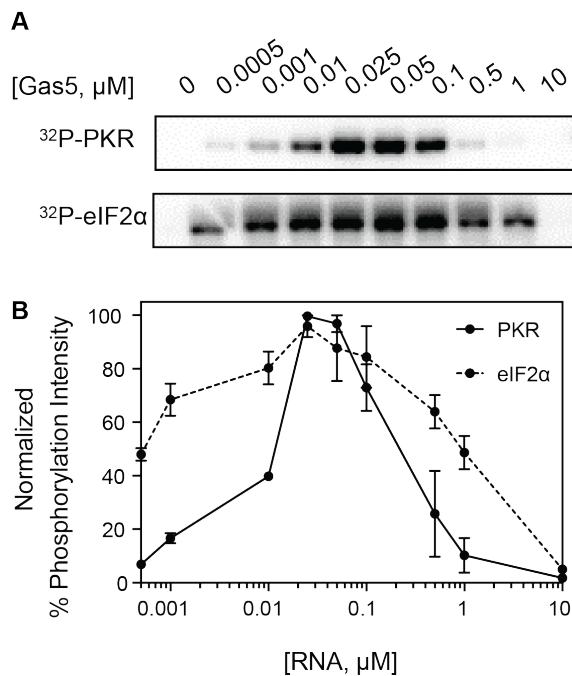


**Figure A.1 Gas5 activates PKR *in vitro*.** A. Sample SDS-PAGE analysis of a radiometric kinase activation assay containing both PKR and eIF2 $\alpha$  in the presence of 0-10  $\mu\text{M}$  Gas5 lincRNA. B. Quantification of radiometric activation assay demonstrating capacity of Gas5 lincRNA to activate PKR autophosphorylation and induce subsequent PKR-mediated phosphorylation of eIF2 $\alpha$ .

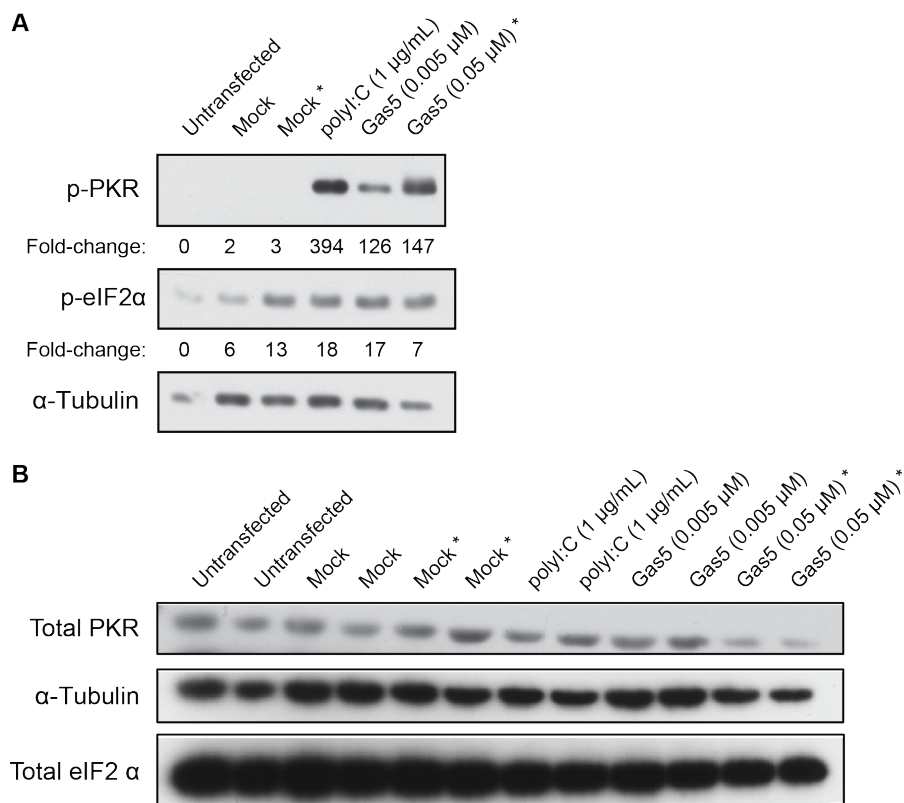


**Figure A.2 Gas5 activates PKR in HEK293T cells.** A. HEK293T cells were untransfected, mock-transfected or transfected with poly(I:C) or Gas5 lincRNA for 4 hours. Cells were lysed, and proteins analyzed by immunoblotting with antibodies against T446 phosphorylated PKR (p-PKR), S51 phosphorylated eIF2 $\alpha$  (p-eIF2 $\alpha$ ), and  $\alpha$ -tubulin. Levels of phosphorylated PKR and eIF2 $\alpha$  were compared to untransfected controls after normalization of each lane to  $\alpha$ -tubulin to determine the fold-change (shown below each lane). \* Indicates larger volume of Lipofectamine 2000 reagent used to allow transfection of the high Gas5 concentration. B. Same as panel A but immunoblotting using antibodies against total PKR, total eIF2 $\alpha$ , and  $\alpha$ -tubulin.

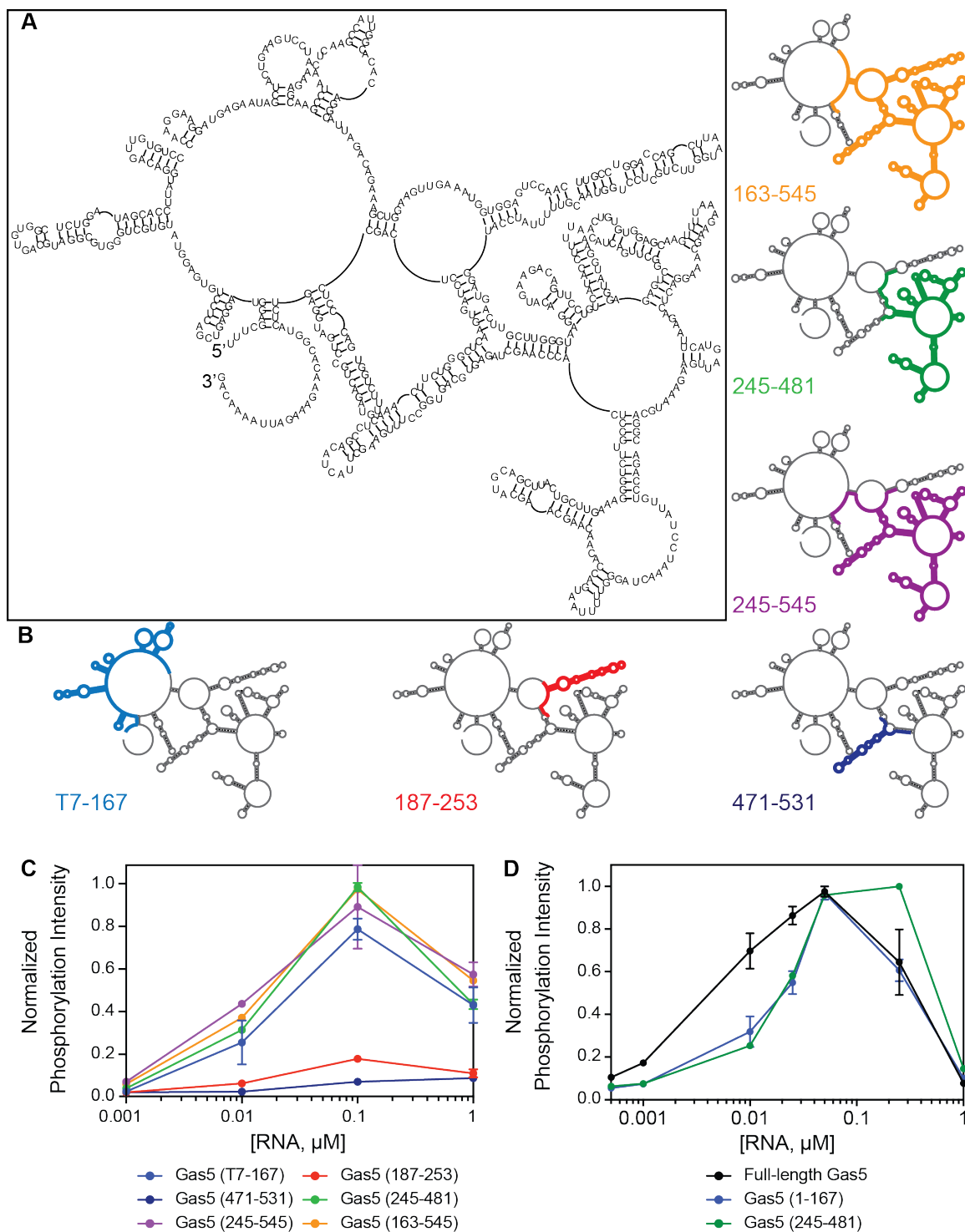


**Figure A.3 Gas5 deletion variants retain PKR activity *in vitro* in a length-dependent manner.** A. Gas5 lincRNA secondary structure. Experimentally confirmed secondary structure of nucleotides 1-600 of mature Gas5 lincRNA based on selective 2'-hydroxyl

acylation analyzed by primer extension (SHAPE) probing (F. Frank and E.A. Ortlund, unpublished). B. Secondary structure maps of full-length Gas5 lincRNA highlighting the regions corresponding to each fragment (color-coded regions). C. Quantification of radiometric PKR activation assay of Gas5 lincRNA truncation variants normalized to highest intensity band on membrane. D. Quantification of radiometric PKR activation assay of Gas5 lincRNA truncation variants T7-167 and 245-481 compared to full-length Gas5 lincRNA normalized to highest intensity band per construct for comparison of shifts in RNA concentration needed to drive maximum PKR activation.

## A.7 References

1. Anonymous (2004) Finishing the euchromatic sequence of the human genome. *Nature* 431(7011):931-945.
2. Pertea M (2012) The Human Transcriptome: An Unfinished Story. *Genes* 3(3):344-360.
3. Mattick JS (2011) The central role of RNA in human development and cognition. *FEBS Letters* 585(11):1600-1616.
4. Kino T, Hurt DE, Ichijo T, Nader N, & Chrousos GP (2010) Noncoding RNA gas5 is a growth arrest- and starvation-associated repressor of the glucocorticoid receptor. *Sci Signal* 3(107):ra8.
5. Hudson WH, *et al.* (2014) Conserved sequence-specific lincRNA-steroid receptor interactions drive transcriptional repression and direct cell fate. *Nat Commun* 5:5395.
6. Pickard MR & Williams GT (2015) Molecular and Cellular Mechanisms of Action of Tumour Suppressor GAS5 LncRNA. *Genes (Basel)* 6(3):484-499.
7. Smith CM & Steitz JA (1998) Classification of gas5 as a multi-small-nucleolar-RNA (snoRNA) host gene and a member of the 5'-terminal oligopyrimidine gene family reveals common features of snoRNA host genes. *Mol Cell Biol* 18(12):6897-6909.
8. Pickard MR, Mourtada-Maarabouni M, & Williams GT (2013) Long non-coding RNA GAS5 regulates apoptosis in prostate cancer cell lines. *Biochim Biophys Acta* 1832(10):1613-1623.
9. Mourtada-Maarabouni M, Pickard MR, Hedge VL, Farzaneh F, & Williams GT (2009) GAS5, a non-protein-coding RNA, controls apoptosis and is downregulated in breast cancer. *Oncogene* 28(2):195-208.
10. Calderon BM & Conn GL (2017) Human noncoding RNA 886 (nc886) adopts two structurally distinct conformers that are functionally opposing regulators of PKR. *RNA* 23(4):557-566.
11. Munir M & Berg M (2013) The multiple faces of protein kinase R in antiviral defense. *Virulence* 4(1):85-89.
12. Balachandran S & Barber GN (2007) PKR in innate immunity, cancer, and viral oncolysis. *Methods Mol Biol* 383:277-301.
13. Liu Y, *et al.* (2015) lncRNA GAS5 enhances G1 cell cycle arrest via binding to YBX1 to regulate p21 expression in stomach cancer. *Sci Rep* 5:10159.
14. Cohen-Chalamish S, *et al.* (2009) Dynamic refolding of IFN- $\gamma$  mRNA enables it to function as PKR activator and translation template. *Nature Chemical Biology* 5(12):896-903.
15. Nussbaum JM (2002) The 3'-untranslated regions of cytoskeletal muscle mRNAs inhibit translation by activating the double-stranded RNA-dependent protein kinase PKR. *Nucleic Acids Research* 30(5):1205-1212.
16. Osman F, Jarrous N, Ben-Asouli Y, & Kaempfer R (1999) A cis-acting element in the 3'-untranslated region of human TNF-alpha mRNA renders splicing dependent on the activation of protein kinase PKR. *Genes & Development* 13(24):3280-3293.
17. Kim Y, *et al.* (2014) PKR is activated by cellular dsRNAs during mitosis and acts

- as a mitotic regulator. *Genes & Development* 28(12):1310-1322.
18. Linpinsel JL & Conn GL (2012) General Protocols for Preparation of Plasmid DNA Template, RNA In Vitro Transcription, and RNA Purification by Denaturing PAGE. in *Recombinant and In Vitro RNA Synthesis* (Springer Science + Business Media), pp 43-58.
  19. Lemaire PA, Anderson E, Lary J, & Cole JL (2008) Mechanism of PKR Activation by dsRNA. *Journal of Molecular Biology* 381(2):351-360.
  20. Sunita S, Schwartz SL, & Conn GL (2015) The Regulatory and Kinase Domains but Not the Interdomain Linker Determine Human Double-stranded RNA-activated Kinase (PKR) Sensitivity to Inhibition by Viral Non-coding RNAs. *J Biol Chem* 290(47):28156-28165.